PREDICTION OF FELT INTENSITY FROM GROUND MOTION PARAMETERS USING ARTIFICIAL NEURAL NETWORK METHOD

A THESIS SUBMITTED TO
THE GRADUATE SCHOOL OF NATURAL AND APPLIED SCIENCES
OF
MIDDLE EAST TECHNICAL UNIVERSITY

BY

SEDA ÖZTÜRK

IN PARTIAL FULFILLMENT OF THE REQUIREMENTS
FOR
THE DEGREE OF MASTER OF SCIENCE
IN
EARTHQUAKE STUDIES

DECEMBER 2019

Approval of the thesis:

PREDICTION OF FELT INTENSITY FROM GROUND MOTION PARAMETERS USING ARTIFICIAL NEURAL NETWORK METHOD

submitted by **SEDA ÖZTÜRK** in partial fulfillment of the requirements for the degree of **Master of Science in Earthquake Studies Department, Middle East Technical University** by,

Prof. Dr. Halil Kalıpçılar
Dean, Graduate School of **Natural and Applied Sciences**

Prof. Dr. Ayşegül Askan Gündoğan
Head of Department, **Earthquake Studies**

Prof. Dr. Ayşegül Askan Gündoğan
Supervisor, **Earthquake Studies, METU**

Prof. Dr. Elçin Kentel Erdoğan
Co-Supervisor, **Civil Engineering, METU**

Examining Committee Members:

Prof. Dr. Murat Altuğ Erberik
Civil Engineering, METU

Prof. Dr. Ayşegül Askan Gündoğan
Earthquake Studies, METU

Prof. Dr. Elçin Kentel Erdoğan
Civil Engineering, METU

Assoc. Prof. Dr. Mustafa Koçkar
Civil Engineering, Hacettepe University

Assist. Prof. Dr. Onur Pekcan
Civil Engineering, METU

Date: 16.12.2019

I hereby declare that all information in this document has been obtained and presented in accordance with academic rules and ethical conduct. I also declare that, as required by these rules and conduct, I have fully cited and referenced all material and results that are not original to this work.

Name, Surname: Seda Öztürk

Signature:

ABSTRACT

PREDICTION OF FELT INTENSITY FROM GROUND MOTION PARAMETERS USING ARTIFICIAL NEURAL NETWORK METHOD

Öztürk, Seda
Master of Science, Earthquake Studies
Supervisor: Prof. Dr. Ayşegül Askan Gündoğan
Co-Supervisor: Prof. Dr. Elçin Kentel Erdoğan

December 2019, 122 pages

Earthquakes are natural phenomena that cause ground shaking and deformations due to the nature of the Earth's surface, which is composed of tectonic plates. The sudden release of energy on these tectonic plates results in earthquakes. One of the ways to measure ground shakings is the macroseismic (or felt) intensity. There are various studies on the correlation between felt intensity and ground motion parameters. Most of them involve a linear regression method to find an empirical formula for this relation. However, assuming a linear correlation may not the best approach since the independent variables affecting intensity values show highly non-linear behaviour. Therefore, a more flexible model capturing the complexities of these independent variables should be constructed. In this thesis, initially, principal component analysis (PCA) is applied to identify main independent variables that affect felt intensity. Based on the results of PCA and expert knowledge, various artificial neural network (ANN) models are built. Feedforward backpropagation method is used with different combinations of input variables to study the best predictions of MMI. Most of the ANN models resulted in better MMI estimations than those provided in the literature.

Keywords: Modified Mercalli Intensity (MMI), Principal Component Analysis, Artificial Neural Network Method, Seismic Ground Motion

ÖZ

YAPAY SİNİR AĞLARI METHODU İLE YER HAREKETİ PARAMETRELERİ KULLANILARAK DEPREM ŞİDDETİNİN TAHMİN EDİLMESİ

Öztürk, Seda
Yüksek Lisans, Deprem Çalışmaları
Tez Danışmanı: Prof. Dr. Ayşegül Askan Gündoğan
Ortak Tez Danışmanı: Prof. Dr. Elçin Kentel Erdoğan

Aralık 2019, 122 sayfa

Depremler, yer yüzeyinin doğası gereği tektonik plakalardan oluşması sebebiyle yer sarsıntısına ve deformasyonlara neden olan doğal olaylardır. Tektonik plakalardaki ani enerji salımı sebebiyle depremler meydana gelmektedir. Yer sarsıntısını ölçmenin yollarından biri makrosismik (veya hissedilen) şiddettir. Hissedilen şiddet ile yer hareketi parametreleri arasındaki korelasyon hakkında değişik çalışmalar vardır. Aralarındaki ilişkiyi ampirik denklem formunda bulmak için, çalışmaların çoğu lineer regresyon metodu içermektedir. Fakat, lineer korelasyon varsayımı, şiddet değerlerini etkileyen bağımsız değişkenlerin yüksek derecede lineer olmayan davranış göstermesi sebebiyle en iyi çözüm olmayabilir. Bu yüzden, bağımsız değişkenlerin karmaşıklığını yakalayan daha esnek bir model oluşturulmalıdır. Bu tezde, öncelikle, hissedilen şiddet değerlerini etkileyen esas bağımsız değişkenler temel bileşen analizi uygulanarak belirlenmiştir. Temel bileşen analizi ve uzman görüşleri sonucunda, çeşitli yapay sinir ağı modelleri kurulmuştur. Farklı kombinasyonlardaki girdi değişkenleri ile ileri beslemeli bir yapay sinir ağları mimarisi ve geri yayılım öğrenme metodu kullanılarak en iyi MMI tahminleri üzerine çalışılmıştır. Geliştirilmiş olan ANN modellerinin neredeyse hepsinin MMI tahminleri litratürde sunulmuş olanlardan daha iyidir.

Anahtar Kelimeler: Değiştirilmiş Mercalli Şiddeti (MMI), Temel Bileşen Analizi, Yapay Sinir Ağları Metodu, Sismik Yer Hareketi

To my love, Cemal …

ACKNOWLEDGEMENTS

Preparing this thesis is not an easy task for me. I have encountered many challenges throughout this journey. The support and contributions of some people should not be ignored. Hence, I would like to thank those people who have made me overcome this challenge and always supported me within this time.

First and foremost important, I would like to express my deepest gratitude to my supervisor, Prof. Dr. Ayşegül Askan. There is so much to talk about her efforts on me. She always encouraged me in every tough situation I have been through. Her patience and guidance throughout this thesis always motivated me. Her vision and thoughts helped me to improve my academic and also my personal life.

Secondly, I would like to express my sincere thanks to my co-supervisor Prof. Dr. Elçin Kentel Erdoğan for her invaluable guidance and supervision. Her dedication, patience, and knowledge helped me in all the time of my research and writing the thesis.

Without my supervisors' help, this thesis would not have been possible.

Besides, I would like to thank my committee members, Prof. Dr. Altuğ Erberik, Assoc. Prof. Dr. Mustafa Koçkar, and Assist. Prof. Dr. Onur Pekcan for their support, suggestions and encouragement.

I would like to thank my family, my dad, my mom and my sister for their valuable support and patience throughout my study. Their presence always gave me strength.

I am very thankful to my best friend, Merve Alımlı for always being by my side, listening and sharing my joy or sadness.

I would like to sincerely thank to my project manager, Mr. Alp Yağcıoğlu from Temelsu International Engineering Services Inc. for his patience and support in that time.

Finally and most importantly, I would like to sincerely thank my dearest husband for his patience in that time. The pep-talks that you have said to me every time I get lost gave me the strength to carry on. Thank you for being in my life and by my side.

TABLE OF CONTENTS

LIST OF TABLES

TABLES

LIST OF FIGURES

FIGURES

LIST OF ABBREVIATIONS

ABBREVIATIONS

ANN	:	Artificial Neural Network
BNN	:	Biological Neural Network
PCA	:	Principal Component Analysis
FD	:	Focal Depth
Repi	:	Epicentral Distance
SC	:	Soil Class
Ia	:	Arias Intensity
D_{5-95}	:	Time intervals between 5-95% of IA- Significant Duration
MMI	:	Modified Mercalli Intensity
PGA	:	Peak Ground Acceleration
PGV	:	Peak Ground Velocity
PGD	:	Peak Ground Displacement
PSA	:	5% Damped Pseudospectral Acceleration
Sa	:	Spectral Acceleration
CAV	:	Cumulative Absolute Velocity
Mw	:	Moment Magnitude
NEHRP	:	National Earthquake Hazards Reduction Program
Vs30	:	The average shear-wave velocity in the top 30 m, based on travel time from the surface

SPSS	: Statistical Package for the Social Sciences
MSE	: Mean Square Error

LIST OF SYMBOLS

SYMBOLS

p	:	number of variables
n	:	number of samples
x_{ij}	:	measured data
$\overline{X_{ij}}$	:	mean value of data
λ_j	:	eigenvalue of j^{th} element
v_j	:	eigenvector of j^{th} element
PC	:	Principal Component
R	:	Correlation matrix
r_{jk}	:	Correlation Coefficient between x_j and x_k
v_{oj}	:	bias value between input and hidden nodes
v_{ij}	:	connection weight between input and hidden nodes
w_{ok}	:	bias value between hidden and output nodes
w_{jk}	:	connection weight between hidden and output nodes
α	:	learning rate
N_h	:	number of hidden neurons in the hidden layer

CHAPTER 1

INTRODUCTION

1.1. Introduction

Earthquakes are natural phenomena that cause ground shaking and deformations due to the nature of the Earth's surface, which is composed of tectonic plates. The sudden release of energy on these tectonic plates results in earthquakes.

There are both subjective and objective measurements to determine the level of ground shaking during a specific earthquake. Measured (instrumental) peak ground motion parameters such as peak ground acceleration or velocity are well-known objective measurements of an earthquake. On the other hand, macroseismic (or felt) intensity is a subjective measurement to classify the earthquake effects based on both human responses and technical observations in the field. Since the ground motion networks are expanding all over the world, the use of objective measures of ground motions has been on the rise. Interestingly, subjective measures, despite their inherent bias and uncertainty, have also regained their historical popularity mostly due to their use in shaking maps in terms of felt intensity (e.g., Wald et al. 1999, AFAD-RED). These maps are used all over the world to determine the meizoseismal area of an earthquake for purposes of immediate disaster response as well as long-term management.

Among various existing intensity scales, the most common ones are the Modified Mercalli Scale (MMI), the European Macroseismic Scale (EMS-98), and the Japanese Meteorological Agency Scale (JMA). According to Musson and Cecić (2012), the MMI scale goes back to the studies of Wood and Neumann (1931), Sieberg (1932), and Richter (1958). The current version mostly belongs to Stover and Coffman (1993).

The MMI scale ranges between I to X, starting from no damage to significant structural damage in the built environment. Appendix A shows the detailed description of the MMI scale. Seismic intensity is significantly dependent on several objective variables such as earthquake magnitude, distance from the earthquake source, soil type, population intensity, building type as well as subjective factors that influence the degree of shaking as reported by humans.

The shaking maps make use of correlations between MMI and instrumental ground motion parameters. Thus, it is essential to mathematically relate these measures of ground shaking to each other. Globally, there has been a major interest in the study of potential correlations between felt intensity and ground motion parameters. A common approach is to use linear regression techniques to find an empirical formula for such relations. However, to find the felt intensity value from different objective measurements assuming a linear correlation between them is not the best approach since the parameters exhibit highly non-linear behavior in nature. Therefore, a more flexible model that could consider potential nonlinearities should be constructed.

Artificial Neural Network Method (ANN) is one of the non-parametric approaches which has been used in many fields. Different than the traditional regression technique, ANN does not convert the input parameters to output value using a parametric (or closed) form, yet it analyses the relations between observed inputs of a system and observed outputs in detail and provides a black-box model that relates inputs to outputs.

The main objective of this study is to develop an ANN model that estimates MMI using measured or computed ground motion parameters. The prerequisite for obtaining this relationship is a dataset comprising of detailed information on previous earthquakes with different ground motion parameters, and the corresponding felt intensity values at locations close to the recording stations. ANN then is trained using these datasets to yield the requested felt intensity value when the selected ground motion parameters are used as inputs.

1.2. Scope and Outline of the Thesis

The scope of this thesis is to study the relationships between felt intensity and various measured or computed ground motion parameters. For this purpose, initially, PCA is performed to study the potential correlations between MMI values and various ground motion parameters. Later, ANN Method is used with selected independent parameters from PCA analysis together with expert knowledge to estimate felt intensity from ground motion parameters.

In Chapter 2, a literature survey is presented, and previous related studies are discussed. Then, previous applications related to PCA and ANN methods are summarized.

In Chapter 3, the details of PCA and ANN methods are described.

In Chapter 4, the seismological parameters that are used in this study are defined, followed by a description of the dataset. Then, applications of PCA and ANN methods are presented, and results are discussed.

Finally, in Chapter 5, summary and conclusions are presented. Recommendations for further studies are also listed in order to advance and improve this study in the future.

CHAPTER 2

LITERATURE REVIEW

2.1. Introduction

In this study, Principal Component Analysis and Artificial Neural Network methods are used in order to study the relations between felt intensity and instrumental ground motion parameters. Both methods have been used in various applications as part of engineering studies. In the following sections, a literature review of related previous studies is presented. In addition, a few past studies on correlations of felt intensity and seismic ground motions are explained.

2.2. Previous Applications of Principal Component Analysis

Although the finance sector is the field that employs this analysis most frequently, it is also used in engineering. Some recent engineering applications of PCA are briefly described here.

Iyengar (1983) analyzed 92 earthquake records from the California region with Principal Component Analysis in order to classify and reduce the 12 ground motion parameters into two principal components. The ground motion parameters used in that study are Richter magnitude and duration of the earthquake, peak ground acceleration, peak ground velocity, and peak ground displacement in horizontal direction, time to the peak horizontal acceleration, ratio of the peak ground acceleration in two horizontal directions, ratio of the vertical peak ground acceleration to the horizontal peak ground acceleration, epicentral distance, soil conditions, maximum of the pseudo relative velocity response spectra, and rate of the zero crossing of the horizontal component. Based on the results of PCA, earthquake records are divided into nine regions in a 2-D principal component plane. Moreover, using PCA, the authors developed an approach for classification and rating of strong motion records in order to analyze the damaging nature of the corresponding earthquakes.

In this study, nine different seismic parameters are selected, which can potentially be used for estimating the felt intensity values. However, these seismic parameters (independent variables) have different effects on the output value. Therefore, in order to eliminate the least effective parameters, PCA analysis is used. The methodology and application of PCA are described in Chapters 3 and 4, respectively.

Nyugen et al. (2017) used PCA to study damage detection in a bridge located in Luxembourg, where artificial damage is applied, and the corresponding changes were monitored for a short-term period. It was observed that ambient temperature could affect the degree of the damage. PCA was applied in order to discriminate the temperature variations in the bridge from the changes related to artificial damage.

2.3. Previous Applications of Artificial Neural Network

There are numerous types of artificial neural network approaches which has been used all over the world. In the field of civil engineering, artificial neural network is used for solving many problems involving prediction of pile capacity as in Teh et al. (1997); liquefaction problems as in Tolon and Ural (2012); classification of soils as in Elarabi et al. (2008); design of underground structures as in Ornthammarath et al. (2008); river flow prediction as in Imrie et al. (2000) or estimating the earthquake performances of buildings as in Arslan et al. (2012). In earthquake engineering, even though there are not as many examples yet, below are some of the applications of neural network method.

Günaydın (2008) studied the prediction of Peak Ground Acceleration (PGA) from various ground motion parameters using an artificial neural network method. Three different ANN methods namely feed-forward backpropagation, radial basis function and generalized regression neural network methods, were used. A total of 95 earthquake records from 15 earthquakes in Turkey in between 1999 and 2001 were used in that study. From these 95 records, 72 were used as training and 23 were used for testing of the analysis. The input parameters were moment magnitude, focal depth, hypocentral distance, and soil conditions. Among the alternative approaches, the feed-forward backpropagation method showed the best performance in terms of the highest R^2 value and the smallest error value.

Tselentis and Vladutu (2010) compiled a ground motion dataset of 310 records from 151 earthquakes in Greece in order to find a relationship between MMI and different seismic parameters such as PGA, PGV, Arias Intensity, acceleration response spectrum, and cumulative absolute velocity using neural networks and genetic algorithms. A combination of ANN and genetic algorithm technique is used, and the model including PGA, Arias intensity, cumulative absolute velocity, moment magnitude, and the focal depth is selected with minimum root mean square error (RMS) value. After the selection of the input values, linear regression analysis is made to find a formula between MMI and the seismic parameters. The performance of the relationship is tested, and the results showed satisfactory results.

Alvarez et al. (2012) carried out a study with a database of 843 ground motion records from 63 earthquakes to predict MMI from PGA, PGV, moment magnitude, and epicentral distance. Three different nonlinear statistical algorithms were used which are support vector regression, artificial neural network, and genetic programming. In addition to the study of nonlinear relationships, a robust linear regression relationship was provided to make a fair comparison with the nonlinear algorithms. The results showed that the neural network method resulted in closer predictions than the other nonlinear methods. Moreover, all the nonlinear techniques yielded better predictions than linear regressions.

Narayanakumar and Raja (2016) worked with Himalayan earthquakes in order to predict the earthquake magnitude (Richter scale) with selected seismicity parameters as input variables. The feed-forward backpropagation method was used with a three-layer structure. The results showed that this structure yield better results for the smaller events with magnitudes between 3 and 5.

In most of the previous studies on predicting felt intensity values, linear functional forms are used, yet the seismic parameters have non-linear behavior. Therefore, in this thesis, Artifical Neural Network Method is used to study the complex relationships between MMI and selected instrumental ground motion parameters. Previous studies mentioned in the literature review (Tselentis and Vladutu, 2010 and Alvarez, 2012) have some similar research with this study. T6yHowever, in this study, earthquake dataset in Turkey is used in the ANN analysis to find a relation between MMI and different seismic parameters. Moreover, additional parameters are included in the analysis such as PGD, Ia, epicentral distance, and focal depth.

2.4. Previous Applications on the Relationship between Felt Intensity and Instrumental Ground Motion Parameters

There are numerous studies all over the world on the correlation of felt intensity with seismic parameters. In this section, selected studies from the literature are briefly described.

In their pioneering study, Trifunac and Brady (1975) worked with 187 strong-motion accelerograms from 57 earthquakes that occurred in the Western United States. The authors used peak ground acceleration, peak ground velocity, and peak ground displacement as strong ground motion input to regression analyses in order to find a correlation between MMI and these parameters. This study showed that local site conditions were effective on intensity values and soil class could be employed in the future correlation equations as an independent parameter.

Soon after, Murphy and O'Brien (1977) made intensity predictions using epicentral distance (R_{epi}), local magnitude (M_L), the geographical region, and earthquake duration as independent variables. The authors suggested that using a filtered PGA dataset reduced the uncertainties and gave a more reliable correlation between intensity and PGA.

Further studies suggested that Peak Ground Velocity (PGV) may be a good parameter for MMI prediction instead of or in addition to PGA. Wald et al. (1999) studied 8 moderate to large earthquakes which occurred in California namely the 1971 San Fernando earthquake (Mw=6.7), the 1979 Imperial Valley earthquake (Mw=6.6), the 1986 North Palm Springs earthquake (Mw=5.9), the 1987 Whittier Narrows earthquake (Mw=5.9), the 1989 Loma Prieta earthquake (Mw=6.9), the 1991 Sierra Madre earthquake (Mw=5.8), the 1992 Landers earthquake (Mw=7.3) and the 1994 Northridge earthquake (Mw=6.7). The authors found a correlation between felt intensity and PGA or PGV using regression analysis. The results showed that PGA correlates well with low MMI intensities, whereas PGV correlated well with higher MMI intensities. The findings of Wald et al. (1999) have accelerated the intensity prediction studies worldwide.

Atkinson and Sonley (2000) studied 29 California earthquakes with Mw=4.9-7.4 in order to find a correlation between MMI and Pseudo Spectral Acceleration (PSA). The results showed that while magnitude affected the relationship between MMI and PSA for low frequencies, distance had an effect on the corresponding relationship for higher frequencies.

Boatwright et al. (2001) employed a dataset of 66 records from the 1994 Northridge earthquake (Mw=6.7) to find a correlation between intensity and selected ground motion parameters such as PGA, PGV, and PSA. Regression analysis results showed that the correlation between MMI and PGV and PSV was better than that with PGA.

Arıoğlu et al. (2001) proposed the first local relationship for Turkey using a database consisting of 14 peak ground motions from the 17 August 1999 Kocaeli earthquake to find a relationship between MMI and maximum PGA with regression analysis technique. This relationship was then compared with that of Wald et al. (1999). It is observed that the latter relationship yielded smaller MMI values. This difference most probably resulted from the different characteristics of the building stocks in California and Turkey. Despite being the first attempt for Turkey, the study has some inherent limitations due to the use of a limited dataset.

Wu et al. (2004) proposed correlations between intensity, earthquake loss, and several ground motion parameters for the 1999 Chi-Chi earthquake with regression analysis. For the earthquake loss analysis, PGA and SA (at 1 s period) were the parameters that gave a higher correlation. However, for the intensity estimations, PGV and SA (at 1 s period) values gave more reliable values within the broad magnitude range. PGA was not found to be stable for smaller earthquakes in the intensity estimations.

Kaka and Atkinson (2004) developed various relationships between MMI and PGV as well as PSA using data from 18 earthquakes in North America with standard least squares regression technique. In addition to comparisons with previous regional studies, this study was verified with the ShakeMap application against the observed shaking map of the earthquake.

Afterward, Atkinson and Kaka (2006) defined a relationship between MMI and PGV in the New Madrid region with regression analysis. This study suggested that including magnitude and distance as independent variables could decrease the standard deviation of the model.

Atkinson and Kaka (2007) proposed a new equation from moderate earthquakes in the central United States (CUS) region applicable to higher intensities.

Tselentis and Danciu (2008) developed new relationships between MMI and ground motion instrumental records such as PGA, PGV, PGD, Ia (Arias Intensity), and Cumulative Absolute Velocity (CAV). The dataset covered 89 earthquakes from Greece. The authors proposed two sets of predictive equations: The first set involved simple equations between MMI and selected ground motion parameters with a weighted least-squares regression technique. In the second set, magnitude, epicentral distance, and local site conditions were also integrated into the model as independent variables. The results showed that, in the first set of equations, PGA gave better results than any other ground motion parameters. The second set showed that local site effects had a small effect on MMI, while magnitude and epicentral distance had more significant effects.

Faenza and Michelini (2010) used the orthogonal distance regression technique with 266 data pairs to find a correlation between MCS Intensity with PGV and PGA. The relations were verified with USGS-ShakeMap (via https://earthquake.usgs.gov/) application.

Yaghmaei-Sabegh, Tsang, and Lam (2011) worked on a ground motion-intensity database which consists of records from events with Mw>6.0 and Repi<250 km. Their results showed that PGV was in good correlation with MMI than were PGA and PSA. The model was found to be highly dependent on the region. The results of this study were consistent with those of Atkinson and Kaka (2007).

Bilal and Askan (2014) developed two sets of predictive relationships for MMI with a linear least-squares regression method. The first set is between MMI and PGA, as well as between MMI and PGV. The database consisted of 92 peak ground motion parameters (PGA and PGV)- MMI pairs from 14 earthquakes with 5.7<Mw<7.4. The results showed that PGA was a more reliable parameter for MMI than PGV since the damaged buildings in Turkey are rigid structures of which the damage is better correlated with PGA than PGV. The authors proposed a second set of equations, which are more refined equations between MMI and PGA/PGV, Mw, Repi. However, this second set of equations is more complex, and they include higher modeling errors. Comparisons with the previous studies showed that intensity relationships are dependent highly on the geographical region due to the dependence of MMI on both regional seismicity and local building styles. The simple set of equations of Bilal and Askan (2014) are the most recent MMI prediction equations for Turkish earthquakes.

As mentioned previously, the MMI values are affected by multiple seismic variables, including moment magnitude, PGA, PGV, SA, soil conditions, Arias Intensity, significant duration, epicentral distance, and focal depth. In order to better predict the felt intensity value, these parameters must be evaluated and should be included as an input value if necessary, mathematically. In this thesis, the most effective parameters are determined using the PCA method to be included in the prediction equation of felt intensity. Most of the previous studies including Arıoğlu et al. (2001) and Bilal and Askan (2014) used linear regression analysis technique which may not fully describe the potential nonlinear relationships between MMI and the mentioned seismic parameters. Therefore, in this thesis, an artificial neural network technique will be used with a larger dataset from Turkish earthquakes to predict MMI from different sets of inputs composed of seismic parameters mentioned above.

CHAPTER 3

METHODOLOGY

3.1. Principal Component Analysis

The main purpose of PCA is to decrease the dimensionality of a dataset that includes interrelated variables while keeping the variation in the dataset as much as possible (Jolliffe, 2002). This can be established by transforming the dataset to a smaller set of uncorrelated attributes that explain most of the variation. Its primary purpose is to decrease a broader set of variables into a smaller set of variables called principal components.

These principal components are, in fact, a linear combination of the original dataset predominantly altered according to the variation scores in the orthogonal dimension (Bohm and Zech, 2010). With the help of this technique, one could reduce the data and visualize it easily. Moreover, identification of the principal components will guide input selection for the ANN Model and improve the quality of the ANN results.

In PCA, the first principal component has the highest variation while the second principal component has the second-highest variation in the data. All of the components are orthogonal with each other. Although the components account for one hundred percent variance as a total, most of the variance is found in the first few variables. For this reason, the data can be described by fewer variables, and the rest of the components may be accepted as unimportant.

3.1.1. Stepwise Explanation of Principal Component Analysis

The flowchart of PCA is given in Figure 3.1 where the steps are explained in detail.

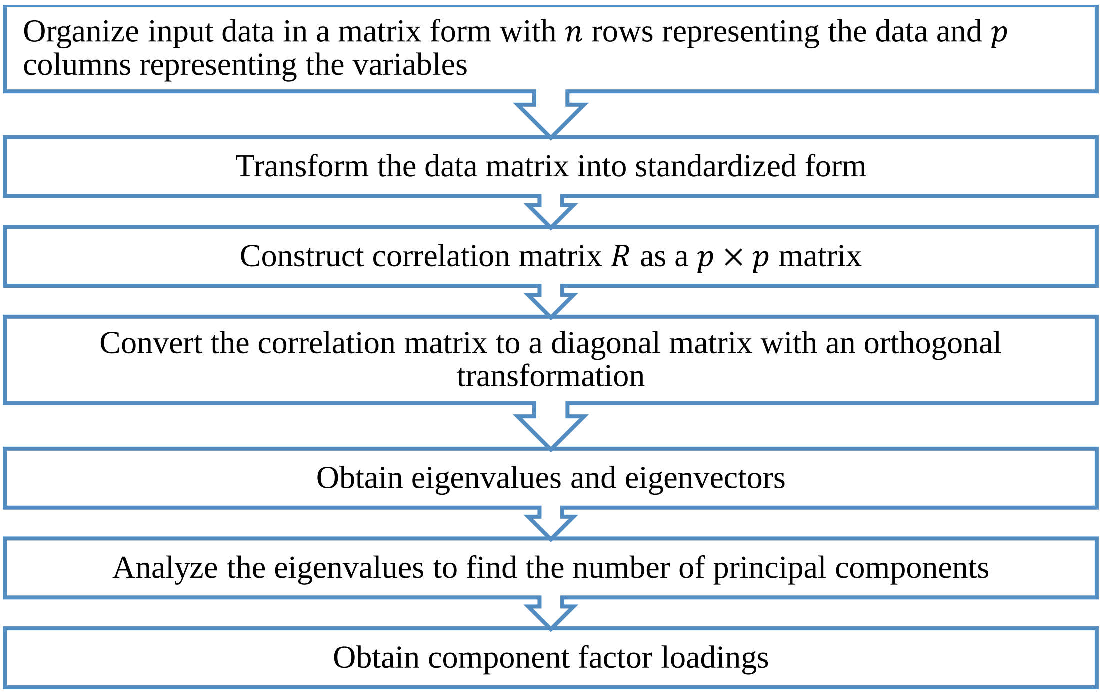

Figure 3.1. Flowchart of Principal Component Analysis

The first step in PCA is to organize the data in a matrix form where columns represent the variables, and rows represent the number of samples. Equation 3.1 shows a sample matrix composed of p columns and n rows:

$$X = \begin{pmatrix} x_{11} & \cdots & x_{1p} \\ \vdots & \ddots & \vdots \\ x_{n1} & \cdots & x_{np} \end{pmatrix} \tag{3.1}$$

where x_{ij} is the measured data, i is the index for the variable $i = 1,2 \ldots, n$, and j is the index for the sample number and $j = 1,2, \ldots, p$.

The next step is to convert the original matrix to a standardized form so that all the data in the matrix is in the same range where mean and variance are zero and one, respectively. If the PCA is performed with variables which have different units, it is necessary to standardize the data.

Standardization can be done as follows:

$$X_s = \begin{pmatrix} (x_{11} - \overline{x_1})/\delta_1 & \cdots & (x_{1p} - \overline{x_p})/\delta_p \\ \vdots & \ddots & \vdots \\ (x_{n1} - \overline{x_1})/\delta_1 & \cdots & (x_{np} - \overline{x_p})/\delta_p \end{pmatrix} \tag{3.2}$$

where

$$\overline{x_j} = \frac{1}{n}\sum_{i=1}^{n} x_{ij}\ , \forall j \tag{3.3}$$

$$\delta_j{}^2 = \frac{1}{n-1}\sum_{i=1}^{n} (x_{ij} - \overline{x_j})^2\ , \forall j \tag{3.4}$$

The third step is to obtain the correlation matrix according to:

$$R = \frac{1}{n-1} X_s{}^T X_s = \begin{pmatrix} 1 & \cdots & r_{1p} \\ \vdots & \ddots & \vdots \\ r_{p1} & \cdots & 1 \end{pmatrix} \tag{3.5}$$

$$r_{jk} = \frac{\delta_{jk}}{\delta_j \delta_k} = \frac{\sum_{i=1}^{n}[(x_{ij} - \overline{x_j})(x_{ik} - \overline{x_k})]}{\sqrt{\sum_{i=1}^{n}(x_{ij} - \overline{x_j})^2}\sqrt{\sum_{i=1}^{n}(x_{ik} - \overline{x_k})^2}}\ \forall i, j \tag{3.6}$$

where r_{jk} is the correlation coefficient between x_j and x_k. $r_{jk} = 1$ whenever j=k.

The result of the correlation matrix is a $p \times p$ symmetric positive matrix. The diagonal elements are equal to 1 due to the normalization.

To represent the correlation matrix with directions and magnitudes (vectors) and also to get rid of the redundant elements, the correlation matrix needs to be diagonalized:

$$R \to V^T R V = diag(\lambda_1 \cdots \lambda_p) \tag{3.7}$$

The uncorrelated feature vectors in the rotated space $y_i = \{y_{i1}, \cdots y_{ip}\}$ are given as:

$$y_i = V^T x_i \, , x_i = V y_i, \forall i \tag{3.8}$$

The next step is to obtain the corresponding eigenvalue and eigenvectors. In order to do that, the following linear equation needs to be solved:

$$\left(R - \lambda_j I\right) v_j = 0 \text{ for } j = 1,2, \ldots , p \tag{3.9}$$

where λ_j is the eigenvalue and v_j is the corresponding eigenvector of the correlation matrix, R. The solution is as follows:

$$R v_j = \lambda_j v_j \text{ for } j = 1,2, \ldots , p \tag{3.10}$$

$$\det(R - \lambda I) = 0 \tag{3.11}$$

where p is the number of eigenvalues that are obtained from the solutions of the characteristic equation (Equation 3.11). The eigenvectors are calculated from Equation 3.9 after inserting the related eigenvalue into the equation. The rotation matrix V is obtained by taking the eigenvectors v_j as its columns:

$$v_{kj} = (v_j)_k \tag{3.12}$$

Rearranging the eigenvalues from the highest to the lowest gives the principal components of the correlation matrix. The first principal component is the first eigenvalue, which gives the most variation. The second principal component value is the second eigenvalue, and so forth. Considering the principal component values in the 2-D axis system, assuming that two of the principal components give the most variance in the original dataset, the first principal component lies in the x-axis, whereas the second PC lies in the y-axis which is the orthogonal axis.

The eigenvalues represent the variances of the data concerning the principal axes since they are the diagonal elements in the correlation matrix. A small eigenvalue means that the projection of the data on the axis has a narrow distribution. Therefore, the related component is of a small contribution to the data and may be ignored (Bohm and Zech, 2010). Similarly, large eigenvalues mean the related component is of large contribution to the data, and they belong to the important principal components.

After finding the principal components, the most crucial step is to analyze the eigenvalues to determine the number of principal components. There are two options for selecting the number of principal components. First is by looking at the eigenvalues. Table 3.1 shows a sample variance table extracted from the Statistical Package for the Social Sciences (SPSS) software indicating the eigenvalues of the principal components and their percent variance values. An arbitrary rule of thumb is to select the principal components such that their eigenvalues are greater than one (Kaiser, 1960) which is known as Kaiser criterion. According to the first column of Table 3.1, eigenvalues of the first two components can be selected as the principal components since the eigenvalues are greater than 1.

Table 3.1. *Sample Variance Table*

Total Variance Explained						
	Initial Eigenvalues			Extraction Sums of Squared Loadings		
Component	Total	% of Variance	Cumulative %	Total	% of Variance	Cumulative %
PC1	6.402	71.136	71.136	6.402	71.136	71.136
PC2	1.665	18.502	89.638	1.665	18.502	89.638
PC3	.732	8.134	97.772			
PC4	.201	2.228	100.000			
PC5	9.238E-16	1.026E-14	100.000			
PC6	3.977E-16	4.419E-15	100.000			
PC7	6.981E-17	7.757E-16	100.000			
PC8	8.253E-18	9.170E-17	100.000			
PC9	-1.939E-16	-2.155E-15	100.000			
Extraction Method: Principal Component Analysis.						

Another method for selecting the principal components is to look at the Scree Plot, which is a plot of the number of principal components versus the eigenvalues. Figure 3.2 shows a sample scree plot extracted from the SPSS software. To determine the number of principal components in the Scree Plot, the starting point of the elbow shape or the largest break between the components is used (Cattell, 1966). According to Figure 3.2, the elbow shape starts at Principal Component 2, so; one can select two principal components.

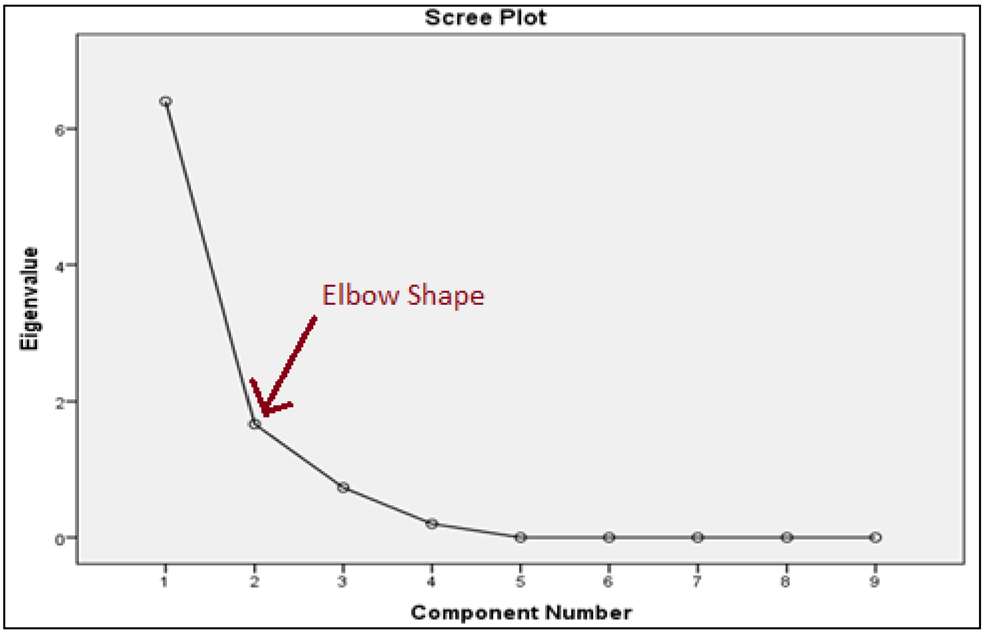

Figure 3.2. Sample Scree Plot

The next step is to obtain the factors f_{ij} by carrying out a standardization of the transformed variables y_{ij}. This is achieved with a division by the square root of the eigenvalues λ_j :

$$f_{ij} = \frac{y_{ij}}{\sqrt{\lambda_j}} \tag{3.13}$$

where i is the index for the variable $i = 1,2 \ldots, n$, and j is the index for the sample number and $j = 1,2, \ldots, p$.

The relation of the factors f_{ij} with the original data x_{ij} is defined as a linear transformation with matrix A in which the elements are called the factor loadings:

$$x_i = Af_i, \forall i \ \text{ or } X^T = AF^T \tag{3.14}$$

The idea of the PCA analysis is to reduce the number of factors so that the data can be described satisfactorily within tolerable deviations, ε:

$$x_1 = a_{11}f_1 + \cdots + a_1 f_k + \varepsilon_1$$
$$x_2 = a_{21}f_1 + \cdots + a_{2k} f_k + \varepsilon_2 \qquad (3.15)$$
$$x_P = a_{p1}f_1 + \cdots + a_{pk} f_k + \varepsilon_p$$

with $k < p$ and the factors $f_1, \ldots f_k$ are uncorrelated.

There exist some computer programs which perform the principal component analysis, do the numerical calculations, and find the component factors. In this thesis, SPSS software is used for PCA.

3.2. Artificial Neural Network Method

3.2.1. Biological Resemblance and General Information about ANN

The artificial neural network (ANN) system idea is based on the biological forms of a human brain. Inside the human brain, there is a large number (approximately 10^{11}) of connected elements called neurons (Hagan, 1996). In order to explain the artificial neural networks, one must fully understand the parts of neurons (see Figure 3.3).

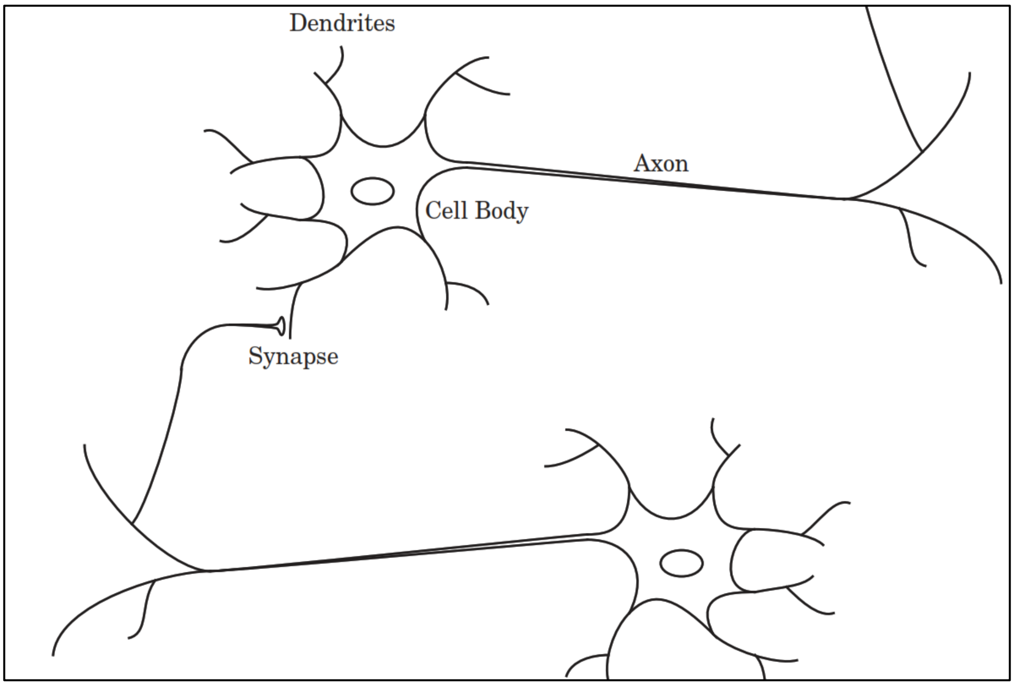

Figure 3.3. Elements of Neurons Inside the Brain (Hagan,1996)

There are three main elements of the neuron: Dendrites, axon, and cell body. Dendrites are receptors that can carry the information to the cell body. They are tree-like structures, and they get messages from other cells and transmit them to the cell body. The cell body is an ellipse-shaped structure, and it is the central part of the neuron. All the information is stored in this area. A nerve cell has a long slender fiber, which is called an axon. The objective of an axon is to get the information from the cell body and transmit it to the other neurons. Although the neurons in the body are not continuous, they can still send the information from one to another through synapses. The synapse is a structure located in between the axon of one neuron and the dendrite of another neuron, and it can pass the chemical or electrical signals from one neuron to the next (Hagan,1996). A schematic presentation of an ANN model, together with its main components, are given in Figure 3.4.

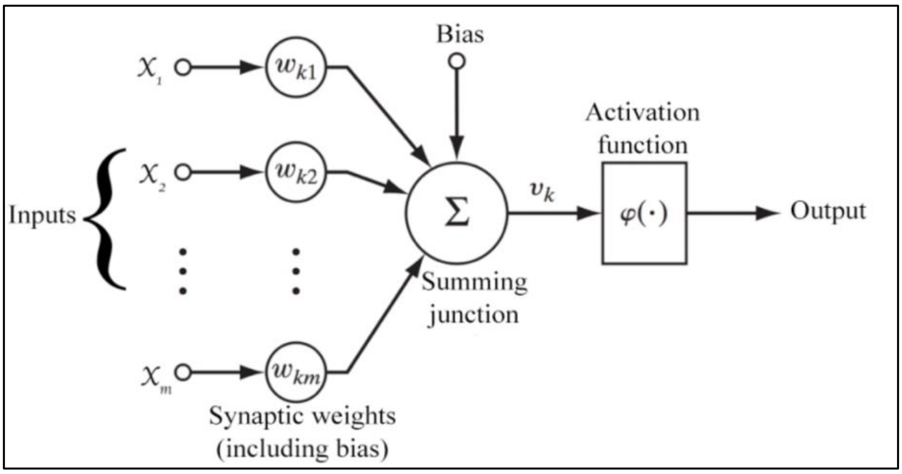

Figure 3.4. Example of an Artificial Neural Network Scheme (Haykin,2009)

Although the structure of an artificial neural network does not have the complexity of a biological neural network, there are yet some similarities between them. The main components of the ANN structure are; the nodes, the input layer, the weights, the hidden layer, summing junctions, activation functions, and the output layer (Hsu et al., 1995).

In ANN, there exist multiple nodes which imitate the neurons in the biological neural network. Nodes are organized in layers and all the nodes in the hidden layer are connected to each node in the previous layer. In ANN, information first comes to the input layer from the information environment similar to the dendrites in a biological neural network (BNN). After the input layer, the information is sent to the hidden layer with a weight function similar to the synapses in BNN. Weight function determines the strength of the connection and this function decides how much effect the input node will have on the output layer.

The hidden layer is an intermediate layer between the input and output layers. Inside the hidden layers, there are hidden neurons. The number of hidden neurons are identified for each problem considering the complexity of the problem and the number of input neurons. If there are not enough hidden neurons in the neural network, then the structure fails to learn the algorithm, and the problem can not be solved. Moreover, if there are a lot of unnecessarily hidden neurons, this will result in the memorization of the network rather than learning.

Summing junctions merges the input values with their corresponding synaptic weights by using a linear combination. After that, the activation function comes into play. The activation function or transfer function is similar to the cell body in BNN. This function aims to gather all weighted inputs and apply generally a nonlinear transformation and transfer them to determine the output layer. The output layer which is similar to the axon in BNN, takes the processed inputs from the activation function and generates the output.

Similar to biological neural networks, in artificial neural networks, information operates in a parallel fashion, which means that all nodes are processing simultaneously.

3.2.2. Classification and Network Types of ANN

There are many classification techniques in ANN. One way is to classify the network according to the number of layers, namely, single layer, bilayer, and multilayer neural network.

The most common taxonomy of the neural networks is according to its architecture. In Figure 3.5, the taxonomy of neural network architecture is given. There are two groups, mainly feed-forward networks and recurrent or feedback networks (Jain et al.,1996).

In the feed-forward neural network, the information flows in only one direction. That means the signal comes to the input layer, and later, this data is processed in the hidden layer. Finally, by processing the input values with associated weights of the connections, calculated data comes to the output layer. Therefore, in this network, the output layer is dependent only on the inputs that receive from the previous layers and corresponding weights (ASCE Task Committee, 2000a).

In feedback networks, data is travelling in both ways creating a loop that is from input layer to output layer or from output layer to the input layer. Therefore, feedback networks are dynamic, the values are changing continuously until to the balance point. Calculations are done and resultant output values feed the network by going back to the analysis (Hagan,1996). In this study, a feedforward networks are developed. Hence, this method is described in detail.

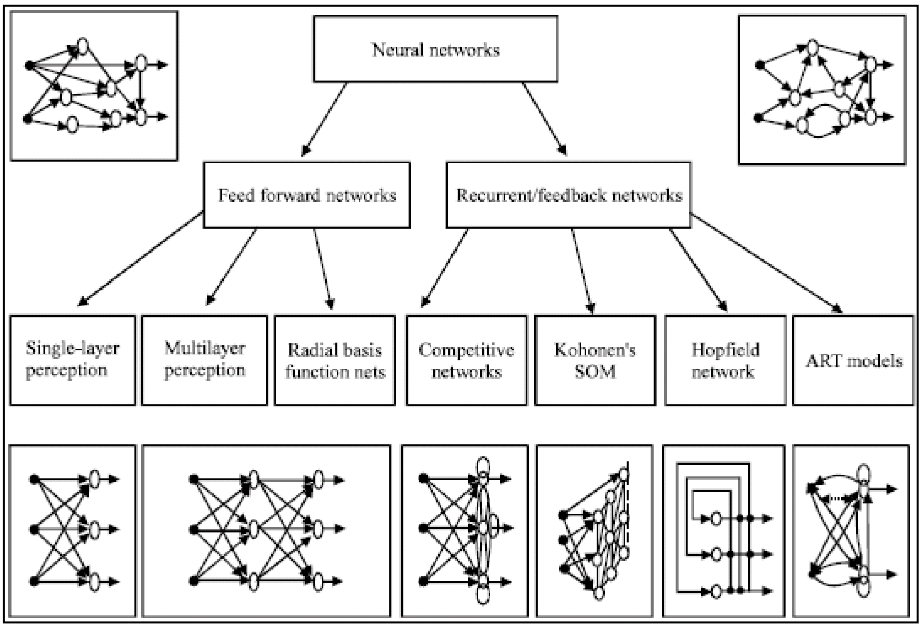

Figure 3.5. Taxonomy of Neural Network Architecture (Jain et al., 1996)

Figure 3.6 summarizes the feedforward neural network architecture. There are multiple layers in the structure. Between the layers, there are connections, and these connections have some weights. In the input layer, there is no calculation, but the information is transmitted to the hidden layer. In the hidden layers, the computations are carried out. After the computations, the information is transferred to the output layer. In a feedforward network, although there can be single input and a single output layer, there is a possibility that there can be no hidden layer (single layer perceptron) (Demuth and Beale, 2003) or multiple hidden layers.

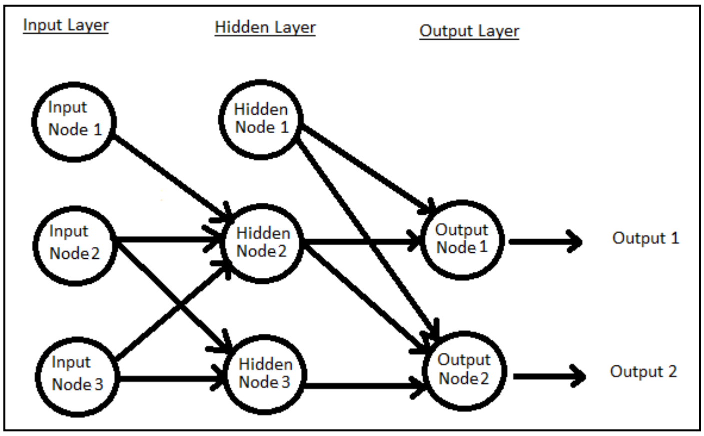

Figure 3.6. Feed Forward Network

There are also numerous network types according to the problem. In Table 3.2, different categories are shown with different network types and intended usage. Some of the networks can be used for only one category, yet some of them can be used for multiple types of problems. For example, a feed-forward backpropagation network can be used almost for all types of problems, and it is commonly used for the first four categories in the Table 3.2. Therefore, it is vital to select a network type suitable for the problem.

Table 3.2. *Network Type Selection (Anderson et. al ,1992)*

Category	**Networks**	**Intended Usage of Network**
Prediction	- Back Propagation - Delta Bar Delta - Extended Delta Bar Delta - Directed Random Search - Higher-Order Neural Networks - Self Organizing Map into Back Propagation	Prediction of output by using input values
Classification	- Learning Vector Quantization - Counter Propagation - Probabilistic Neural Network	Using input values for the classification
Data Association	- Hopfield - Boltzmann Machine - Hamming Network - Bidirectional Associative Memory - Spatiotemporal Pattern Recognition	Similar to the classification but it identifies the errors in the data
Data Conceptualization	- Adaptive Resonance Network - Self Organizing Map	Group the data having relationships via analyzing the inputs
Data Filtering	- Recirculation	Smoothen the input data

According to Table 3.2, estimation of the felt intensity from several ground motion parameters is a prediction problem. In other words, prediction of output values (MMI) from input values (such as PGA, PGV) is performed in this study. The most used algorithm for prediction is the feed-forward backpropagation method, which will be described in the below section.

3.2.3. Designing the ANN Model

3.2.3.1. Feed-Forward Back Propagation Algorithm

In the feed-forward backpropagation algorithm, there is one input layer, one or more hidden layers, and one output layer. In each layer, one or more neurons are present. Calculation steps of the feed-forward backpropagation are summarized below (ASCE Task Committee, 2000):

ANN architecture:

- Identify the input variables
- Determine the number of neurons in the hidden layer using trial and error

Feed-Forward:

- Initialize weights using random small numbers
- Feed input values to the nodes of the input layer ($X_i, i = 1,2,..,n$)
- Propagate values to the hidden layer and then to the output layer using weights. This is achieved through repeating the following procedure until the termination criteria is satisfied:
  - Sum input signals reaching to each hidden neuron

$$Zin_j = v_{oj} + \sum x_i\, v_{ij} \text{ for } i = 1,2,..,n \tag{3.16}$$

where v_{ij} is the connection weight between input and hidden nodes, and v_{oj} is the bias value, i is the number of input nodes, and j is the number of hidden nodes. The output signal is computed with the application of the activation function, f (i.e., hyperbolic tangent, sigmoid, etc.)

$$Z_j = f(Zin_j) \tag{3.17}$$

and this signal is sent to the next layer (e.g., the output layer if there is only one hidden layer).

- Sum each weighted input signal at the output neuron

$$Yin_k = w_{ok} + \sum z_j \, w_{jk} \text{ for j} = 1,2,..,p \qquad (3.18)$$

where w_{ok} is the bias and w_{jk} is the connection weight between hidden and output nodes, k is the number of output nodes.

Output signal is computed with the application of the activation function, f_2 (i.e., hyperbolic tangent, sigmoid, etc.).

$$Y_k = f_2(Yin_k) \qquad (3.19)$$

Back-propagation of error :

- Each output neuron generates an output, y_k related to the input training pattern, and the error term is computed using the observed target, t_k (Equation 3.20). Later, with that error term, weight correction terms to update w_{jk} (see Equation 3.21), and bias correction terms to update w_{ok} (see Equation 3.22) are computed and δ_k values are sent to the nodes in the previous layer.

$$\delta_k = (t_k - y_k) f'(Yin_k) \qquad (3.20)$$

$$\Delta w_{jk} = \partial \delta_k Z_j \qquad (3.21)$$

$$\Delta w_{ok} = \alpha \delta_k \qquad (3.22)$$

where α is the learning rate.

- Each hidden neuron sums the delta values (see Equation 3.23), and multiplies with the derivative of the activation functions to calculate the error term (Equation 3.24). Later, weight correction terms to update v_{ij} (see Equation 3.25), and a bias correction terms to update v_{oj} (see Equation 3.26) are computed from the error term.

$$\delta in_j = \sum \delta_k \, w_{jk} \text{ for } k = 1,2,..,m \tag{3.23}$$

$$\delta_j = \delta in_j f'(Zin_j) \tag{3.24}$$

$$\Delta v_{ij} = \partial \delta_j x_i \tag{3.25}$$

$$\Delta v_{oj} = \alpha \delta_j \tag{3.26}$$

Update weights and biases :

- Bias and weights are updated for each output neuron

$$w_{jk}(updated) = w_{jk}(old) + \Delta w_{jk} \quad \text{for } j = 0,1,..,p \tag{3.27}$$

- Bias and weights are updated for each hidden neuron

$$v_{ij}(updated) = v_{ij}(old) + \Delta v_{ij} \quad \text{for } i = 0,1,..,n \tag{3.28}$$

There are various transfer functions in ANN, yet in multilayer networks, generally, the functions in Equation 3.29, 3.30 and 3.31 are used. In Figure 3.7, an example showing the transfer functions is shown.

Sigmoid Function:

$$f(x) = \frac{1}{1 + e^{-x}} \tag{3.29}$$

Hyperbolic Tangent Sigmoid Function:

$$f(x) = \frac{2}{1 + e^{-2x}} - 1 \tag{3.30}$$

Linear: $f(x) = x$ (3.31)

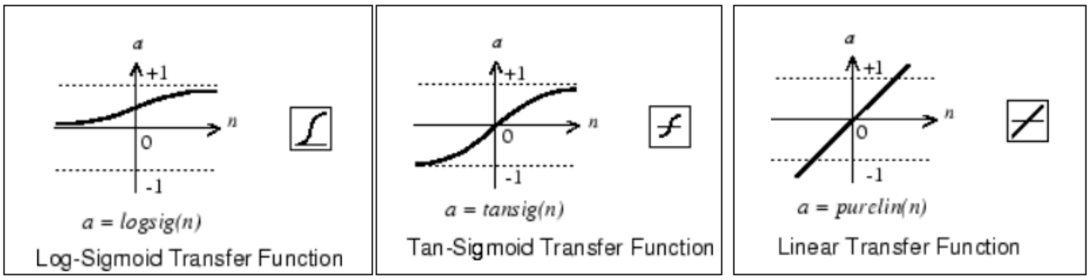

Figure 3.7. Example of Transfer Functions (Demuth and Beale, 2003)

In ANN analysis, selecting the number of hidden neurons is an essential procedure since increasing the hidden neurons a lot may result in overfitting. There are various empirical relationships from different studies to determine the number of hidden neurons. For instance, Hecht-Nielsen (1987) suggested an empirical formula for the upper limit of the number of hidden neurons:.

$$N_h = 2 * N_i + 1 \tag{3.32}$$

where N_h is the number of hidden neurons in the hidden layer, N_i is the number of inputs.

Also, there is a lower bound for the determination of hidden layers. Lai (1997) suggested that a minimum number of hidden neurons is equal to the number of inputs. In this study, as a starting point, the lower bound suggested by Lai (1997) is used. Then, a trial and error procedure is followed to find the most suitable number of hidden nodes.

CHAPTER 4

CASE STUDY FOR TURKEY: RELATIONSHIP BETWEEN MMI AND SELECTED PARAMETERS

4.1. Introduction

In this Chapter, the relationships between MMI and selected seismic parameters are studied for Turkey. Initially, the available data is briefly described followed by the definitions of the parameters. Then, results of principal component analysis and artificial neural network method are presented.

4.2. Available Data

In this study, correlations of MMI with several seismic parameters are studied. Thus, available MMI values are paired with the seismic parameters from earthquakes in Turkey. Focal Depth, Moment Magnitude (Mw), Epicentral Distance (Repi) parameters regarding each earthquake and 30 m-average shear wave velocity (Vs30) as well as latitude and longitude values of each station are directly downloaded from the Strong Ground Motion Database of Turkey (http://kyhdata.deprem.gov.tr). This is a national data portal with data from a total of approximately 750 equipped stations all over Turkey.

The dataset in this thesis is composed of 195 ground motion records from 18 earthquakes covering a range of moment magnitude values from 5.1 to 7.4 (Figure 4.1).

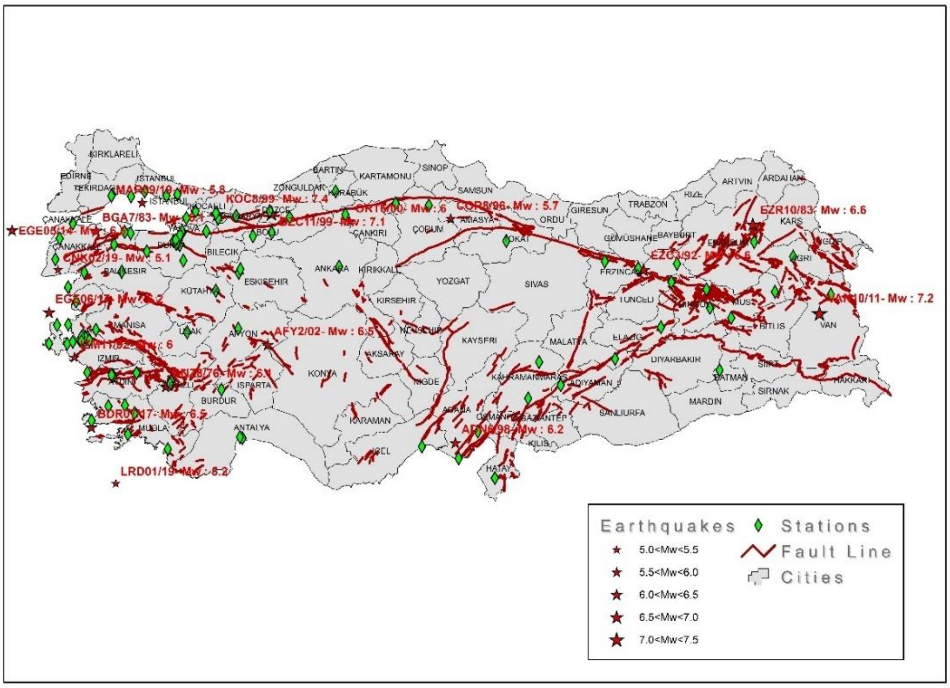

Figure 4.1. Locations and magnitudes of earthquakes and corresponding recording stations used in this thesis

Raw accelograms corresponding to these earthquakes are downloaded from the mentioned strong motion data portal. In order to produce different ground motion parameters, a series of computations are made. MATLAB software is used for that purpose where PGA (cm/s^2), PGV(cm/s), PGD (cm), Arias Intensity (cm/s), Significant Duration (sec) values are extracted from the code. The code employed in this thesis is given in Appendix B.

Among those 195 ground motion records, 92 are gathered from the study of Bilal and Askan (2014). Raw ground motion dataset (PGA, and PGV values) is obtained from the database of Prime Ministry Disaster and Emergency Management Presidency (http://daphne.deprem.gov.tr). For the calculation of other seismic parameters (PGD, Arias Intensity, and Significant Duration), the MATLAB code given in Appendix B is used. Intensity dataset of Bilal and Askan (2014) was collected from the unpublished bulletins and maps prepared by the Earthquake Research Department of AFAD.

The additional intensity data in this thesis are gathered from the USGS Earthquake Hazards Program which is a part of the National Earthquake Hazards Reduction Program (NEHRP) (https://earthquake.usgs.gov/). In this website, MMI values are computed from online public surveys where public from all over the world summarize the effects of shaking in nearby regions. Figure 4.2 shows a sample snapshot of MMI values obtained from the website.

MMI values are assigned to the ground motion stations using the nearest MMI value within an uncertainty of ±1 MMI unit. The ground motion stations located within a range of approximately 5 km distance are paired with the MMI values.

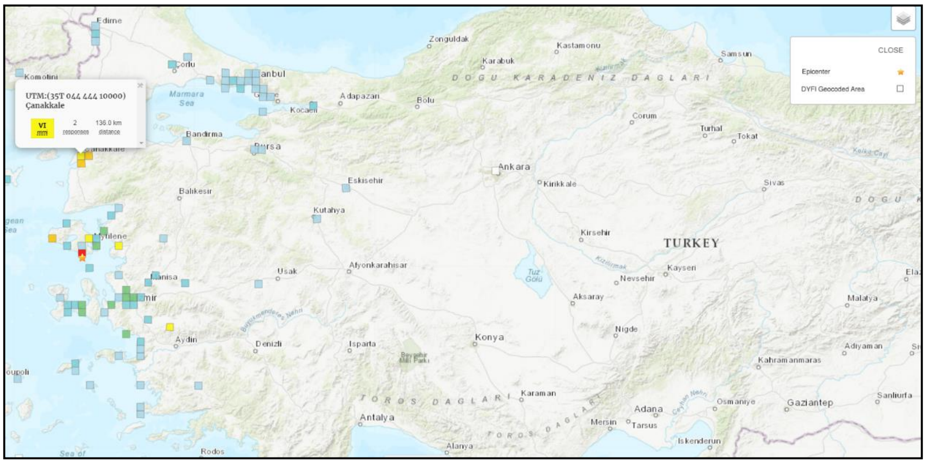

Figure 4.2. Reported *MMI values of a sample earthquake (https://earthquake.usgs.gov/)*

In this thesis, there are a total of 195 input data patterns which include MMI, and seismic parameters such as PGA, PGV, PGD, Arias Intensity, Epicentral Distance, Focal Depth, Moment Magnitude, Soil Class, and Significant Duration from 18 earthquakes. A sample raw dataset composed of 14 input data patterns is demonstrated in Table 4.1. The whole dataset is given in Appendix C.

Table 4.1. *Sample Dataset Used in This Study*

Record No.	*Earthquake ID*	*Station ID*	*Mw*	*PGA(N-S)(cm/sec2)*	*PGA(E-W)(cm/sec2)*	*PGV(N-S)(cm/sec)*	*PGV(E-W)(cm/sec)*	*PGD(N-S)(cm)*	*PGD(E-W)(cm)*	*Ia(N-S)(cm/s)*	*Ia (E-W) (cm/s)*
1	KOC8/99	1604	7.4	54.32	45.81	9.50	71.67	198.60	4765.80	7.93	7.39
2	KOC8/99	5903	7.4	90.36	101.36	20.62	12.75	227.74	66.20	15.62	16.32
3	KOC8/99	3401	7.4	60.67	42.66	9.59	8.57	79.73	264.34	4.06	4.84
4	KOC8/99	3403	7.4	118.03	89.61	14.94	16.53	49.04	20.15	19.38	12.55
5	KOC8/99	1612	7.4	91.89	123.32	17.97	31.69	110.15	82.17	31.07	53.78
6	KOC8/99	4106	7.4	264.82	141.45	97.13	127.99	2313.87	3047.92	61.75	37.53
7	KOC8/99	8101	7.4	314.88	373.76	59.55	52.65	63.24	86.82	113.52	141.00
8	KOC8/99	4101	7.4	171.17	224.91	92.79	76.30	2413.70	1874.53	75.65	100.00
9	KOC8/99	5401	7.4	0.21	407.04	8.11	82.35	1466.11	1279.89	0.001	199.00
10	KOC8/99	6001	7.4	0.85	1.16	1.81	1.86	54.35	79.90	0.01	0.01
11	KOC8/99	4302	7.4	50.05	59.66	9.41	17.15	60.83	148.13	14.70	22.13
12	KOC8/99	901	7.4	5.98	5.25	3.56	4.49	333.96	278.60	0.34	0.31
13	KOC8/99	2002	7.4	5.92	11.69	4.48	14.21	104.09	527.85	0.21	0.37
14	KOC8/99	3502	7.4	9.89	10.80	3.92	3.20	149.88	102.43	0.44	0.56

Table 4.1 *(continued)*

Record No.	*D_5_95(N-S)sec*	*D_5_95(E-W)sec*	*MMI*	*LAT*	*LON*	*STATION CITY*	*Focal Depth(km)*	*Repi (Epicentral Distance)*	*Vs30 (m/s)*	*SOIL CLASSIFICATION*	*CLASSIFICATION (IN NUMBERS*
1	34.05	34.91	VI	40.183	29.127	Bursa/Merkez	17	95	459	C	3
2	19.795	14.87	VI	40.972	27.950	Tekirdağ/Marmara Ereğlisi	17	170	325	D	2
3	38.12	37.5	VI	41.058	29.009	İstanbul/Merkez	17	86	595	C	3
4	9.79	8.975	VII	41.026	28.758	İstanbul/K.Çekmece	17	105	283	D	2
5	33.63	32.53	VII	40.441	29.716	Bursa/İznik	17	40	197	D	2
6	29.645	29.62	VIII	40.786	29.450	Kocaeli/Gebze	17	43	701	C	3
7	11.88	12.07	IX	40.843	31.148	Düzce/Merkez	17	101	282	D	2
8	34.08	34.57	IX	40.766	29.917	Kocaeli/Kozluk	17	3	826	B	4
9	3.43E+02	44.32	X	40.736	30.380	Sakarya/Merkez	17	36	412	C	3
10	70.07	60.64	II	40.329	36.555	Tokat/Merkez	17	561	324	D	2
11	54.88	57.4	IV	39.419	29.997	Kütahya/Merkez	17	149	243	D	2
12	1.40E+02	133	II	37.836	27.838	Aydın/Merkez	17	374	311	D	2
13	44.3	30.85	IV	37.812	29.111	Denizli/Merkez	17	336	356	D	2
14	76.71	73.41	IV	38.455	27.226	İzmir/Bornova	17	349	270	D	2

Figures 4.3 and 4.4 display the distance and magnitude distribution of the MMI dataset, respectively. As expected, despite significant scatter, MMI values increase with increasing Mw while they decrease with increasing epicentral distances. Next, Figure 4.5 and 4.6 show the variation of MMI with respect to PGA and PGV, respectively. In the same figures, the linear regressions from previous studies which are mentioned in Chapter 2 are also presented. The uneven distribution of PGA and PGV values at each MMI level is noticeable. To account for this scatter, in most of the past studies, mean PGA and PGV values are assigned to each MMI level. In this study, a number of ANN models which accept different combinations of input variables are developed. While training these models, values of the input variables are directly used. Thus, each ANN model is capable of handling all MMI and peak ground motion levels.

As an additional observation, the differences between previous models indicate the need for local relationships between intensity and seismic parameters. Therefore, in this study, ANN models for Turkey utilizing Turkish earthquake data are developed. Additional parameters such as soil classification, epicentral depth, and focal depth parameters are included in the analysis in order to further account the regional effects.

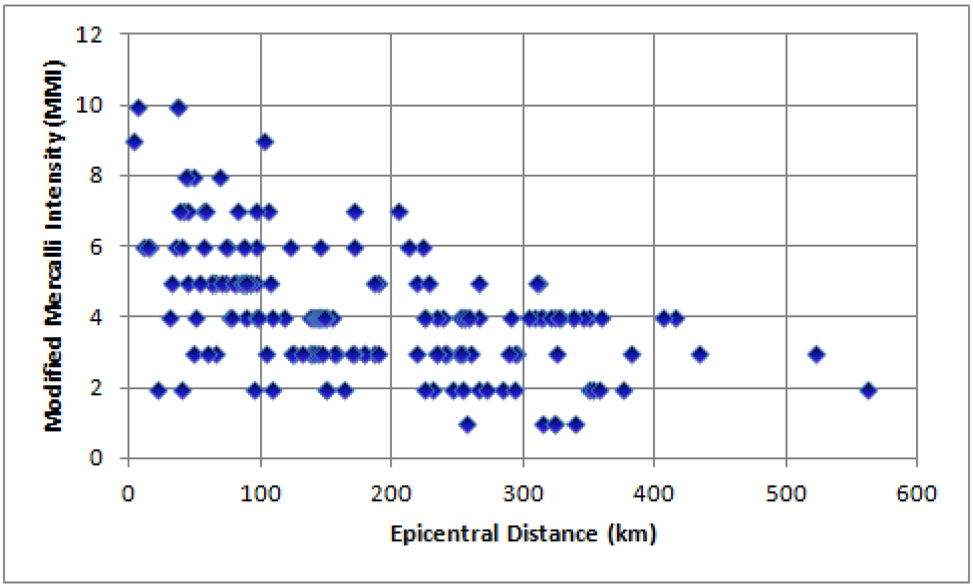

Figure 4.3. Distance distribution of MMI values

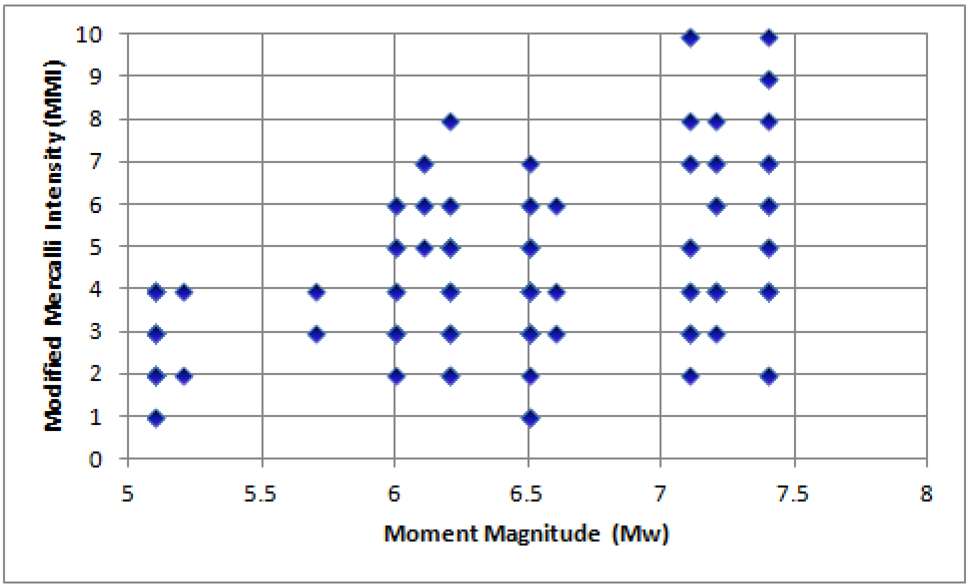

Figure 4.4. Moment Magnitude distribution of MMI values

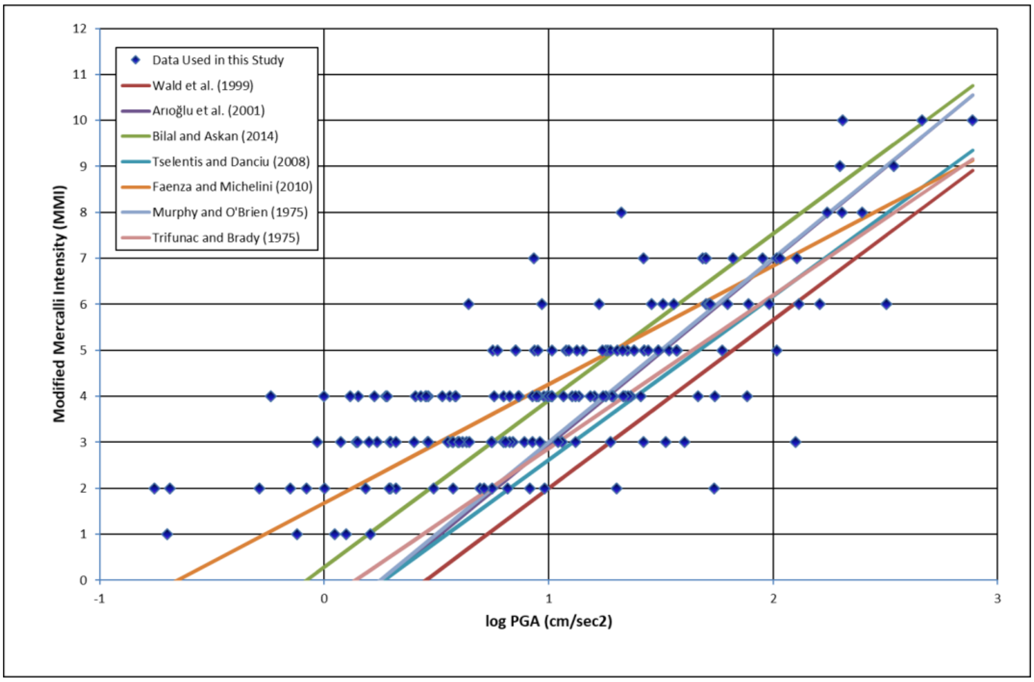

Figure 4.5. Variation of MMI with respect to PGA and comparisons with previous studies

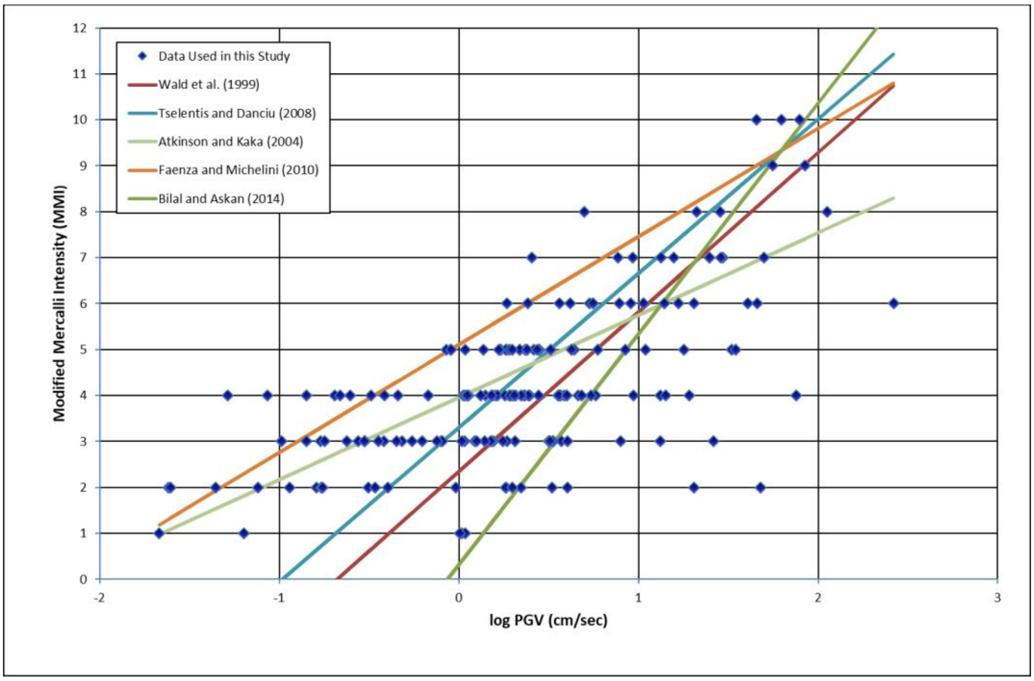

Figure 4.6. Variation of MMI with respect to PGA and comparisons with previous studies

4.3. Definition of Parameters

In this section, the ground motion parameters that are used in this study are explained briefly.

PGA, PGV, PGD: The maximum acceleration, velocity, and displacement of the ground shaking at a particular time of earthquake are defined as peak ground acceleration, peak ground velocity, and peak ground displacement, respectively. Since the shaking occurs in 3 directions, 2 horizontal and 1 vertical PGA, PGV, and PGD are reported for each records.

Accelerogram data is downloaded for all earthquake stations related to each earthquake (http://kyhdata.deprem.gov.tr). An example of an accelerograph and a snapshot of the raw data is given in Figure 4.7.

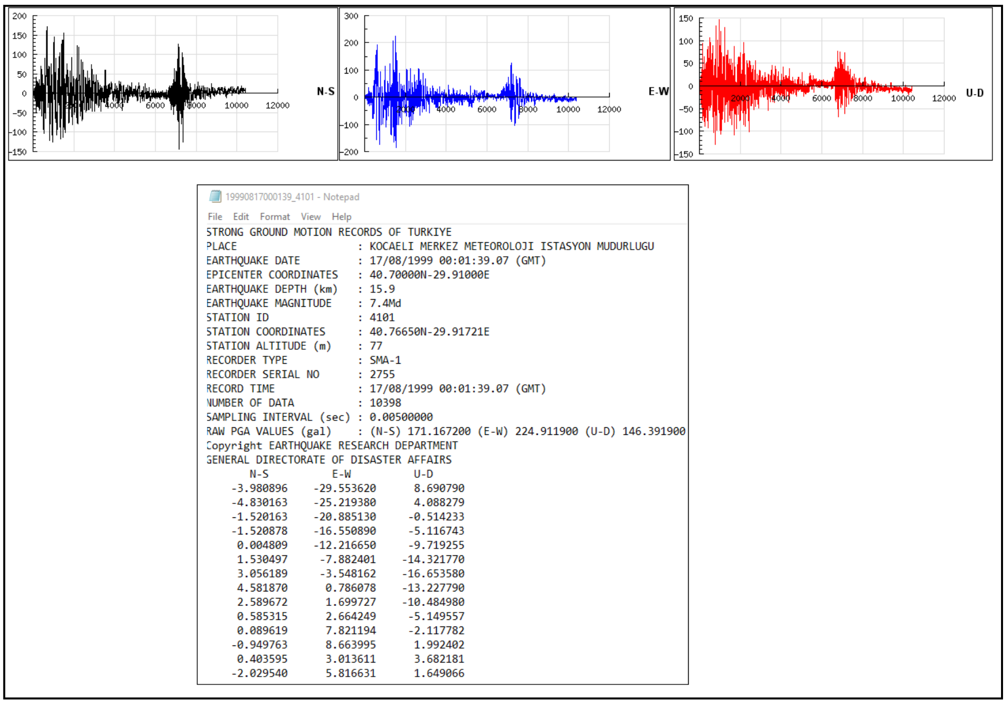


```
19990817000139_4101 - Notepad
File  Edit  Format  View  Help
STRONG GROUND MOTION RECORDS OF TURKIYE
PLACE                    : KOCAELI MERKEZ METEOROLOJI ISTASYON MUDURLUGU
EARTHQUAKE DATE          : 17/08/1999 00:01:39.07 (GMT)
EPICENTER COORDINATES    : 40.70000N-29.91000E
EARTHQUAKE DEPTH (km)    : 15.9
EARTHQUAKE MAGNITUDE     : 7.4Md
STATION ID               : 4101
STATION COORDINATES      : 40.76650N-29.91721E
STATION ALTITUDE (m)     : 77
RECORDER TYPE            : SMA-1
RECORDER SERIAL NO       : 2755
RECORD TIME              : 17/08/1999 00:01:39.07 (GMT)
NUMBER OF DATA           : 10398
SAMPLING INTERVAL (sec)  : 0.00500000
RAW PGA VALUES (gal)     : (N-S) 171.167200 (E-W) 224.911900 (U-D) 146.391900
Copyright EARTHQUAKE RESEARCH DEPARTMENT
GENERAL DIRECTORATE OF DISASTER AFFAIRS
      N-S          E-W          U-D
   -3.980896   -29.553620     8.690790
   -4.830163   -25.219380     4.088279
   -1.520163   -20.885130    -0.514233
   -1.520878   -16.550890    -5.116743
    0.004809   -12.216650    -9.719255
    1.530497    -7.882401   -14.321770
    3.056189    -3.548162   -16.653580
    4.581870     0.786078   -13.227790
    2.589672     1.699727   -10.484980
    0.585315     2.664249    -5.149557
    0.089619     7.821194    -2.117782
   -0.949763     8.663995     1.992402
    0.403595     3.013611     3.682181
   -2.029540     5.816631     1.649066
```

Figure 4.7. An example of an accelerograph and snapshot of the values (http://kyhdata.deprem.gov.tr)

Arias Intensity: Arias intensity is calculated as the square of the acceleration integrated over the total duration of the shaking. Similar to the PGA, I_a is also used as an indicator of intensity of the ground motion. The corresponding formula is given as follows:

$$I_a = \frac{\pi}{2g}\int_0^T [a(t)]^2 dt \qquad (4.1)$$

where $a(t)$is the acceleration data in time domain, g is the gravitational acceleration, and T is the total duration of the earthquake.

Significant Duration: Strong motion duration is an important parameter to measure the potential damage during an earthquake. This parameter usually depends on local site conditions, fault characteristics and the distance from the source to the station. There are different measures for the strong motion duration namely, bracket, uniform, and significant duration. Significant duration is the time between %5 and %95 of Arias Intensity (I_a) (Trifunac and Brady,1975). This value is determined from the Husid plots which are the time history of Arias Intensity scaled to the total intensity. An example computation is given in Figure 4.8.

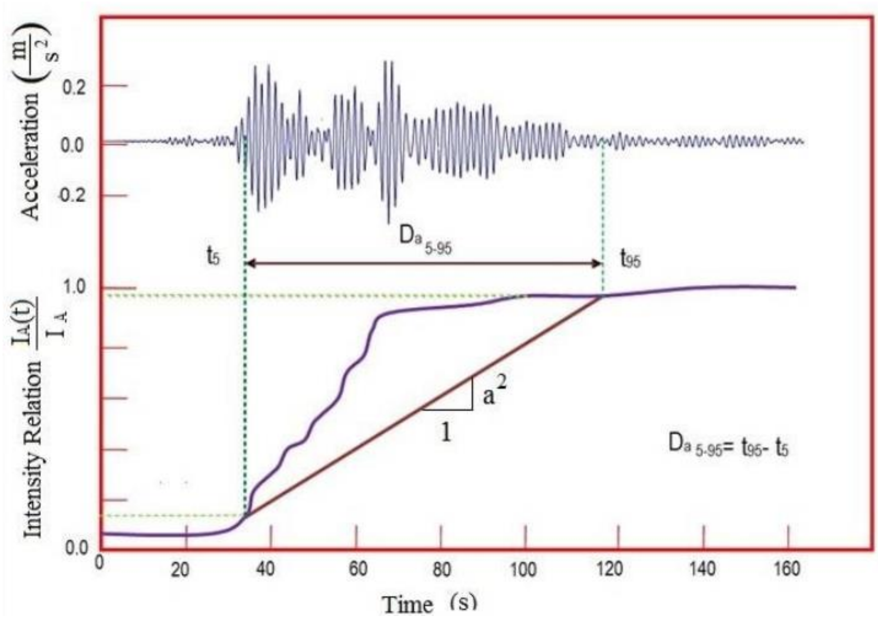

Figure 4.8. Example for computation of Significant Duration ($D_{5\text{-}95}$) determined from Husid Plot (Husid,1969)

Focal Depth and Epicentral Distance: The point at which the earthquake occurs is the focus or hypocenter of the earthquake. The epicenter is the projection of the focus to the Earth’s surface. The focal depth is the distance from the focus to the epicenter location. The epicentral distance is the distance from the epicenter point to the station point where the earthquake ground motion parameters are gathered (Figure 4.9).

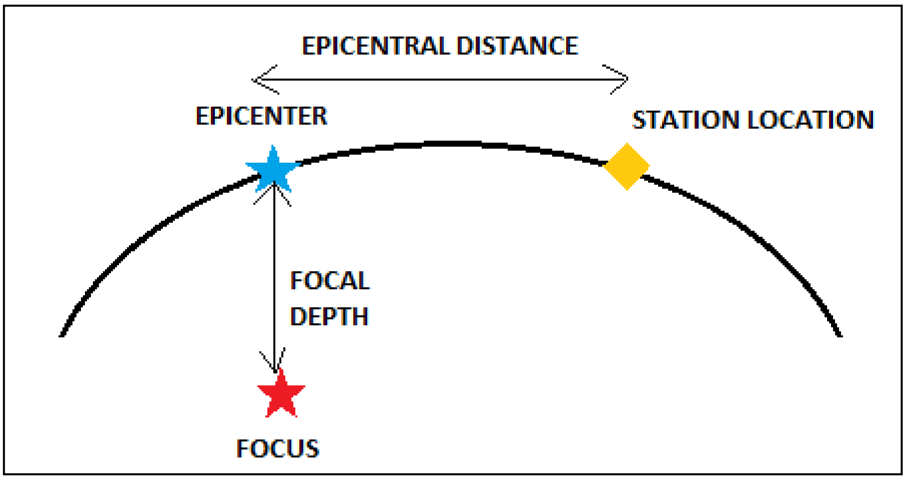

Figure 4.9. Visual Description of Epicentral Distance and Focal Depth

Soil Classification (Vs30): Shear wave velocity is an important parameter for determining the site class. Vs30 is the average shear wave velocity in the top 30 m of the soil. According to the National Earthquake Hazards Program- Uniform Building Code (NEHRP- UBC), the soils are divided into some classes according to their Vs30 values (Table 4.2). In this study, soil classes are converted to categoric numbers in order to insert as an input value to ANN analyses. Table 4.2 shows the corresponding information.

Table 4.2. *Vs30 Soil Classification and Categoric Definitions used in this thesis (NEHRP-UBC)*

Soil Class	*Soil Class In Numbers*	*Soil Type*	*Vs30 Criteria*
A	5	Hard Rock	Vs30 > 1500 m/s
B	4	Rock	760 m/s < Vs30 ≤1500
C	3	Very Dense Soil and Soft Rock	360 m/s < Vs30 ≤ 760
D	2	Stiff Soil	180 m/s <Vs30 ≤ 360
E	1	Soft Clay Soil	Vs30 < 180 m/s
F	Not Applicable	Soils Requiring Additional Response	-

4.4. Application of Principal Component Analysis using SPSS Software

Principal Component Analysis is carried out using the factor analysis tool of the Statistical Package for the Social Sciences (SPSS) program. For each MMI value, the analysis is performed seperately. Results of the analysis include the following calculation steps;

- Generation of the Correlation matrix
- Generation of the Total Variance Plot
- Generation of the Scree Plot
- Generation of the Component Matrix

Each calculation step is shown in detail in Appendix D, Appendix E, Appendix F, and Appendix G, respectively. For MMI=IX, due to the fact that there are only 2 data, PCA analysis is not conducted.

Arithmetic mean of two components of the ground motion parameters (PGA, PGV, PGD, Ia, $D_{5\text{-}95}$) are used in order to take into account the widely distributed data values. The input values are;

- Moment Magnitude (Mw)
- Focal Depth (FD)
- Epicentral Distance (Repi)
- Soil Classification (SC)
- PGA
- PGV
- PGD
- Arias Intensity (Ia)
- Significant Duration ($D_{5\text{-}95}$)

Using these input variables, PCA analysis for each MMI level is conducted. The component matrices generated are given in Appendix G.
A summary table of the component matrix is given in Table 4.3 for ease of reference.

The component matrix shows the correlations between the input variables and the principal component. In the component matrix, the principal components and their relations with the variables are shown. By definition, the first principal component has the largest variation and the second principal component has the second-largest variation.

As can be seen in Table 4.3, for most of the MMI levels, PGA which has a high correlation with MMI is included in the first principal component. This makes sense that this parameter is an important indicator of the seismic-resistant design because of the fact that the product of PGA and mass represents the inertial force loading the structures (Krinitzsky and Chang, 1988). PGV, PGD and Arias Intensity are identifed as other variables that have high correlations with MMI levels. This is also expected since these parameters are known to correlate with damage to structures with different fundamental periods.

PGA, PGV, PGD, and Arias intensities will be separately included in the analysis since highly correlated parameters do not make a drastic change to the outcome value. Moreover, PCA results are also compatible with previous studies. Almost all of the regression equations developed in the literature use PGA, PGV, PGD, and Ia, seperately. This fact is also confirmed with expert knowledge.

Table 4.3. *Summary Table for the Component Matrix*

MMI =I							
Components	*Variables*						
PC1	PGV	FD	Mw	PGA	D_{5-95}	Ia	PGD
PC2	Repi	SC					
MMI =II							
Components	*Variables*						
PC1	PGA	Repi	Ia	D_{5-95}			
PC2	PGV	PGD	FD	SC			
PC3	Mw						
MMI =III							
Components	*Variables*						
PC1	PGV	Ia	PGA	FD			
PC2	Mw	Repi	D_{5-95}				
PC3	SC	PGD					
MMI =IV							
Components	*Variables*						
PC1	Mw	D_{5-95}	PGV	PGD	Repi		
PC2	PGA	Ia					
PC3	FD						
PC4	SC						
MMI =V							
Components	*Variables*						
PC1	PGV	PGD	Ia	PGA			
PC2	Repi	Mw	D_{5-95}				
PC3	FD	SC					
MMI =VI							
Components	*Variables*						
PC1	PGA	Ia	PGV	Repi	D_{5-95}	PGD	
PC2	FD	Mw					
PC3	SC						
MMI =VII							
Components	*Variables*						
PC1	PGV	PGD	FD	D_{5-95}	Repi		
PC2	Ia	PGA	Mw				
PC3	SC						
MMI =VIII							
Components	*Variables*						
PC1	D_{5-95}	Ia	FD	SC	Mw	PGA	
PC2	PGV	PGD	Repi				
MMI =X							
Components	*Variables*						
PC1	FD	SC	Mw	D_{5-95}	Ia	PGD	PGV
PC1	PGA						
PC2	Repi						

4.5. Application of Artificial Neural Network Analysis using NF Toolbox

Neural Network Analysis is carried out using MATLAB software which contains different types of toolboxes in various engineering fields. Using Neural Network Toolbox with Neural Net Fitting Toolbar (nftool), several multilayer models are created with one input layer, different numbers of hidden neurons in one hidden layer and one output layer.

A two-layer feed-forward network with sigmoid hidden neurons and output neuron is used and the models are trained with the Levenberg-Marquardt backpropagation algorithm. MATLAB manual states that 'This algorithm is the fastest backpropagation algorithm in the toolbox and is highly recommended as a first-choice supervised algorithm, although it does require more memory than other algorithms.' In Figure 4.10, the sample feed-forward algorithm which is extracted from the MATLAB NF Toolbar is given.

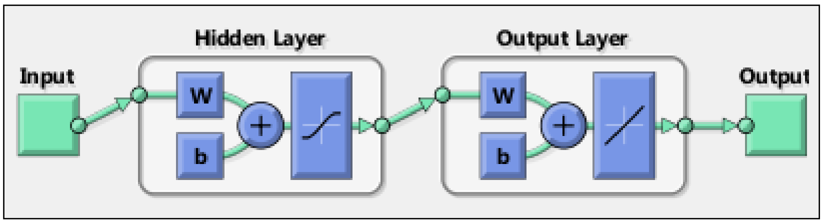

Figure 4.10. Sample Representation of Feed Forward Algorithm in MATLAB NFTOOL (MatLab, M.,2012)

In the first part of neural network analysis, the dataset is trained with different combinations of input variables chosen based on the results of the principal component analysis and expert knowledge. Table 4.4 shows the description of the models created using different input variable sets.

Table 4.4. *Model Descriptions for ANN*

Model	**Variables included in the Model**								
M1	Mw	PGA	Repi						
M2	Mw	PGA	Repi	SC					
M3	Mw	PGA	Repi	SC	FD				
M4	Mw	PGA	Repi	SC	FD	$D_{5\text{-}95}$			
M5	Mw	PGV	Repi						
M6	Mw	PGV	Repi	SC					
M7	Mw	PGV	Repi	SC	FD				
M8	Mw	PGV	Repi	SC	FD	$D_{5\text{-}95}$			
M9	Mw	PGD	Repi						
M10	Mw	PGD	Repi	SC					
M11	Mw	PGD	Repi	SC	FD				
M12	Mw	PGD	Repi	SC	FD	$D_{5\text{-}95}$			
M13	Mw	Ia	Repi						
M14	Mw	Ia	Repi	SC					
M15	Mw	Ia	Repi	SC	FD				
M16	Mw	Ia	Repi	SC	FD	$D_{5\text{-}95}$			

According to the Neural Network Toolbox, the inputs are randomly divided into three sets, namely; training, validation, and testing. In this part of the analysis, a total of 170 datasets are gathered. Due to the limited number of available data, the distribution of data for training, validation, and testing is carried out by allocating most of the data for training. In other words, to maintain proper training (i.e., adjustment of the weights of the ANN models), most of the data is used in the training process. Therefore, training, validation and testing data are selected as 90%, 5% and 5%, respectively (Figure 4.11). The trained model is then run with 25 new datasets to compare ANN model results with other published models in the literature.

To evaluate the impact of hidden neurons used in the hidden layer, the number of hidden neurons is changed, and different models are built. The number of input variables are set as the minimum number of hidden neurons and this number is increased progressively. Different number of hidden neurons are used, and the program is trained for 10 times for each different number of hidden neurons in order to evaluate the effect of training data selection on the model performance. The performance of the model is evaluated using the mean square error (MSE) and the Pearson's Correlation Coefficient (R).

Mean Square Error (MSE):

$$MSE = \frac{1}{n}\sum_{i=1}^{n}(y_i - x_i)^2 \tag{4.2}$$

Pearson's Correlation Coefficient (R):

$$R = \frac{\sum_{i=1}^{n}(x_i - \bar{x})(y_i - \bar{y})}{\sqrt{\sum_{i=1}^{n}(x_i - \bar{x})^2}\sqrt{\sum_{i=1}^{n}(y_i - \bar{y})^2}} \tag{4.3}$$

where n is the number of data, x, y, $\bar{x}$, and $\bar{y}$ depict the observed values, predicted values, mean value of observed values, and mean value of predicted values respectively.

A summary table is generated for each model with different numbers of hidden neurons (Table 4.5). Figure 4.12 shows an example regression plot for ANN training model for M3 model and 5 hidden neurons. The other plots are given in Appendix H.

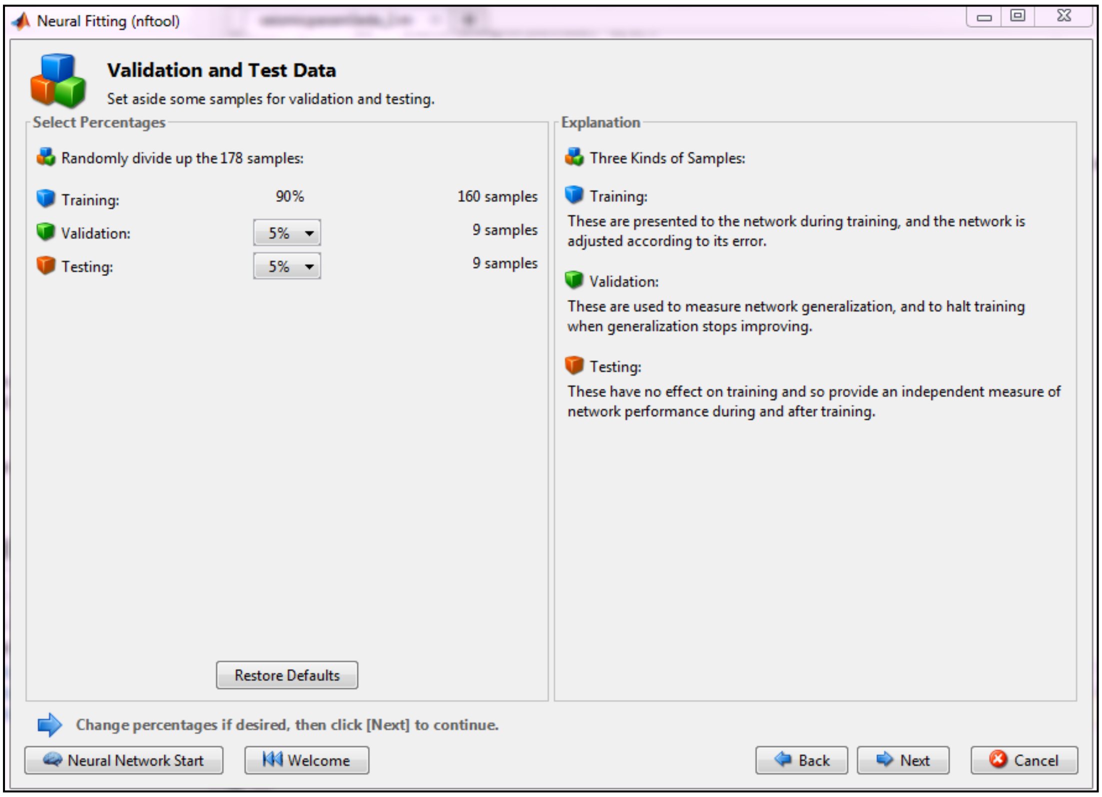

Figure 4.11. Input Percentage Selection in NF Tool

Table 4.5. *Training performances of various ANN models with different number of hidden neurons*

Model	**# of Hidden Neurons**	**Regression Value (R)**	**Mean Square Error (MSE)**
M1 (Mw,PGA,Repi)	**3**	**0.87**	**0.79**
	4	0.86	0.84
M2 (Mw,PGA, Repi,SC)	4	0.86	0.76
	5	**0.89**	**0.60**
M3 (Mw,PGA, Repi,SC,FD)	5	0.93	0.40
	6	**0.93**	**0.40**
M4 (Mw,PGA, Repi,SC,FD, $D_{5\text{-}95}$)	6	0.92	0.42
	7	**0.93**	**0.39**
M5 (Mw,PGV, Repi)	3	0.84	0.98
	4	**0.87**	**0.76**
M6 (Mw,PGV, Repi,SC)	4	0.85	0.85
	5	**0.86**	**0.83**
M7 (Mw,PGV, Repi,SC,FD)	5	0.87	0.72
	6	**0.93**	**0.45**
M8 (Mw,PGV, Repi,SC,FD, $D_{5\text{-}95}$)	6	0.91	0.52
	7	**0.93**	**0.45**
M9 (Mw,PGD, Repi)	3	0.83	0.85
	4	**0.87**	**0.69**

Table 4.5. *(continued)*

Model	**# of Hidden Neurons**	**Regression Value (R)**	**Mean Square Error (MSE)**
M10	4	0.84	0.90
(Mw,PGD, Repi,SC)	**5**	**0.84**	**0.86**
M11	5	0.87	0.73
(Mw,PGD, Repi,SC,FD)	**6**	**0.89**	**0.62**
M12	6	0.91	0.49
(Mw,PGD,Repi, SC,FD, $D_{5\text{-}95}$)	**7**	**0.92**	**0.46**
M13	3	0.84	0.89
(Mw,Ia, Repi)	**4**	**0.87**	**0.76**
M14	**4**	**0.87**	**0.69**
(Mw, Ia, Repi,SC)	5	0.87	0.75
M15	5	0.87	0.74
(Mw, Ia, Repi,SC,FD)	**6**	**0.91**	**0.5**
M16	6	0.91	0.55
(Mw, Ia, Repi,SC,FD, $D_{5\text{-}95}$)	**7**	**0.94**	**0.36**

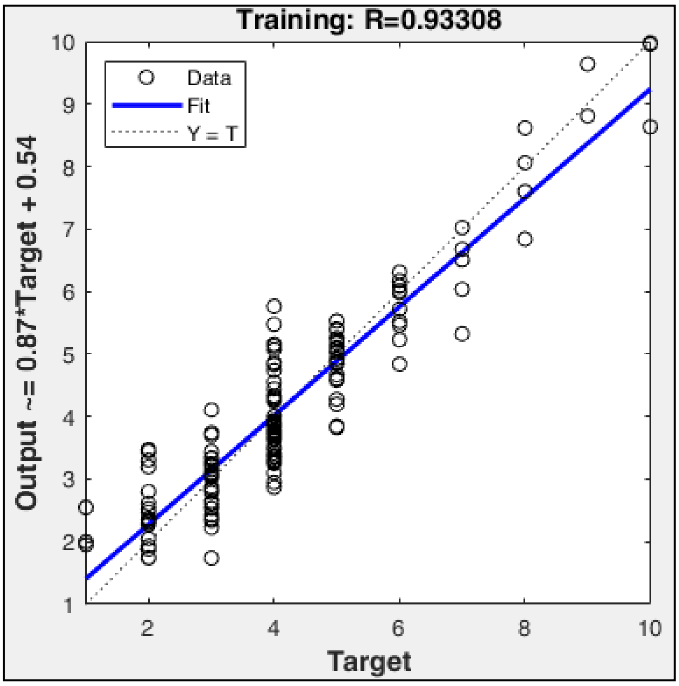

Figure 4.12. Example Regression Plot for ANN Training Model (M3 Model with 5 hidden neurons)

The models highlighted in bold in Table 4.5 are the models with the highest training performance. In the second part of the neural network analysis, these models are tested with a new dataset for testing purposes. This new data set is composed of 25 patterns which are provided in Table 4.6. The data from the earthquake that occurred on 26th of September 2019 at Istanbul is also included in the test data. As a result, observed and predicted values for the trials are tabulated and MSE and R^2 values are calculated. These results are also compared with the previous studies which used linear regression. In addition to the restrictions recommended by the authors' and estimated MMI values less than or equal to zero are not used in R^2 calculations. In Table 4.7, Table 4.8 and Table 4.9, previous equations proposed for MMI-PGA, MMI-PGV, and MMI-Ia are shown.

Table 4.6. *Testing Dataset*

Record No.	Earthquake ID	Station ID	Mw	PGA (cm/sec2)	PGV (cm/sec)	PGD(cm)	Arias Intensity (cm/s)	D_5_95 (sec)	Focal Depth (km)	ED(Epicentral Distance)	SOIL CLASSIFICATION (IN NUMBERS)	MMI	MMI_NUMBERS
1	CNK02/19	4104	5.1	0.20	0.02	0.16	0.00	59.275	5.80	322	4	I	1
2	MAR09/19	619	5.8	0.45	0.17	18.22	0.00	111.415	7.97	402	2	I	1
3	DNZ08/19	3509	6.0	1.95	0.34	7.31	0.02	61.37	6.96	149	2	II	2
4	MAR09/19	1710	5.8	1.75	0.21	0.83	0.01	76.82	7.97	141	2	II	2
5	BDR07/17	701	6.5	1.39	0.38	2.08	0.02	200.24	19.44	287	4	III	3
6	CNK02/19	1628	5.1	1.59	0.14	4.76	0.00	35.325	5.80	239	3	III	3
7	MAR09/19	301	5.8	1.36	0.24	0.38	0.01	85.71	7.97	309	2	III	3
8	VAN10/11	4404	7.2	1.00	0.67	7.50	0.01	87.74	19.02	405	4	IV	4
9	VAN10/11	7201	7.2	8.45	2.48	18.53	0.34	38.685	19.02	223	3	IV	4
10	MAR09/19	4125	5.8	4.50	0.65	0.61	0.04	33.03	7.97	144	4	IV	4
11	MAR09/19	1628	5.8	15.40	1.30	4.53	0.22	10.41	7.97	101	3	IV	4
12	MAR09/19	1620	5.8	4.12	0.62	4.41	0.05	38.28	7.97	110	3	IV	4
13	MAR09/19	1627	5.8	11.87	1.50	6.87	0.40	48.02	7.97	103	2	IV	4
14	MAR09/19	7708	5.8	13.67	1.48	1.13	0.46	45.725	7.97	91	2	IV	4
15	ADN6/98	110	6.2	30.80	17.90	186.82	2.29	17.3975	46.6	31	3	V	5
16	IZM11/92	3501	6	34.42	10.90	41.61	3.27	12.8725	17.2	43	2	V	5
17	DZC11/99	5902	7.1	5.91	1.84	19.80	0.10	27.58	10.4	309	3	V	5
18	MAR09/19	1642	5.8	17.88	1.19	0.23	0.26	14.47	7.97	97	3	V	5
19	MAR09/19	1629	5.8	24.18	1.59	1.75	1.01	22.185	7.97	95	2	V	5
20	MAR09/19	1630	5.8	17.53	1.17	1.34	0.43	12.74	7.97	96	2	V	5
21	EZR10/83	2503	6.6	161.78	45.73	107.94	51.27	19.225	16.1	35	2	VI	6
22	ORT6/00	1801	6	62.81	7.80	69.54	10.36	36.632	10	15	2	VI	6
23	BDR07/17	4810	6.5	36.04	1.85	2.24	1.54	16.42	19.44	72	3	VI	6
24	KOC8/99	3403	7.4	103.82	15.73	34.60	15.97	9.3825	17	105	2	VII	7
25	VAN10/11	4902	7.2	50.25	13.34	198.77	8.53	32.2455	19.02	95	2	VII	7

Table 4.7. *Linear Regression Equations proposed for MMI-PGA relationships*

Linear Relationships proposed for MMI-PGA relationships		
No	**Name**	**Equation**
1	Wald et al. (1999)	MMI= $-1.66+3.66 \log_{10}(PGA)$ $\log_{10}(PGA) > 1.82$
2	Tselentis and Danciu (2008)	MMI= $-0.946+ 3.563 \log_{10}(PGA)$
3	Murphy and O'Brien (1977)	MMI= $(\log_{10}(PGA)-0.25)/0.25$
4	Trifunac and Brady (1975)	MMI= $(\log_{10}(PGA)-0.14)/0.30$
5	Bilal and Askan (2014)	MMI= $0.132+ 3.884 \log_{10}(PGA)$
6	Arıoğlu et. Al. (2001)	MMI= $1.748*\ln(PGA) -1.078$
7	Faenza and Michelini (2010)	MMI= $1.68+ 2.58 \log_{10}(PGA)$
8	Tselentis and Danciu (2008)	MMI= $2.355+ 1.384*\log_{10}(PGA)+0.297Mw-0.832*\log_{10}(Repi)-0.108*SC$
9	Bilal and Askan (2014)	MMI=$-1.692+ 0.793*\log(PGA)+1.653Mw-2.746*\log(Repi)$

Table 4.8. *Linear Regression Equations proposed for MMI-PGV relationships*

Linear Relationships proposed for MMI-PGV relationships		
No	**Name**	**Equation**
1	Wald et al. (1999)	MMI= 2.35+3.47 $\log_{10}$ (PGV) $\log_{10}$ (PGV) > 0.76
2	Atkinson and Kaka (2007)	MMI= 4.37+1.32 $\log_{10}$ (PGV) for $\log_{10}$ (PGV) ≤ 0.48
		MMI= 3.54+3.03 $\log_{10}$ (PGV) $\log_{10}$ (PGV) > 0.48
3	Tselentis and Danciu (2008)	MMI= 3.30+ 3.358 $\log_{10}$ (PGV)
4	Atkinson and Kaka (2004)	MMI= 3.96+ 1.79 $\log_{10}$ (PGV)
5	Faenza and Michelini (2010)	MMI= 5.11+ 2.35 $\log_{10}$ (PGV)
6	Bilal and Askan (2014)	MMI= 2.673+ 4.340 $\log_{10}$ (PGV)
7	Tselentis and Danciu (2008)	MMI= 5.582+ 1.397*$\log_{10}$ (PGV)-0.78*log (Repi)-0.073* SC
8	Bilal and Askan (2014)	MMI=0.788+ 0.914*log (PGV)+1.412Mw-2.904* log (Repi)

Table 4.9. *Linear Regression Equations proposed for MMI-Ia relationships*

Linear Relationships proposed for MMI-Ia relationships		
1	Tselentis and Danciu (2008)	MMI= 4.395+ 2.040 $\log_{10}$ (Ia)
2	Tselentis and Danciu (2008)	MMI= 5.919+ 0.844*$\log_{10}$ (Ia)-0.997*$\log_{10}$ (Repi)-0.105* SC

The ANN model results and linear regression results are tabulated in Table 4.10, 4.11, 4.12, and 4.13 depicting the comparison of MMI-PGA, MMI-PGV, MMI-PGD, and MMI-Ia, respectively. In the literature, since PGD regression relationships do not exist, only the ANN analysis results are shown for the case of PGD.

Table 4.10. *Comparison of MMI-PGA relationship with Previous Studies*

PGA (cm/sec2)	OBSERVED_ MMI_NUMBERS	PREDICTED MMI NUMBERS												
		M1	M2	M3	M4	Wald et al. (1999) (1)	Tselentis and Danciu (2008) (2)-univariate	Murphy and O'Brien (1977) (3)	Trifunac and Brady (1975) (4)	Bilal and Askan (2014) (5)	Arıoğlu et. Al. (2001) (6)	Faenza and Michelini (2010) (7)	Tselentis and Danciu (2008) (8)-multivariate	Bilal and Askan (2014) (9)-multivariate
0.20	1	2	2	2	1	NA	NA	NA	NA	NA	NA	NA	NA	NA
0.45	1	2	2	3	3	NA	NA	NA	NA	NA	NA	1	NA	NA
1.95	2	4	3	4	3	NA	NA	NA	1	1	NA	2	NA	2
1.75	2	4	4	4	3	NA	NA	NA	NA	1	NA	2	NA	2
1.39	3	3	4	2	4	NA	NA	NA	NA	1	NA	2	NA	2
1.59	3	3	3	3	3	NA	NA	NA	NA	1	NA	2	NA	NA
1.36	3	3	2	3	3	NA	NA	NA	NA	1	NA	2	NA	1
1.00	4	3	4	3	4	NA	NA	NA	NA	NA	NA	2	2	3
8.45	4	4	5	5	5	NA	2	3	3	4	3	4	4	4
4.50	4	4	3	4	5	NA	1	2	2	3	2	3	3	2
15.40	4	4	5	4	4	NA	3	4	3	5	4	5	4	3
4.12	4	4	4	4	4	NA	1	1	2	3	1	3	3	3
11.87	4	4	5	4	4	NA	3	3	3	4	3	4	4	3
13.67	4	4	5	4	4	NA	3	4	3	5	3	5	4	3
30.80	5	5	7	2	2	4	4	5	4	6	5	6	5	6
34.42	5	5	5	6	5	4	5	5	5	6	5	6	5	5
5.91	5	4	4	4	3	1	2	2	2	3	2	4	3	4
17.88	5	4	5	4	4	3	4	4	4	5	4	5	4	3
24.18	5	4	5	5	4	3	4	5	4	6	4	5	4	4
17.53	5	4	5	4	4	3	3	4	4	5	4	5	4	3
161.78	6	7	6	7	7	6	7	8	7	9	8	7	6	7
62.81	6	5	4	6	6	5	5	6	6	7	6	6	6	6
36.04	6	5	4	4	5	4	5	5	5	6	5	6	5	5
103.82	7	7	7	7	6	6	6	7	6	8	7	7	6	7
50.25	7	6	6	6	4	5	5	6	5	7	6	6	5	6
MSE VALUES		**0.66**	**0.97**	**1.32**	**1.83**	**3.76**	**2.55**	**1.81**	**2.00**	**1.68**	**1.90**	**0.66**	**0.89**	**0.97**
R^2 VALUES		**0.76**	**0.63**	**0.50**	**0.35**	**0.48**	**0.66**	**0.66**	**0.74**	**0.81**	**0.66**	**0.80**	**0.65**	**0.74**

Table 4.10 shows that the best ANN model among those with PGA as the main ground motion parameter is found to be M1 with the inclusion of Mw, and Repi into the inputs.

R^2 values for the dataset used in Faenza and Michelini (2010) and Bilal and Askan (2014) are higher than other regression equations. The result for M1 model has similar performances to the regression equations developed by Faenza and Michelini (2010) and Bilal and Askan (2014). The reason for this situation is the fact that the dataset used in those regression equations belong to Italy and Turkey, respectively, where the building stock is similar.

Predicted results for Arıoğlu et al. (2001) clearly underestimate the observed values by at least one intensity unit. The reason for this may be the utilization of only one earthquake in the mentioned study. Equations from other previous studies also underestimate the observed values. These studies are performed in the California region where the structures are considered to be different and more earthquake-resistant than the building stock in Turkey. Therefore, MMI values from those equations (Wald et al., Trifunac and Brady) are lower for the same peak ground motion parameters.

Table 4.11. *Comparison of MMI-PGV relationship with Previous Studies*

PGV (cm/sec)	OBSERVED _MMI_NUMBERS	PREDICTED MMI NUMBERS											
		M5	M6	M7	M8	Wald et al. (1999) (1)	Atkinson and Kaka (2007) (2)	Tselentis and Danciu (2008) (3) univariate	Atkinson and Kaka (2004) (4)	Faenza and Michelini (2010) (5)	Bilal and Askan (2014) (6) univariate	Tselentis and Danciu (2008) (7) multivariate	Bilal and Askan (2014) (8)-multivariate
0.02	1	2	2	2	3	NA	2	NA	NA	1	NA	NA	NA
0.17	1	2	2	2	3	NA	3	NA	NA	3	NA	NA	1
0.34	2	4	4	4	3	NA	4	NA	NA	4	1	NA	3
0.21	2	3	4	4	4	NA	3	NA	NA	4	NA	NA	2
0.38	3	3	3	3	3	NA	4	NA	NA	4	1	NA	2
0.14	3	3	3	3	3	NA	3	NA	NA	3	NA	NA	NA
0.24	3	3	2	2	2	NA	4	NA	NA	4	NA	NA	1
0.67	4	4	4	3	3	NA	4	3	NA	5	2	3	3
2.48	4	4	5	4	5	NA	5	5	NA	6	4	4	4
0.65	4	3	4	4	4	NA	4	3	NA	5	2	4	3
1.30	4	3	4	4	4	NA	5	4	NA	5	3	4	3
0.62	4	3	4	4	4	NA	4	3	NA	5	2	4	3
1.50	4	3	4	4	5	NA	5	4	NA	6	3	4	3
1.48	4	3	4	4	5	NA	5	4	NA	6	3	4	3
17.90	5	5	5	4	7	7	7	8	6	8	8	6	6
10.90	5	6	5	5	5	6	7	7	6	8	7	6	5
1.84	5	4	4	4	3	3	5	4	4	6	4	4	4
1.19	5	3	4	4	4	3	4	4	4	5	3	4	3
1.59	5	3	4	4	4	3	5	4	4	6	4	4	3
1.17	5	3	4	4	4	3	4	4	4	5	3	4	3
45.73	6	6	9	7	8	8	9	9	7	9	10	7	7
7.80	6	6	5	5	6	5	6	6	6	7	7	6	7
1.85	6	4	5	5	5	3	5	4	4	6	4	4	5
15.73	7	7	6	7	7	7	7	7	6	8	8	6	6
13.34	7	6	6	6	5	6	7	7	6	8	8	6	6
MSE VALUES		**0.85**	**0.96**	**0.69**	**1.39**	**3.19**	**1.30**	**1.83**	**0.90**	**2.17**	**3.44**	**0.71**	**1.11**
R^2 VALUES		**0.69**	**0.63**	**0.75**	**0.50**	**0.26**	**0.65**	**0.51**	**0.26**	**0.76**	**0.61**	**0.48**	**0.72**

Table 4.11 shows that the best ANN model among those with PGV as the main ground motion parameter is found to be M7 which includes Mw, Repi, SC, and FD into the inputs. However, the ANN model for the PGA relationship has slightly better performance than that of the PGV relationship. This is believed to arise from the fact that most damaged structures in Turkey are rigid where the damage is better correlated with PGA than PGV.

R^2 values for the dataset used in Faenza and Michelini (2010) is the highest from the other regression equations. Also, the multivariate relationship proposed for Bilal and Askan (2014) has closer performances than that of the ANN model. The reason for this situation is the fact that the dataset of the building stocks is similar.

Moreover, the multivariate relationship proposed for Bilal and Askan (2014) includes PGV, Mw, and Epicentral Distance (Repi). The univariate relationships developed by Bilal and Askan (2014) have higher MSE and lower R^2 than that of multivariate relationship. Therefore, including additional parameters apart from PGV improved the performance and have closer performances with that of ANN model.

On the other hand, some of the previous studies suggested that high levels of seismic intensity correlate well with PGV (Atkinson and Kaka, 2007; Tselentis and Danciu, 2008). The probable reason is the fact that the building stock in these regions has more ductile properties than that of Turkey.

Moreover, similar observation as in PGA indicates that equations from other previous studies such as Wald et al. (1999), Atkinson and Kaka (2004), and Atkinson and Kaka (2007) also underestimate the observed values. These studies are performed in the California region where the structures are considered to be different and more earthquake-resistant than the building stock in Turkey. Therefore, MMI values from those equations are lower for the same peak ground motion parameters.

Table 4.12. *Results of MMI-PGD relationship*

PGD(cm)	OBSERVED_ MMI_ NUMBERS	PREDICTED MMI NUMBERS			
		M9	M10	M11	M12
0.16	1	2	2	3	3
18.22	1	3	2	NA	NA
7.31	2	3	3	4	3
0.83	2	4	3	3	3
2.08	3	3	3	3	4
4.76	3	3	3	3	3
0.38	3	3	3	2	2
7.50	4	3	4	4	4
18.53	4	4	5	5	6
0.61	4	4	4	4	4
4.53	4	5	4	4	5
4.41	4	4	4	4	4
6.87	4	5	4	4	4
1.13	4	5	4	4	4
186.82	5	6	5	5	2
41.61	5	5	5	5	5
19.80	5	4	4	4	3
0.23	5	5	4	4	5
1.75	5	5	4	4	5
1.34	5	5	4	4	5
107.94	6	6	7	6	6
69.54	6	6	6	6	5
2.24	6	5	5	5	5
34.60	7	7	7	7	7
198.77	7	6	7	7	7
MSE VALUES		**0.69**	**0.62**	**0.61**	**1.12**
R^2 VALUES		**0.75**	**0.77**	**0.73**	**0.51**

Table 4.12 shows that the best ANN model when PGD is used as the main ground motion parameter is found to be M10 with the inclusion of Mw, Repi, and SC into the inputs. Inclusion of soil class among the input variables is particularly reasonable for softer soils, since long period site effects influence the peak ground displacement values significantly.

In the literature, PGD is not commonly used in felt intensity prediction equations since PGD is obtained by integrating twice of the acceleration record. This integration might involve numerical errors or differences per each numerical method. Thus, PGD value is not always constant and stable. Moreover, PGD corresponds mainly to longer structural periods.

However, the ANN model with PGD presented in this study could be used in future studies to indirectly predict the potential damage to flexible structures with longer periods.

Table 4.13. *Comparison of MMI-Ia relationship with Previous Studies*

Arias Intensity(cm/s)	OBSERVED _MMI_NUMBERS	PREDICTED MMI NUMBERS					
		M13	M14	M15	M16	Tselentis and Danciu (2008) (1) univariate	Tselentis and Danciu (2008) (2) multivariate
0.0001	1	2	2	2	3	NA	NA
0.0014	1	NA	2	2	2	NA	NA
0.02	2	4	4	4	3	NA	NA
0.01	2	4	4	4	3	NA	NA
0.02	3	3	4	4	5	NA	NA
0.005	3	3	3	3	3	NA	NA
0.01	3	2	2	3	2	NA	NA
0.01	4	3	4	4	4	NA	2
0.34	4	5	5	4	6	3	3
0.04	4	4	4	4	4	1	3
0.22	4	4	5	4	4	3	3
0.05	4	4	4	4	4	2	3
0.40	4	4	5	4	4	4	3
0.46	4	4	5	4	4	4	4
2.29	5	6	6	4	4	5	5
3.27	5	5	5	5	5	5	5
0.10	5	4	4	4	3	2	3
0.26	5	4	5	4	4	3	3
1.01	5	4	5	4	4	4	4
0.43	5	4	5	4	4	4	4
51.27	6	6	7	6	7	8	6
10.36	6	6	5	5	5	6	5
1.54	6	4	5	5	5	5	4
15.97	7	7	6	6	6	7	5
8.53	7	6	6	5	5	6	5
MSE VALUES		**0.79**	**0.74**	**0.81**	**1.05**	**1.86**	**2.02**
R^2 VALUES		**0.65**	**0.73**	**0.74**	**0.59**	**0.64**	**0.53**

Table 4.13 shows that the best ANN model when Ia is used as the main ground motion parameter is selected as M15 with the inclusion of Mw, Repi, SC, and FD into the inputs. Utilization of Arias Intensity improved predictions of lower MMI values while it did not increase the performance for higher MMI values.

The multivariate relationship proposed by Tselentis and Danciu (2008) includes Ia, Epicentral Distance (Repi) and Soil Class (SC). The ANN model with Ia yielded higher performance than Ia-based predictive models by Tselentis and Danciu (2008).

Therefore, including additional parameters such as Mw, and FD improved the performance.

However, when the performances of the Ia ANN model are compared with the other ANN models which employ PGA, PGV, and PGD, it is observed that the arias intensity is not a particularly representative parameter for the prediction of felt intensity.

CHAPTER 5

CONCLUSIONS

5.1. Conclusions

In this thesis, the non-linear relationships between felt intensity (macroseismic) and various sets of ground motion parameters are studied through the ANN method using data from recent earthquakes in Turkey. The dataset includes a total of 195 ground motion records from 18 earthquakes. In order to select the input parameters of the ANN models, a combination of the PCA analysis, literature and expert knowledge is used.

The following main conclusions are derived from this study:

- When PGA is used as the main ground motion parameter, the inclusion of Mw and Repi as the inputs to the ANN model, the best model is obtained. The performance of the ANN models developed in this study is closer to those of Bilal and Askan (2014), and Faenza and Michelini (2010).
- When PGV is used as the main ground motion parameter, ANN model performances are increased by adding Mw, Repi, SC, and FD. Although previous studies suggest that only high levels of seismic intensity correlate well with PGV, it is observed in this study that including additional variables such as Mw, Repi, SC, and FD to the PGV increase the performance at all intensity levels. Similar to the case of PGA, the performance of the ANN model is similar to those of Bilal and Askan (2014), and Faenza and Michelini (2010).
- When PGD is used as the main ground motion parameter, ANN model performance improves when Mw, Repi, and SC are added to the inputs. In the literature, PGD is not commonly used in felt intensity prediction equations

since PGD corresponds only to longer structural periods. The ANN model with PGD presented in this study could be used in future studies to indirectly predict the potential damage to flexible structures with longer periods.

- When Ia is used as the main ground motion parameter together with Mw, Repi, SC, and FD the best ANN model is obtained. The ANN model with Ia yielded smaller error than Ia based predictive models by Tselentis and Danciu (2008). However, when the performances of the Ia model are compared with the others, it is observed that the arias intensity is not a representative parameter for the prediction of felt intensity.
- The ANN models with best performances (M1 for PGA, M7 for PGV, M10 for PGD, M15 for Ia) showed that the addition of significant duration (D_{5-95}) to the input variable set does not improve the prediction performance of felt intensity.
- For ANN models with PGD, and Ia, it is observed that addition of site class term yields a drastically better performance when compared to the ANN model without this term.
- Most of the existing intensity prediction models exhibit varying performance levels at different intensity ranges. However, since trained for the whole felt intensity range, developed ANN models give consistent performances throughout the entire felt intensity scale.
- As a final remark, it is observed that ANN handles the inherent complexity due to the nonlinearity of the felt intensity prediction problem.

5.2. Future Work and Recommendations

Although the analysis presented in this study suggest some promising findings that can be used in future ShakeMap applications in Turkey, there are indeed some constraints due to the fact that this study depends solely on a limited dataset. Following are some recommendations and future works that can be made for further investigation:

- For reliable analysis, the dataset must be correct and complete in terms of all independent variables. For the future studies, it is recommended to use multiple sources to achieve a complete dataset such as online databases, catalogues or digitized maps.
- In this study, various parameters such as PGA, PGV, PGD, Ia, Mw, Repi, Vs30, FD, $D_{5\text{-}95}$ are used. In the future studies, additional parameters such as building types, population density, duration of earthquake, cumulative absolute velocity and any other quantitative seismic parameters could be inserted to the dataset for further analysis and investigation.
- In this study, MMI values are used from both United States Geological Survey-Did You Feel It? (DYFI) website, and from the previous study of Bilal and Askan (2014). As previously mentioned, DYFI values are an online public survey that people can summarize the effects of shaking in their regions. In Turkey, a similar project could be implemented where people should be encouraged to actively participate. Such a data source could provide abundant data.
- In the dataset, some of the intensity maps are taken from the study of Bilal and Askan (2014) which are not in a digitized form. Those maps could be digitized for more accurate felt intensity values.
- Most of the recorded data belongs to earthquakes which occurred on strike-slip faults. Therefore, fault type is not included as a parameter in the analysis steps. For the future studies, fault type can be added as an additional input variable.

- An important point which affects the MMI values in a region is the seismic design of the nearby buildings. In other words, in regions where most buildings comply with the seismic code, lower MMI values will be assigned. Thus, the seismic quality of the buildings may be inserted into the dataset for future analyses.

REFERENCES

AFAD Deprem Ön Hasar ve Kayıp Tahmin Sistemi (AFAD-RED): https://deprem.afad.gov.tr/icerik?id=13

Alvarez, D. A., Hurtado, J. E. and Bedoya-Ruíz, D. A. (2012), Prediction of modified Mercalli intensity from PGA, PGV, moment magnitude, and epicentral distance using several nonlinear statistical algorithms', *Journal of Seismology*, 16(3), pp. 489–511.

American Society of Civil Engineers (ASCE) Task Committee (2000), Artificial Neural Networks in Hydrology I: Preliminary Concepts. By the ASCE Task Committee on Application of Artificial Neural Networks in Hydrology', *Journal of Hydrologic Engineering*.

Arıoğlu, E., Arıoğlu, B., Girgin, C., (2001), Doğu Marmara Depreminin İvme Değerleri Açısından Değerlendirilmesi, Beton Prefabrikasyon, 57-58, 5-15.

Arslan, M. H., Ccylan, M. and Koyuncu, T. (2012), An ANN Approaches on Estimating Earthquake Performances of Existing RC Buildings, *Neural Network World*.

ASCE Task Committee (2000), Artificial Neural Networks in hydrology. II: Hydrologic applications, *Journal of Hydrologic Engineering*.

Atkinson, G. M. and Kaka, S. I. (2006), Relationships Between Felt Intensity and Instrumental Ground Motion for New Madrid ShakeMaps, (March), pp. 1–27.

Atkinson, G. M. and Kaka, S. L. I. (2007), Relationships between felt intensity and instrumental ground motion in the Central United States and California, *Bulletin of the Seismological Society of America*, 97(2), pp. 497–510.

Atkinson, G. M. and Sonley, E. (2000), Empirical relationships between Modified Mercalli Intensity and response spectra, *Bulletin of the Seismological Society of America*, 90(2), pp. 537–544.

Bilal, M. and Askan, A. (2014), Relationships between felt intensity and recorded ground-motion parameters for Turkey, *Bulletin of the Seismological Society of America*, 104(1), pp. 484–496.

Boatwright, J., Thywissen, K. and Seekins, L. C. (2001), Correlation of ground motion and intensity for the 17 January 1994 Northridge, California, earthquake, *Bulletin of the Seismological Society of America*, 91(4), pp. 739–752.

Bohm, G. and Zech, G. (2010), *Introduction to statistics and data analysis for physicists, Statsref.Com*.

Cattell, R. B. (1966). The Scree Plot Test for the Number of Factors. Multivariate Behavioral Research, 1, 140-161.

Demuth, H. and Beale Mark (2003), Neural Network Toolbox for Use with MATLAB - User Guide, *The MathWorks*.

Elarabi, H., and Khadheeja, A. (2008), Soil Classification Modelling Using Artificial Neural Network.

Faenza, L. and Michelini, A. (2010), Regression analysis of MCS intensity and ground motion parameters in Italy and its application in ShakeMap, *Geophysical Journal International*, 180(3), pp. 1138–1152.

Günaydın, K. and Günaydn, A. (2008), Peak ground acceleration prediction by artificial neural networks for northwestern Turkey, *Mathematical Problems in Engineering*, 2008.

Hagan, M. T., Demuth, H. B. and Beale, M. H. (1995), Neural Network Design, *Boston Massachusetts PWS*.

Haykin, S. (2009), *Neural Networks and Learning Machines*, *Pearson Prentice Hall New Jersey USA 936 pLinks*.

Hecht-Nielsen, R. (1987), Kolmogorov's Mapping Neural Network Existence Theorem.

Hsu, K. -l, Gupta, H. V. and Sorooshian, S. (1995), Artificial Neural Network Modeling of the Rainfall-Runoff Process, *Water Resources Research*.

Husid, L.R. (1969). Caracteristicas de Terremotos. Analisis General. Revista del IDIEM 8, Santiago de Chile, 21-42.

IBM Corp. Released in 2016. IBM SPSS Statistics for Windows, Version 24.0. Armonk, NY: IBM Corp.

Imrie, C. E., Durucan, S. and Korre, A. (2000), River flow prediction using artificial neural networks: Generalisation beyond the calibration range, *Journal of Hydrology*.

Iyengar, R. N. and Prodhan, K. C. (1983), Classification and rating of strong-motion earthquake records, *Earthquake Engineering & Structural Dynamics*.

Jain, A. K., Mao, J. and Mohiuddin, K. M. (1996), Artificial neural networks: A tutorial, *Computer*.

Jolliffe, I. T. (2002), Principal Component Analysis, Second Edition, *Encyclopedia of Statistics in Behavioral Science*.

Kaiser, H. F. (1960). The application of electronic computers to factor analysis. Educational and Psychological Measurement, 20, 141-151.

Kaka, S. L. I. and Atkinson, G. M. (2004), Relationships between instrumental ground-motion parameters and modified Mercalli intensity in eastern North America, *Bulletin of the Seismological Society of America*, 94(5), pp. 1728–1736.

Krinitzsky, E. L. and CHANG, F. K. (1988), Intensity-Related Earthquake Ground Motions, *Environmental & Engineering Geoscience*.

MatLab, M. (2012), The Language of Technical Computing, *The MathWorks, Inc. http://www. mathworks. com*.

Mazlum, N., Özer, A. and Mazlum, S. (1999), Interpretation of water quality data by principal components analysis, *Turkish Journal of Engineering and Environmental Sciences*, 23(1), pp. 19–26.

Modified Mercalli Intensity Scale, https://www.usgs.gov/media/images/modified-mercalli-intensity-scale

Murphy, J. R., and O'Brien, L. J. (1977), The correlation of peak ground acceleration amplitude with seismic intensity and other physical parameters, Bull. Seismol. Soc. Am. 67, 877–915

Musson, R. M., Cecić, I. (2012): Intensity and Intensity Scales. - In: Bormann, P. (Ed.), New Manual of Seismological Observatory Practice 2 (NMSOP-2), Potsdam: Deutsches GeoForschungsZentrum GFZ, pp. 1—41. (DOI: http://doi.org/10.2312/GFZ.NMSOP-2_ch12)

Narayanakumar, S. and Raja, K. (2016), A BP Artificial Neural Network Model for Earthquake Magnitude Prediction in Himalayas, India, *Circuits and Systems*, 07(11), pp. 3456–3468.

National Earthquake Hazards Reduction Program (NEHRP) (https://www.nehrp.gov/).

Nguyen, V. H., Mahowald, J., Golinval, J. C., Maas, S. (2014), Damage detection in civil engineering structure considering temperature effect, Conference Proceedings of the Society for Experimental Mechanics Series, 4, pp. 187–196.

Ornthammarath, T., Corigliano, M., and Lai, C.G. (2008), Artificial Neural Networks Applied to The Seismic Design of Deep Tunnels.

Richter CF (1958). Elementary seismology. W. H. Freeman and Company, San Francisco and London, viii + 768 pp.

Sieberg A (1932). Geologie der Erdbeben. Handbuch der Geophysik, Gebrüder Bornträger, Berlin, 2(4): 550-555.

Stover, C. W. and Coffman, J. L. (1993), Seismicity of the United States, 1568-1989 (revised), *US Geological Survey Professional Paper*

Teh, C. I. *et al.* (1997), Prediction of pile capacity using neural networks, *Journal of Computing in Civil Engineering*.

Tolon, M., & Ural, D. (2012). Liquefaction Analysis in 3 D based on Neural Network Algorithm.

Trifunac, M. D. and Brady, A. G. (1975), On the correlation of seismic intensity scales with the peaks of recorded strong ground motion, *Bulletin of the Seismological Society of America*.

Tselentis, G. A. and Danciu, L. (2008), Empirical relationships between modified Mercalli intensity and engineering ground-motion parameters in Greece, *Bulletin of the Seismological Society of America*, 98(4), pp. 1863–1875.

Tselentis, G. A. and Vladutu, L. (2010), An attempt to model the relationship between MMI attenuation and engineering ground-motion parameters using artificial neural networks and genetic algorithms, *Natural Hazards and Earth System Science*, 10(12), pp. 2527–2537.

U.S. Geological Survey (USGS), USGS-ShakeMap (via https://earthquake.usgs.gov/).

Uniform Building Code (1997), Uniform building code, American Association of Building Officials, Whittier, CA.

Wald, DJ., Quitoriano, V., Heaton, TH., Kanamori, H., Scrivner, CW., Worden, BC. (1999). TriNet “ShakeMaps”: Rapid generation of peak ground-motion and intensity maps for earthquakes in southern California. Earthquake Spectra 15(3): 537–556

Web Page of Strong Ground Motion Database of Turkey, http://kyhdata.deprem.gov.tr/2K/kyhdata_v4.php

Wood, H.O. and Neumann, F. (1931), Modified Mercalli Intensity Scale of 1931, Bulletin of the Seismological Society of America, Vol. 21, No. 4, pp. 277-283.

Wu, Y. M., Hsiao, N. C. and Teng, T. L. (2004), Relationships between strong ground motion peak values and seismic loss during 1999 Chi-Chi, Taiwan Earthquake, *Natural Hazards*, 32(3), pp. 357–373.

Yaghmaei-Sabegh, S., Tsang, H. H. and Lam, N. T. K. (2011), Conversion Between Peak Ground Motion Parameters and Modified Mercalli Intensity Values, *Journal of Earthquake Engineering*, 15(7), pp. 1138–1155.

APPENDICES

A. Detailed Description of MMI Scale

Figure A.1 shows the detailed description of MMI scale.

Intensity	Shaking	Description/Damage
I	Not felt	Not felt except by a very few under especially favorable conditions.
II	Weak	Felt only by a few persons at rest,especially on upper floors of buildings.
III	Weak	Felt quite noticeably by persons indoors, especially on upper floors of buildings. Many people do not recognize it as an earthquake. Standing motor cars may rock slightly. Vibrations similar to the passing of a truck. Duration estimated.
IV	Light	Felt indoors by many, outdoors by few during the day. At night, some awakened. Dishes, windows, doors disturbed; walls make cracking sound. Sensation like heavy truck striking building. Standing motor cars rocked noticeably.
V	Moderate	Felt by nearly everyone; many awakened. Some dishes, windows broken. Unstable objects overturned. Pendulum clocks may stop.
VI	Strong	Felt by all, many frightened. Some heavy furniture moved; a few instances of fallen plaster. Damage slight.
VII	Very strong	Damage negligible in buildings of good design and construction; slight to moderate in well-built ordinary structures; considerable damage in poorly built or badly designed structures; some chimneys broken.
VIII	Severe	Damage slight in specially designed structures; considerable damage in ordinary substantial buildings with partial collapse. Damage great in poorly built structures. Fall of chimneys, factory stacks, columns, monuments, walls. Heavy furniture overturned.
IX	Violent	Damage considerable in specially designed structures; well-designed frame structures thrown out of plumb. Damage great in substantial buildings, with partial collapse. Buildings shifted off foundations.
X	Extreme	Some well-built wooden structures destroyed; most masonry and frame structures destroyed with foundations. Rails bent.

Figure A.1. Description of MMI Scale (https://www.usgs.gov/media/images/modified-mercalli-intensity-scale)

B. Matlab Script for Converting Seismic Ground Motion Parameters

Matlab Script for converting seismic ground motion parameters (Brian Carlton, 2005) are given below.

```
%seismicparam
% This function calculates seismic parameters from an acceleration time
% series. Specifically, it calculates velocity vs time, displacement vs
% time, peak ground acceleration (PGA), peak ground velocity (PGV), peak
% ground displacement (PGD), Arias intensity vs time, total Arias intensity
% (Ia), time between when 5% and 75% of Ia has occurred (significant
% duration D5-75), time between when 5% and 95% of Ia has occurred
% (significant duration D5-95), mean period (Tm), pseudo-acceleration
% response spectrum (Sa), pseudo-velocity response spectrum (Sv),
% displacement response spectrum (Sd), and the Fourier amplitude spectrum
% (FAS).
%
% Written by Brian Carlton 18 March 2015
%
% SYNTAX
% [param]=seismicparam(time,acc,damp,LUF,HUF)
%
% MANDATORY INPUTS
% acc = acceleration vector in g
% time = time vector in seconds, must be the same length as acc
%
% OPTIONAL INPUTS
% damp = damping ratio for response spectra
%       default = 0.05
% LUF = lowest usable frequency of response spectra
%       default = 0.10
% HUF = highest usable frequency of response spectra
%       default = (1/dt)/2 (Nyquist frequency)
%
% OUTPUT
% param = MATLAB structure with the following fields
%
% param.vel = velocity time series in cm/s
% param.disp = displacement time series in cm
% param.PGA = peak ground acceleration in g
% param.PGV = peak ground velocity in cm/s
% param.PGD = peak ground displacement in cm
% param.aint2 = cumulative fraction of Arias intensity occurring with time
% param.arias = total arias intensity at end of time series in m/s
```

```
% param.D_5_75 = time between when 5% and 75% of Ia has occurred (significant
%       duration D5-75) in seconds
% param.t_5_75 = time when 5% and 75% of Ia has occurred in seconds
% param.D_5_95 = time between when 5% and 95% of Ia has occurred (significant
%       duration D5-95) in seconds
% param.t_5_95 = time when 5% and 95% of Ia has occurred in seconds
% param.Tm = mean period in seconds according to Rathje et al (2004)
% param.Period = periods for response spectra
% param.Sa = pseudo-acceleration response spectrum in g
% param.Sv = pseudo-velocity response spectrum in cm/s
% param.Sd = displacement response spectrum in cm
% param.FAS = Fourier amplitude spectrum in g
% param.freq = frequencies for Fourier amplitude spectrum in Hz
function[param]=seismicparam(time,acc,damp,LUF,HUF)
acc = acc(:);
time = time(:);
g = 9.81;
A   = acc*g; %convert to m/s^2
dt = time(2)-time(1);
% Check what variables are specified by the user, if a variable is not
% specified, then assign the default value
if exist('damp','var') == 0;
   damp = 0.05;
end
if exist('LUF','var') == 0;
   LUF = 0.10;
end
if exist('HUF','var') == 0;
   HUF = (1/dt)/2;
   if HUF > 100;
      HUF = 100;
   end
end
% TIME SERIES
param.vel = cumsum(A)*dt*100;
param.disp = cumsum(param.vel)*dt;
% PEAK RESPONSES
param.PGA = max(abs(A))/g;
param.PGV = max(abs(param.vel));
param.PGD = max(abs(param.disp));
% ARIAS INTENSITY
aint2 = cumsum(A.^2)*pi*dt/(2*g);
arias = aint2(end);
param.aint2 = aint2/arias;
```

```
param.arias = arias;
% DURATION
timed = time(aint2>=0.05*arias & aint2<=0.75*arias);
param.t_5_75 = [timed(1),timed(end)];
param.D_5_75 = timed(end)-timed(1);
timed = time(aint2>=0.05*arias & aint2<=0.95*arias);
param.t_5_95 = [timed(1),timed(end)];
param.D_5_95 = timed(end)-timed(1);
% RESPONSE SPECTRA
[Sa,Sv,Sd,T]=rs(acc,dt,damp,LUF,HUF);
param.Sd=Sd(:);
param.Sv=Sv(:);
param.Sa=Sa(:);
param.Period = T(:);
% FOURIER AMPLITUDE SPECTRUM
[f,U]=FAS(dt,acc);
param.FAS = U;
param.freq = f;
% MEAN PERIOD (Rathje et al, 2004)
fi = f(f>0.25 & f<20);
Ci = U(f>0.25 & f<20);
Tm = ((Ci(:)'.^2)*(1./fi(:)))/(Ci(:)'*Ci(:));
param.Tm = Tm;
function[Sa,Sv,Sd,T]=rs(acc,dt,damp,LUF,HUF)
Acccms=acc*981;%convert from g to cm/s^2
if dt > .005;
    beta = .25;
else beta = 1/6;
end
gamma= 0.5; %parameters for Newmark's method
%average acceleration method gamma = 0.5, beta = .25, linear acceleration
%method gamma = 0.5, beta = 1/6.  Average acceleration method is
%unconditionally stable, but less accurate.  Linear acceleration method is
%stable for dt/T < 0.551 but more accurate (Chopra, 2011)
Tlong = LUF^-1; %lowest usable frequency = 1/max period
Tshort = HUF^-1; %highest usable frequency = 1/min period
T = 10.^linspace(log10(Tshort),log10(Tlong),150); %150 points
umax = zeros(1,length(T));
for j=1:length(T)
   wn = 2*pi/T(j);
   m = 1;%then c and k are in terms of damping and natural period
   k = wn^2;
   c = 2*wn*damp;
   khat = k+gamma/beta/dt*c+m/beta/dt^2;
```

```
    a = m/beta/dt+gamma*c/beta;
    b = 1/2/beta*m+dt*(gamma/2/beta-1)*c;
    u = zeros(length(Acccms),1); %oscillator starting from rest
    udot = zeros(length(Acccms),1);%pre-allocate for speed
    uddot = zeros(length(Acccms),1);
    du = zeros(length(Acccms)-1,1);
    dudot = zeros(length(Acccms)-1,1);
    duddot = zeros(length(Acccms)-1,1);
    for i = 1:length(Acccms)-1
       du(i) = (Acccms(i+1)-Acccms(i)+a*udot(i)+b*uddot(i))/khat;
       u(i+1) = u(i)+du(i);
       dudot(i)          =          gamma*du(i)/beta/dt-gamma*udot(i)/beta+dt*(1-
gamma/2/beta)*uddot(i);
       udot(i+1) = udot(i)+dudot(i);
       duddot(i) = du(i)/beta/dt^2-udot(i)/beta/dt-uddot(i)/2/beta;
       uddot(i+1) = uddot(i)+duddot(i);
    end
    umax(j) = max(abs(u));%max displacement for every period T (cm)
end
Sd = umax; %displacement in cm
Sv=2*pi*Sd./T;%pseudo velocity in cm/s
Sa=2*pi*Sv./T/981;%pseudo acceleration in g
function[f,U]=FAS(dt,acc)
Ny = (1/dt)/2; %Nyquist frequency (highest frequency)
L  = length(acc); %number of points in acc
NFFT = 2^nextpow2(L); % Next power of 2 from length of acc
df = 1/(NFFT*dt); %frequency spacing
U = abs(fft(acc,NFFT))*dt; %Fourier amplitudes
U = U(2:Ny/df+1); %single sided FAS
f = linspace(df,Ny,Ny/df)'; %[small, large, number] frequencies
```

C. Dataset used in the Study

Table C.1. *Dataset Used in the Study*

Record No.	Earthquake ID	Station ID	Mw	PGA (cm/sec2)	PGV (cm/sec)	PGD (cm)	Arias Intensity (cm/s)	D_5_95 (sec)	Focal Depth (km)	Epicentral Distance (km)	Soil Classification (in numbers)	Soil Classification	MMI	MMI_ Numbers
1	KOC8/99	1604	7.4	50.065	40.58	2482.20	7.65745	34.48	17	95	3	C	VI	6
2	KOC8/99	5903	7.4	95.86	16.68	146.97	15.9708	17.3325	17	170	2	D	VI	6
3	KOC8/99	3401	7.4	51.665	9.08	172.04	4.44877	37.81	17	86	3	C	VI	6
4	KOC8/99	3403	7.4	103.82	15.73	34.60	15.9663	9.3825	17	105	2	D	VII	7
5	KOC8/99	1612	7.4	107.605	24.83	96.16	42.4251	33.08	17	40	2	D	VII	7
6	KOC8/99	4106	7.4	203.135	112.56	2680.89	49.6382	29.6325	17	43	3	C	VIII	8
7	KOC8/99	8101	7.4	344.32	56.10	75.03	127.086	11.975	17	101	2	D	IX	9
8	KOC8/99	4101	7.4	198.04	84.55	2144.12	88.03	34.325	17	3	4	B	IX	9
9	KOC8/99	5401	7.4	203.625	45.23	1373.00	99.3768	193.805	17	36	3	C	X	10
10	KOC8/99	6001	7.4	1.005	1.83	67.12	0.00575	65.355	17	561	2	D	II	2
11	KOC8/99	4302	7.4	54.855	13.28	104.48	18.4138	56.14	17	149	2	D	IV	4
12	KOC8/99	901	7.4	5.615	4.03	306.28	0.32764	136.095	17	374	2	D	II	2
13	KOC8/99	2002	7.4	8.805	9.35	315.97	0.2904	37.575	17	336	2	D	IV	4
14	KOC8/99	3502	7.4	10.345	3.56	126.16	0.50207	75.06	17	349	2	D	IV	4
15	KOC8/99	3701	7.4	10.3	5.80	168.17	0.62564	81.965	17	344	3	C	IV	4
16	KOC8/99	1701	7.4	26.6	8.46	61.34	4.05165	57.42	17	310	2	D	V	5
17	KOC8/99	6401	7.4	12.755	5.46	183.39	0.68653	49.53	17	237	2	D	IV	4
18	KOC8/99	1001	7.4	17.975	5.91	207.48	1.07198	45.22	17	218	3	C	V	5
19	KOC8/99	301	7.4	14.25	32.88	2990.95	1.43548	62.6255	17	226	2	D	V	5
20	KOC8/99	4501	7.4	9.5	75.52	6355.46	0.54616	89.121	17	327	2	D	IV	4
21	KOC8/99	1404	7.4	127.795	29.49	363.59	23.5251	11.5875	17	82	2	D	VII	7
22	AFY2/02	1006	6.5	1.605	1.04	17.14	0.01312	30.71	22.1	338	2	D	I	1
23	AFY2/02	5401	6.5	1.115	1.09	38.37	0.00466	46.53	22.1	256	3	C	I	1
24	AFY2/02	1001	6.5	1.255	1.01	22.63	0.00824	48.125	22.1	313	3	C	I	1
25	AFY2/02	1502	6.5	2.515	3.36	82.35	0.02363	33.59	22.1	125	2	D	III	3

Table C.1 *Dataset Used in the Study (continued)*

Record No.	Earthquake ID	Station ID	Mw	PGA (cm/sec2)	PGV (cm/sec)	PGD (cm)	Arias Intensity (cm/s)	D_5_95 (sec)	Focal Depth (km)	Epicentral Distance (km)	Soil Classification (in numbers)	Soil Classification	MMI	MMI_ Numbers
26	AFY2/02	6401	6.5	6.915	1.56	11.50	0.17454	26.115	22.1	157	2	D	III	3
27	AFY2/02	4302	6.5	21.955	3.68	21.73	1.68609	25.38	22.1	144	2	D	IV	4
28	AFY2/02	301	6.5	103.75	34.82	2570.00	1599.75	15.5585	22.1	65	2	D	V	5
29	BGA7/83	1012	6.1	49.975	28.64	247.67	3.29067	10.55	6.9	55	3	C	VII	7
30	BGA7/83	1013	6.1	26.58	4.38	15.56	0.64771	9.65	6.9	84	2	D	V	5
31	BGA7/83	1014	6.1	48.44	49.84	366.28	3.03684	12.145	6.9	44	3	C	VII	7
32	BGA7/83	5901	6.1	32.4	10.65	66.38	1.38991	8.65	6.9	74	3	C	VI	6
33	DNZ8/76	2001	6.1	319.445	262.83	2046.46	74.9273	8.49	19.8	10	2	D	VI	6
34	EZR10/83	2503	6.6	161.78	45.73	107.94	51.2728	19.225	16.1	35	2	D	VI	6
35	COR8/96	1902	5.7	23.265	3.84	11.68	0.55773	7.0325	11.9	49	2	D	IV	4
36	COR8/96	502	5.7	40.25	3.16	66.42	1.95385	8.0035	11.9	48	3	C	III	3
37	ORT6/00	1801	6	62.81	7.80	69.54	10.3645	36.632	10	15	2	D	VI	6
38	ORT6/00	1401	6	6.305	1.93	10.10	0.05299	17.808	10	116	2	D	IV	4
39	ORT6/00	8101	6	4.135	1.07	4.36	0.03354	16.98	10	155	2	D	III	3
40	ORT6/00	3701	6	11.935	1.72	61.15	0.27862	30.125	10	95	3	C	V	5
41	ORT6/00	7801	6	5.625	0.89	37.80	0.05722	35.056	10	63	3	C	V	5
42	ORT6/00	4302	6	3.925	3.19	169.71	0.0663	67.16	10	293	2	D	III	3
43	ADN6/98	3301	6.2	125.705	26.24	280.54	8.75164	11.35	46.6	65	3	C	III	3
44	ADN6/98	202	6.2	3.75	20.28	879.97	0.09803	57.977	46.6	230	3	C	II	2
45	ADN6/98	105	6.2	248.415	28.61	75.60	100.142	13.175	46.6	48	2	D	VIII	8
46	ADN6/98	4603	6.2	8.25	47.97	2950.85	0.28193	64.8045	46.6	163	3	C	II	2
47	ADN6/98	4605	6.2	4.93	3.29	67.33	0.07096	25.31	46.6	223	2	D	II	2
48	ADN6/98	3102	6.2	26.46	3.73	16.31	1.64557	15.955	46.6	103	3	C	III	3
49	ADN6/98	110	6.2	30.8	17.90	186.82	2.28917	17.3975	46.6	31	3	C	V	5
50	IZM11/92	3501	6	34.415	10.90	41.61	3.26826	12.8725	17.2	43	2	D	V	5

Table C.1 *Dataset Used in the Study (continued)*

Record No.	Earthquake ID	Station ID	Mw	PGA (cm/sec2)	PGV (cm/sec)	PGD (cm)	Arias Intensity (cm/s)	D_5_95 (sec)	Focal Depth (km)	Epicentral Distance (km)	Soil Classification (in numbers)	Soil Classification	MMI	MMI_ Numbers
51	IZM11/92	905	6	77.645	13.93	134.95	8.07432	10.14	17.2	39	3	C	VI	6
52	EZC3/92	2403	6.6	76.57	19.15	139.25	5.55945	11.2875	22.6	76	3	C	IV	4
53	EZC3/92	2405	6.6	33.175	13.28	100.98	3.38298	17.9625	22.6	59	2	D	III	3
54	DZC11/99	5902	7.1	5.905	1.84	19.80	0.10018	27.58	10.4	309	3	C	V	5
55	DZC11/99	4302	7.1	18.905	7.95	96.98	3.22612	50.915	10.4	185	2	D	III	3
56	DZC11/99	5401	7.1	21.025	5.00	93.12	1.31162	27.285	10.4	68	3	C	VIII	8
57	DZC11/99	301	7.1	9	14.14	898.81	0.44833	56.3405	10.4	233	2	D	IV	4
58	DZC11/99	1604	7.1	8.655	2.62	22.66	0.2813	35.29	10.4	188	3	C	V	5
59	DZC11/99	1701	7.1	3.635	1.99	42.14	0.11866	51.7	10.4	414	2	D	IV	4
60	DZC11/99	2002	7.1	3.585	4.03	110.38	0.15533	58.45	10.4	380	2	D	III	3
61	DZC11/99	1404	7.1	26.355	9.28	79.33	2.03917	22.0375	10.4	57	2	D	VII	7
62	DZC11/99	1406	7.1	89.665	24.90	309.47	15.5121	16.7225	10.4	38	2	D	VII	7
63	DZC11/99	1001	7.1	2.55	2.33	51.45	0.03384	56.9	10.4	313	3	C	IV	4
64	DZC11/99	3502	7.1	1.725	2.06	95.53	0.03559	89.815	10.4	433	2	D	III	3
65	DZC11/99	3701	7.1	7.78	3.33	57.07	0.34757	53.785	10.4	240	3	C	III	3
66	DZC11/99	6401	7.1	3.065	2.22	37.55	0.05561	55.11	10.4	283	2	D	II	2
67	DZC11/99	8101	7.1	460.735	78.67	257.13	294.024	11.02	10.4	5	2	D	X	10
68	DZC11/99	3401	7.1	7.11	3.24	102.40	0.16339	33.09	10.4	185	3	C	V	5
69	DZC11/99	1401	7.1	772.695	62.22	71.22	319.75	8.785	10.4	36	2	D	X	10
70	VAN10/11	208	7.2	0.93	0.48	2.13	0.0059	47.89	19.02	521	3	C	III	3
71	VAN10/11	401	7.2	16.775	5.35	56.26	2.32683	94.915	19.02	121	2	D	VI	6
72	VAN10/11	1206	7.2	9.305	3.63	13.48	0.55988	61.62	19.02	222	2	D	VI	6
73	VAN10/11	1211	7.2	4.395	2.43	9.11	0.1665	79.48	19.02	211	3	C	VI	6
74	VAN10/11	2307	7.2	1.88	1.14	10.83	0.04964	94.1	19.02	307	2	D	IV	4
75	VAN10/11	2401	7.2	1.415	1.05	5.05	0.02323	85.51	19.02	358	2	D	IV	4

Table C.1 *Dataset Used in the Study (continued)*

Record No.	Earthquake ID	Station ID	Mw	PGA (cm/sec2)	PGV (cm/sec)	PGD (cm)	Arias Intensity (cm/s)	D_5_95 (sec)	Focal Depth (km)	Epicentral Distance (km)	Soil Classification (in numbers)	Soil Classification	MMI	MMI_ Numbers
76	VAN10/11	2407	7.2	2.905	2.07	8.98	0.07847	84.045	19.02	289	2	D	IV	4
77	VAN10/11	4404	7.2	1	0.67	7.50	0.01131	87.74	19.02	405	4	B	IV	4
78	VAN10/11	4901	7.2	8.585	2.55	16.44	0.52882	56.56	19.02	170	2	D	VII	7
79	VAN10/11	4902	7.2	50.25	13.34	198.77	8.53144	32.2455	19.02	95	2	D	VII	7
80	VAN10/11	6503	7.2	174	21.10	65.72	66.4334	20.752	19.02	42	2	D	VIII	8
81	VAN10/11	7201	7.2	8.445	2.48	18.53	0.34043	38.685	19.02	223	3	C	IV	4
82	EGE05/14	3408	6.5	8.98	2.34	12.17	0.36123	76.85	25.02	265	3	C	V	5
83	EGE05/14	3518	6.5	9.875	3.63	682.61	0.39719	60.755	25.02	254	2	D	IV	4
84	EGE05/14	3523	6.5	5.145	1.83	228.32	0.12918	57.725	25.02	245	3	C	II	2
85	EGE05/14	3515	6.5	8.445	3.22	705.96	0.45514	60.825	25.02	249	1	E	III	3
86	EGE05/14	4501	6.5	5.585	1.51	14.94	0.19525	69.365	25.02	253	2	D	III	3
87	EGE05/14	3530	6.5	8.855	1.41	6.70	0.32612	51.46	25.02	257	2	D	IV	4
88	EGE05/14	1613	6.5	15.93	1.60	8.86	0.67333	26.345	25.02	336	3	C	IV	4
89	EGE05/14	1614	6.5	19.365	2.31	7.20	0.9694	44.03	25.02	264	2	D	IV	4
90	EGE05/14	1625	6.5	10.24	1.90	3.86	0.49575	59.52	25.02	322	3	C	IV	4
91	EGE05/14	1626	6.5	19.065	3.65	9.25	1.07909	56.895	25.02	312	3	C	IV	4
92	EGE05/14	3513	6.5	13.675	2.45	132.07	0.98212	53.08	25.02	253	2	D	IV	4
93	EGE05/14	3514	6.5	3.83	1.54	181.29	0.06443	65.295	25.02	251	4	B	IV	4
94	EGE05/14	3525	6.5	3.56	1.51	217.72	0.0517	59.97	25.02	258	3	C	III	3
95	EGE05/14	3415	6.5	21.43	2.23	8.85	1.23332	37.95	25.02	303	2	D	IV	4
96	EGE05/14	1627	6.5	15.375	4.61	12.43	1.66156	74.785	25.02	320	2	D	IV	4
97	EGE05/14	1620	6.5	7.37	1.65	4.22	0.20072	53.76	25.02	325	3	C	IV	4
98	EGE05/14	3407	6.5	4.32	1.04	7.97	0.05706	39.545	25.02	324	3	C	III	3
99	EGE05/14	3510	6.5	6.285	1.85	175.89	0.15679	49.845	25.02	251	2	D	III	3
100	EGE05/14	3519	6.5	11.655	3.59	447.43	0.81475	70.515	25.02	251	1	E	IV	4

Table C.1 *Dataset Used in the Study (continued)*

Record No.	Earthquake ID	Station ID	Mw	PGA (cm/sec2)	PGV (cm/sec)	PGD (cm)	Arias Intensity (cm/s)	D_5_95 (sec)	Focal Depth (km)	Epicentral Distance (km)	Soil Classification (in numbers)	Soil Classification	MMI	MMI_ Numbers
101	EGE05/14	3520	6.5	3.865	1.80	179.64	0.07698	51.56	25.02	254	4	B	IV	4
102	EGE05/14	3522	6.5	7.35	1.52	28.49	0.30418	55.005	25.02	257	2	D	IV	4
103	EGE05/14	5902	6.5	66.395	7.71	72.86	5.42328	13.47	25.02	204	3	C	VII	7
104	EGE06/17	3516	6.2	22.37	1.81	1.97	0.86851	20.255	15.86	73	3	C	V	5
105	EGE06/17	3527	6.2	46.1	4.82	3.43	3.76778	14.765	15.86	29	2	D	IV	4
106	EGE06/17	3518	6.2	18.335	2.18	4.75	1.11863	37.695	15.86	86	2	D	V	5
107	EGE06/17	3503	6.2	52.265	5.59	4.79	7.45463	25.43	15.86	56	2	D	VI	6
108	EGE06/17	1005	6.2	37.25	1.68	1.59	2.9243	20.2	15.86	61	3	C	V	5
109	EGE06/17	1701	6.2	28.74	4.18	2.22	2.71187	33.045	15.86	144	2	D	VI	6
110	EGE06/17	3528	6.2	37.165	2.39	1.40	2.58662	17.98	15.86	61	3	C	V	5
111	EGE06/17	3515	6.2	18.815	2.17	1.63	1.02986	28.045	15.86	80	1	E	V	5
112	EGE06/17	3523	6.2	30.77	2.81	1.59	1.76676	16.34	15.86	70	3	C	V	5
113	EGE06/17	3510	6.2	27.77	2.80	1.78	1.49685	17.525	15.86	80	2	D	V	5
114	EGE06/17	3512	6.2	13.39	0.85	1.32	0.34477	26.095	15.86	88	3	C	V	5
115	EGE06/17	3524	6.2	23.97	1.67	1.26	0.99901	16.565	15.86	79	3	C	V	5
116	EGE06/17	4501	6.2	18	1.93	1.42	0.63896	28.885	15.86	97	2	D	IV	4
117	EGE06/17	3513	6.2	20.24	2.40	2.87	1.11919	55.7	15.86	86	2	D	V	5
118	EGE06/17	3514	6.2	12.29	1.08	1.70	0.2874	26.89	15.86	84	4	B	V	5
119	EGE06/17	3525	6.2	17.475	1.32	1.08	0.55886	16.135	15.86	87	3	C	IV	4
120	EGE06/17	3511	6.2	10.015	1.08	1.05	0.21774	18.96	15.86	95	4	B	IV	4
121	EGE06/17	3520	6.2	10.365	0.91	1.65	0.28101	25.765	15.86	88	4	B	V	5
122	EGE06/17	3522	6.2	21.33	2.73	1.74	1.29454	28.2	15.86	90	2	D	V	5
123	EGE06/17	905	6.2	10.31	1.11	1.13	0.32052	19.45	15.86	138	3	C	IV	4
124	EGE06/17	3530	6.2	17.41	1.92	3.43	0.93365	33.935	15.86	91	2	D	V	5
125	EGE06/17	1710	6.2	13.17	1.22	1.41	0.4755	46.11	15.86	178	2	D	III	3

Table C.1 *Dataset Used in the Study (continued)*

Record No.	Earthquake ID	Station ID	Mw	PGA (cm/sec2)	PGV (cm/sec)	PGD (cm)	Arias Intensity (cm/s)	D_5_95 (sec)	Focal Depth (km)	Epicentral Distance (km)	Soil Classification (in numbers)	Soil Classification	MMI	MMI_ Numbers
126	EGE06/17	1006	6.2	6.7	0.79	1.61	0.21338	43.495	15.86	218	2	D	III	3
127	BDR07/17	709	6.5	1.185	0.45	2.68	0.02037	212.22	19.44	292	3	C	III	3
128	BDR07/17	4803	6.5	25.705	2.79	3.59	2.06241	35.04	19.44	153	2	D	IV	4
129	BDR07/17	4806	6.5	59.265	4.24	15.46	5.93807	25.335	19.44	52	2	D	V	5
130	BDR07/17	4807	6.5	22.49	2.04	3.59	0.76949	18.555	19.44	77	3	C	IV	4
131	BDR07/17	4801	6.5	23.94	1.98	2.40	1.17913	15.66	19.44	87	3	C	V	5
132	BDR07/17	905	6.5	7.15	1.37	2.00	0.18838	54.95	19.44	106	3	C	V	5
133	BDR07/17	4809	6.5	130.385	20.36	18.70	18.4879	7.035	19.44	13	3	C	VI	6
134	BDR07/17	910	6.5	21.54	3.98	5.52	1.64972	86.115	19.44	108	2	D	IV	4
135	BDR07/17	2002	6.5	9.12	1.76	3.64	0.32257	97.37	19.44	177	2	D	III	3
136	BDR07/17	4810	6.5	36.04	1.85	2.24	1.54049	16.42	19.44	72	3	C	VI	6
137	BDR07/17	914	6.5	13.14	3.98	20.19	1.55058	91.96	19.44	136	2	D	IV	4
138	BDR07/17	3522	6.5	4.42	1.39	2.26	0.13665	80.53	19.44	170	2	D	III	3
139	BDR07/17	4501	6.5	1.96	0.81	1.83	0.03524	147.725	19.44	188	2	D	III	3
140	BDR07/17	701	6.5	1.39	0.38	2.08	0.01787	200.24	19.44	287	4	B	III	3
141	CNK02/19	1704	5.1	54.53	1.98	2.22	1.41005	8.405	5.80	20	3	C	II	2
142	CNK02/19	1005	5.1	20.02	0.96	0.18	0.40308	14.145	5.80	39	3	C	II	2
143	CNK02/19	1710	5.1	6.575	0.31	0.31	0.06963	24.905	5.80	94	2	D	II	2
144	CNK02/19	3415	5.1	1.98	0.16	7.51	0.01042	47.445	5.80	252	2	D	II	2
145	CNK02/19	7708	5.1	1.53	0.17	2.78	0.01021	54.395	5.80	265	2	D	II	2
146	CNK02/19	3534	5.1	9.575	0.40	3.98	0.10067	21.3	5.80	108	2	D	II	2
147	CNK02/19	1628	5.1	1.585	0.14	4.76	0.00485	35.325	5.80	239	3	C	III	3
148	CNK02/19	1620	5.1	1.97	0.17	3.98	0.00513	43.145	5.80	239	3	C	III	3
149	CNK02/19	1017	5.1	6.435	0.36	0.24	0.06272	19.255	5.80	123	3	C	III	3
150	CNK02/19	1003	5.1	11.465	0.62	0.33	0.13103	9.025	5.80	123	3	C	III	3

Table C.1 *Dataset Used in the Study (continued)*

Record No.	Earthquake ID	Station ID	Mw	PGA (cm/sec2)	PGV (cm/sec)	PGD (cm)	Arias Intensity (cm/s)	D_5_95 (sec)	Focal Depth (km)	Epicentral Distance (km)	Soil Classification (in numbers)	Soil Classification	MMI	MMI_ Numbers
151	CNK02/19	3524	5.1	3.72	0.24	0.12	0.01434	17.21	5.80	136	3	C	III	3
152	CNK02/19	3521	5.1	5.56	0.55	0.76	0.05983	25.825	5.80	138	1	E	III	3
153	CNK02/19	3515	5.1	3.76	0.30	0.12	0.02527	18.4	5.80	139	1	E	III	3
154	CNK02/19	3514	5.1	1.905	0.14	0.11	0.00711	25.945	5.80	140	4	B	IV	4
155	CNK02/19	3519	5.1	5.72	0.39	0.33	0.05626	25.445	5.80	141	1	E	IV	4
156	CNK02/19	3520	5.1	1.675	0.20	2.13	0.00527	27.915	5.80	142	4	B	IV	4
157	CNK02/19	3513	5.1	2.83	0.32	0.19	0.02164	38.015	5.80	143	2	D	IV	4
158	CNK02/19	3510	5.1	3.985	0.28	0.13	0.0194	14.245	5.80	143	2	D	III	3
159	CNK02/19	3518	5.1	2.695	0.22	0.21	0.0187	33.36	5.80	144	2	D	IV	4
160	CNK02/19	3530	5.1	2.855	0.25	0.16	0.02116	31.535	5.80	145	2	D	IV	4
161	CNK02/19	3506	5.1	1.41	0.10	0.11	0.00187	27.955	5.80	146	4	B	III	3
162	CNK02/19	3512	5.1	1.305	0.09	0.16	0.00445	32.46	5.80	148	3	C	IV	4
163	CNK02/19	3525	5.1	2.085	0.17	0.12	0.00688	22.255	5.80	149	3	C	II	2
164	CNK02/19	3408	5.1	0.58	0.05	0.46	0.001	54.455	5.80	224	3	C	IV	4
165	CNK02/19	1622	5.1	2.08	0.18	0.31	0.01165	52.345	5.80	233	3	C	III	3
166	CNK02/19	1623	5.1	2.89	0.30	0.23	0.02563	22.56	5.80	233	3	C	III	3
167	CNK02/19	3407	5.1	0.515	0.04	0.33	0.00081	76.36	5.80	270	3	C	II	2
168	CNK02/19	4105	5.1	0.755	0.06	0.36	0.00345	58.81	5.80	322	2	D	I	1
169	CNK02/19	4104	5.1	0.2	0.02	0.16	0.00012	59.275	5.80	322	4	B	I	1
170	CNK02/19	2606	5.1	0.835	0.08	0.98	0.00182	49.835	5.80	348	2	D	II	2
171	CNK02/19	2601	5.1	0.705	0.11	0.39	0.00225	72.885	5.80	351	2	D	II	2
172	CNK02/19	5401	5.1	0.205	0.02	0.20	0.00015	67.975	5.80	356	3	C	II	2
173	LRD01/19	3524	5.2	0.175	0.02	0.36	0.00012	92.795	51.33	292	3	C	II	2
174	LRD01/19	4810	5.2	6.68	0.46	0.17	0.07344	12.995	51.33	97	3	C	IV	4
175	DNZ08/19	3509	6.0	1.950117	0.34	7.31	0.02144	61.37	6.96	149	2	D	II	2

Table C.1 *Dataset Used in the Study (continued)*

Record No.	Earthquake ID	Station ID	Mw	PGA (cm/sec2)	PGV (cm/sec)	PGD (cm)	Arias Intensity (cm/s)	D_5_95 (sec)	Focal Depth (km)	Epicentral Distance (km)	Soil Classification (in numbers)	Soil Classification	MMI	MMI_ Numbers
176	DNZ08/19	0301	6.0	11.028	1.26	1.50	0.33188	33.915	6.96	131	2	D	III	3
177	DNZ08/19	0709	6.0	3.352234	0.68	0.55	0.05799	66.285	6.96	147	3	C	IV	4
178	DNZ08/19	0711	6.0	2.915884	0.76	0.52	0.04496	43.29	6.96	168	3	C	III	3
179	MAR09/19	3408	5.8	67.24603	3.57222	1.62507	1.40506	18.185	7.97	22	3	C	V	5
180	MAR09/19	1701	5.8	2.520613	0.25738	0.67041	0.0255	71.89	7.97	175	2	D	IV	4
181	MAR09/19	3407	5.8	18.51473	0.90654	0.41829	0.21699	17.26	7.97	70	3	C	IV	4
182	MAR09/19	1622	5.8	6.048146	0.88137	0.60578	0.11045	32.9	7.97	104	3	C	IV	4
183	MAR09/19	1623	5.8	8.005991	0.87386	0.63155	0.15758	36.37	7.97	98	3	C	IV	4
184	MAR09/19	1642	5.8	17.88347	1.19058	0.2328	0.25937	14.47	7.97	97	3	C	V	5
185	MAR09/19	1710	5.8	1.749111	0.21169	0.83326	0.01455	76.82	7.97	141	2	D	II	2
186	MAR09/19	5401	5.8	3.515944	0.36928	0.29609	0.02411	24.67	7.97	183	3	C	IV	4
187	MAR09/19	4125	5.8	4.498716	0.65464	0.60645	0.03731	33.03	7.97	144	4	B	IV	4
188	MAR09/19	619	5.8	0.449587	0.16913	18.2167	0.0014	111.415	7.97	402	2	D	I	1
189	MAR09/19	1628	5.8	15.39719	1.29882	4.53062	0.22148	10.41	7.97	101	3	C	IV	4
190	MAR09/19	1620	5.8	4.124638	0.61764	4.40635	0.04639	38.28	7.97	110	3	C	IV	4
191	MAR09/19	1627	5.8	11.87209	1.49528	6.87295	0.39926	48.02	7.97	103	2	D	IV	4
192	MAR09/19	1629	5.8	24.17922	1.59053	1.7486	1.01284	22.185	7.97	95	2	D	V	5
193	MAR09/19	1630	5.8	17.53156	1.16559	1.33874	0.42894	12.74	7.97	96	2	D	V	5
194	MAR09/19	7708	5.8	13.67018	1.4788	1.13071	0.45766	45.725	7.97	91	2	D	IV	4
195	MAR09/19	301	5.8	1.357565	0.24499	0.37666	0.01378	85.71	7.97	309	2	D	III	3

D. Principal Component Analysis- Correlation Matrix

Table D.2. *Correlation Matrix for MMI=I*

Correlation Matrix										
		Mw	PGA	PGV	PGD	Ia	D_{5-95}	FD	ED	SC
Correlation	Mw	1.000	0.868	0.998	0.876	0.760	-0.811	1.000	-0.341	-0.218
	PGA	0.868	1.000	0.869	0.621	0.947	-0.892	0.868	-0.015	-0.656
	PGV	0.998	0.869	1.000	0.894	0.748	-0.809	0.998	-0.378	-0.236
	PGD	0.876	0.621	0.894	1.000	0.393	-0.530	0.876	-0.752	-0.030
	Ia	0.760	0.947	0.748	0.393	1.000	-0.927	0.760	0.283	-0.634
	D_{5-95}	-0.811	-0.892	-0.809	-0.530	-0.927	1.000	-0.811	-0.095	0.473
	FD	1.000	0.868	0.998	0.876	0.760	-0.811	1.000	-0.341	-0.218
	ED	-0.341	-0.015	-0.378	-0.752	0.283	-0.095	-0.341	1.000	-0.263
	SC	-0.218	-0.656	-0.236	-0.030	-0.634	0.473	-0.218	-0.263	1.000

Table D.3. *Correlation Matrix for MMI=II*

Correlation Matrix										
		Mw	PGA	PGV	PGD	Ia	D_{5-95}	FD	ED	SC
Correlation	Mw	1.000	-0.167	0.260	0.255	-0.054	0.459	0.355	0.470	-0.225
	PGA	-0.167	1.000	0.036	0.007	0.978	-0.481	-0.138	-0.593	0.297
	PGV	0.260	0.036	1.000	0.990	0.114	0.114	0.586	-0.122	0.317
	PGD	0.255	0.007	0.990	1.000	0.091	0.159	0.551	-0.101	0.308
	Ia	-0.054	0.978	0.114	0.091	1.000	-0.309	-0.073	-0.496	0.316
	D_{5-95}	0.459	-0.481	0.114	0.159	-0.309	1.000	0.247	0.668	-0.075
	FD	0.355	-0.138	0.586	0.551	-0.073	0.247	1.000	0.090	0.303
	ED	0.470	-0.593	-0.122	-0.101	-0.496	0.668	0.090	1.000	-0.307
	SC	-0.225	0.297	0.317	0.308	0.316	-0.075	0.303	-0.307	1.000

Table *D.4*. *Correlation Matrix for MMI=III*

Correlation Matrix										
		Mw	PGA	PGV	PGD	Ia	D_{5-95}	FD	ED	SC
Correlation	Mw	1.000	0.066	0.267	0.279	0.160	0.414	0.502	0.464	-0.166
	PGA	0.066	1.000	0.918	0.300	0.962	-0.266	0.560	-0.426	0.092
	PGV	0.267	0.918	1.000	0.398	0.964	-0.191	0.563	-0.302	-0.022
	PGD	0.279	0.300	0.398	1.000	0.313	-0.019	0.375	0.075	-0.305
	Ia	0.160	0.962	0.964	0.313	1.000	-0.223	0.543	-0.387	0.059
	D_{5-95}	0.414	-0.266	-0.191	-0.019	-0.223	1.000	0.122	0.434	0.130
	FD	0.502	0.560	0.563	0.375	0.543	0.122	1.000	-0.061	0.015
	ED	0.464	-0.426	-0.302	0.075	-0.387	0.434	-0.061	1.000	0.073
	SC	-0.166	0.092	-0.022	-0.305	0.059	0.130	0.015	0.073	1.000

Table *D.5*. *Correlation Matrix for MMI=IV*

Correlation Matrix										
		Mw	PGA	PGV	PGD	Ia	D_{5-95}	FD	ED	SC
Correlation	Mw	1.000	0.190	0.333	0.248	0.232	0.550	0.311	0.593	-0.138
	PGA	0.190	1.000	0.217	-0.030	0.718	-0.299	0.208	-0.381	-0.147
	PGV	0.333	0.217	1.000	0.957	0.180	0.224	0.020	0.127	-0.147
	PGD	0.248	-0.030	0.957	1.000	-0.019	0.270	0.000	0.188	-0.127
	Ia	0.232	0.718	0.180	-0.019	1.000	-0.025	0.069	-0.200	-0.142
	D_{5-95}	0.550	-0.299	0.224	0.270	-0.025	1.000	0.112	0.654	-0.145
	FD	0.311	0.208	0.020	0.000	0.069	0.112	1.000	0.211	0.025
	ED	0.593	-0.381	0.127	0.188	-0.200	0.654	0.211	1.000	-0.013
	SC	-0.138	-0.147	-0.147	-0.127	-0.142	-0.145	0.025	-0.013	1.000

Table D.6. *Correlation Matrix for MMI=V*

Correlation Matrix										
		Mw	PGA	PGV	PGD	Ia	D_{5-95}	FD	ED	SC
Correlation	Mw	1.000	-0.117	0.326	0.365	0.027	0.501	-0.065	0.835	-0.011
	PGA	-0.117	1.000	0.570	0.450	0.792	-0.403	0.285	-0.362	-0.340
	PGV	0.326	0.570	1.000	0.924	0.655	0.069	0.393	0.079	-0.306
	PGD	0.365	0.450	0.924	1.000	0.634	0.172	0.138	0.145	-0.248
	Ia	0.027	0.792	0.655	0.634	1.000	-0.176	0.153	-0.122	-0.181
	D_{5-95}	0.501	-0.403	0.069	0.172	-0.176	1.000	0.041	0.651	-0.064
	FD	-0.065	0.285	0.393	0.138	0.153	0.041	1.000	-0.174	0.035
	ED	0.835	-0.362	0.079	0.145	-0.122	0.651	-0.174	1.000	0.041
	SC	-0.011	-0.340	-0.306	-0.248	-0.181	-0.064	0.035	0.041	1.000

Table D.7. *Correlation Matrix for MMI=VI*

Correlation Matrix										
		Mw	PGA	PGV	PGD	Ia	D_{5-95}	FD	ED	SC
Correlation	Mw	1.000	-0.326	-0.242	0.121	-0.266	0.558	0.425	0.652	0.106
	PGA	-0.326	1.000	0.900	0.497	0.964	-0.535	0.208	-0.581	-0.248
	PGV	-0.242	0.900	1.000	0.683	0.875	-0.313	0.237	-0.383	-0.234
	PGD	0.121	0.497	0.683	1.000	0.473	-0.166	0.176	-0.211	0.070
	Ia	-0.266	0.964	0.875	0.473	1.000	-0.413	0.195	-0.499	-0.359
	D_{5-95}	0.558	-0.535	-0.313	-0.166	-0.413	1.000	0.250	0.639	-0.181
	FD	0.425	0.208	0.237	0.176	0.195	0.250	1.000	0.234	-0.002
	ED	0.652	-0.581	-0.383	-0.211	-0.499	0.639	0.234	1.000	-0.092
	SC	0.106	-0.248	-0.234	0.070	-0.359	-0.181	-0.002	-0.092	1.000

Table *D.8*. *Correlation Matrix for MMI=VII*

Correlation Matrix										
		Mw	PGA	PGV	PGD	Ia	D_{5-95}	FD	ED	SC
Correlation	Mw	1.000	0.398	-0.456	-0.346	0.557	0.386	0.453	0.025	-0.953
	PGA	0.398	1.000	0.334	0.302	0.805	-0.499	0.166	-0.263	-0.234
	PGV	-0.456	0.334	1.000	0.817	0.199	-0.522	-0.652	-0.671	0.403
	PGD	-0.346	0.302	0.817	1.000	0.044	-0.483	-0.541	-0.558	0.256
	Ia	0.557	0.805	0.199	0.044	1.000	-0.023	0.199	-0.355	-0.429
	D_{5-95}	0.386	-0.499	-0.522	-0.483	-0.023	1.000	0.333	0.300	-0.448
	FD	0.453	0.166	-0.652	-0.541	0.199	0.333	1.000	0.800	-0.224
	ED	0.025	-0.263	-0.671	-0.558	-0.355	0.300	0.800	1.000	0.145
	SC	-0.953	-0.234	0.403	0.256	-0.429	-0.448	-0.224	0.145	1.000

Table *D.9*. *Correlation Matrix for MMI=VIII*

Correlation Matrix										
		Mw	PGA	PGV	PGD	Ia	D_{5-95}	FD	ED	SC
Correlation	Mw	1.000	-0.410	0.404	0.534	-0.631	0.889	-0.914	-0.050	0.597
	PGA	-0.410	1.000	0.471	0.274	0.935	-0.553	0.744	-0.863	-0.580
	PGV	0.404	0.471	1.000	0.977	0.129	0.457	-0.082	-0.551	0.407
	PGD	0.534	0.274	0.977	1.000	-0.083	0.629	-0.264	-0.391	0.584
	Ia	-0.631	0.935	0.129	-0.083	1.000	-0.807	0.876	-0.742	-0.811
	D_{5-95}	0.889	-0.553	0.457	0.629	-0.807	1.000	-0.893	0.256	0.899
	FD	-0.914	0.744	-0.082	-0.264	0.876	-0.893	1.000	-0.345	-0.690
	ED	-0.050	-0.863	-0.551	-0.391	-0.742	0.256	-0.345	1.000	0.500
	SC	0.597	-0.580	0.407	0.584	-0.811	0.899	-0.690	0.500	1.000

Table D.10. *Correlation Matrix for MMI=X*

Correlation Matrix										
		Mw	PGA	PGV	PGD	Ia	D_{5-95}	FD	ED	SC
Correlation	Mw	1.000	-0.837	-0.871	0.991	-0.994	1.000	1.000	0.500	1.000
	PGA	-0.837	1.000	0.459	-0.902	0.891	-0.843	-0.837	0.056	-0.837
	PGV	-0.871	0.459	1.000	-0.798	0.813	-0.865	-0.871	-0.861	-0.871
	PGD	0.991	-0.902	-0.798	1.000	-1.000	0.993	0.991	0.381	0.991
	Ia	-0.994	0.891	0.813	-1.000	1.000	-0.995	-0.994	-0.405	-0.994
	D_{5-95}	1.000	-0.843	-0.865	0.993	-0.995	1.000	1.000	0.491	1.000
	FD	1.000	-0.837	-0.871	0.991	-0.994	1.000	1.000	0.500	1.000
	ED	0.500	0.056	-0.861	0.381	-0.405	0.491	0.500	1.000	0.500
	SC	1.000	-0.837	-0.871	0.991	-0.994	1.000	1.000	0.500	1.000

E. Principal Component Analysis-Total Variance Table

Table E.1. *Total Variance Table for MMI=I*

Total Variance Explained[a]						
Component	Initial Eigenvalues			Extraction Sums of Squared Loadings		
	Total	% of Variance	Cumulative %	Total	% of Variance	Cumulative %
1	6.175	68.608	68.608	6.175	68.608	68.608
2	2.095	23.272	91.881	2.095	23.272	91.881
3	0.618	6.865	98.746			
4	0.113	1.254	100.000			
5	3.207E-16	3.563E-15	100.000			
6	1.771E-16	1.968E-15	100.000			
7	-2.611E-17	-2.901E-16	100.000			
8	-2.534E-16	-2.815E-15	100.000			
9	-4.191E-16	-4.657E-15	100.000			
Extraction Method: Principal Component Analysis.						
a. Only cases for which MMI = 1 are used in the analysis phase.						

Table E.2. *Total Variance Table for MMI=II*

Total Variance Explained[a]						
Component	Initial Eigenvalues			Extraction Sums of Squared Loadings		
	Total	% of Variance	Cumulative %	Total	% of Variance	Cumulative %
1	3.126	34.733	34.733	3.126	34.733	34.733
2	2.778	30.864	65.597	2.778	30.864	65.597
3	1.164	12.928	78.525	1.164	12.928	78.525
4	0.816	9.063	87.588			
5	0.538	5.978	93.566			
6	0.316	3.510	97.076			
7	0.253	2.815	99.892			
8	0.007	0.076	99.967			
9	0.003	0.033	100.000			
Extraction Method: Principal Component Analysis.						
a. Only cases for which MMI = II are used in the analysis phase.						

Table E.3. *Total Variance Table for MMI=III*

Total Variance Explained[a]						
Component	Initial Eigenvalues			Extraction Sums of Squared Loadings		
	Total	% of Variance	Cumulative %	Total	% of Variance	Cumulative %
1	3.717	41.298	41.298	3.717	41.298	41.298
2	2.096	23.285	64.583	2.096	23.285	64.583
3	1.259	13.986	78.569	1.259	13.986	78.569
4	0.638	7.088	85.658			
5	0.538	5.980	91.638			
6	0.458	5.087	96.724			
7	0.227	2.526	99.250			
8	0.049	0.540	99.790			
9	0.019	0.210	100.000			
Extraction Method: Principal Component Analysis.						
a. Only cases for which MMI = III are used in the analysis phase.						

Table E.4. *Total Variance Plot for MMI=IV*

Total Variance Explained[a]						
Component	Initial Eigenvalues			Extraction Sums of Squared Loadings		
	Total	% of Variance	Cumulative %	Total	% of Variance	Cumulative %
1	2.754	30.595	30.595	2.754	30.595	30.595
2	2.125	23.606	54.201	2.125	23.606	54.201
3	1.514	16.819	71.020	1.514	16.819	71.020
4	1.004	11.155	82.175	1.004	11.155	82.175
5	0.783	8.697	90.872			
6	0.394	4.373	95.245			
7	0.260	2.887	98.132			
8	0.159	1.762	99.894			
9	0.010	0.106	100.000			
Extraction Method: Principal Component Analysis.						
a. Only cases for which MMI = IV are used in the analysis phase.						

Table *E.5. Total Variance Table for MMI=V*

Total Variance Explained[a]						
Component	Initial Eigenvalues			Extraction Sums of Squared Loadings		
	Total	% of Variance	Cumulative %	Total	% of Variance	Cumulative %
1	3.289	36.547	36.547	3.289	36.547	36.547
2	2.612	29.019	65.566	2.612	29.019	65.566
3	1.054	11.706	77.272	1.054	11.706	77.272
4	0.880	9.777	87.049			
5	0.505	5.613	92.662			
6	0.416	4.620	97.282			
7	0.142	1.578	98.860			
8	0.079	0.878	99.738			
9	0.024	0.262	100.000			
Extraction Method: Principal Component Analysis.						
a. Only cases for which MMI = V are used in the analysis phase.						

Table *E.6. Total Variance Table for MMI=VI*

Total Variance Explained[a]						
Component	Initial Eigenvalues			Extraction Sums of Squared Loadings		
	Total	% of Variance	Cumulative %	Total	% of Variance	Cumulative %
1	4.053	45.032	45.032	4.053	45.032	45.032
2	2.066	22.954	67.987	2.066	22.954	67.987
3	1.205	13.386	81.373	1.205	13.386	81.373
4	0.697	7.740	89.113			
5	0.390	4.332	93.446			
6	0.293	3.259	96.705			
7	0.243	2.700	99.405			
8	0.045	0.495	99.901			
9	0.009	0.099	100.000			
Extraction Method: Principal Component Analysis.						
a. Only cases for which MMI = VI are used in the analysis phase.						

Table E.7. *Total Variance Table for MMI=VII*

Total Variance Explained[a]						
	Initial Eigenvalues			Extraction Sums of Squared Loadings		
Component	Total	% of Variance	Cumulative %	Total	% of Variance	Cumulative %
1	3.803	42.252	42.252	3.803	42.252	42.252
2	2.770	30.779	73.030	2.770	30.779	73.030
3	1.336	14.849	87.879	1.336	14.849	87.879
4	0.515	5.718	93.597			
5	0.444	4.930	98.527			
6	0.086	0.953	99.480			
7	0.042	0.469	99.949			
8	0.004	0.046	99.995			
9	0.000	0.005	100.000			
Extraction Method: Principal Component Analysis.						
a. Only cases for which MMI = VII are used in the analysis phase.						

Table E.8. *Total Variance Table for MMI=VIII*

Total Variance Explained[a]						
	Initial Eigenvalues			Extraction Sums of Squared Loadings		
Component	Total	% of Variance	Cumulative %	Total	% of Variance	Cumulative %
1	5.183	57.588	57.588	5.183	57.588	57.588
2	3.050	33.885	91.473	3.050	33.885	91.473
3	0.767	8.527	100.000			
4	1.411E-15	1.568E-14	100.000			
5	2.380E-16	2.644E-15	100.000			
6	1.212E-16	1.347E-15	100.000			
7	1.002E-17	1.113E-16	100.000			
8	-4.035E-16	-4.483E-15	100.000			
9	-5.063E-16	-5.626E-15	100.000			
Extraction Method: Principal Component Analysis.						
a. Only cases for which MMI = VIII are used in the analysis phase.						

Table *E.9*. *Total Variance Table for MMI=X*

Total Variance Explained[a]						
	Initial Eigenvalues			Extraction Sums of Squared Loadings		
Component	Total	% of Variance	Cumulative %	Total	% of Variance	Cumulative %
1	7.683	85.370	85.370	7.683	85.370	85.370
2	1.317	14.630	100.000	1.317	14.630	100.000
3	5.475E-16	6.084E-15	100.000			
4	4.865E-16	5.406E-15	100.000			
5	1.020E-16	1.134E-15	100.000			
6	-1.318E-16	-1.464E-15	100.000			
7	-2.146E-16	-2.384E-15	100.000			
8	-3.207E-16	-3.563E-15	100.000			
9	-6.703E-16	-7.447E-15	100.000			
Extraction Method: Principal Component Analysis.						

F. Principal Component Analysis – Scree Plot

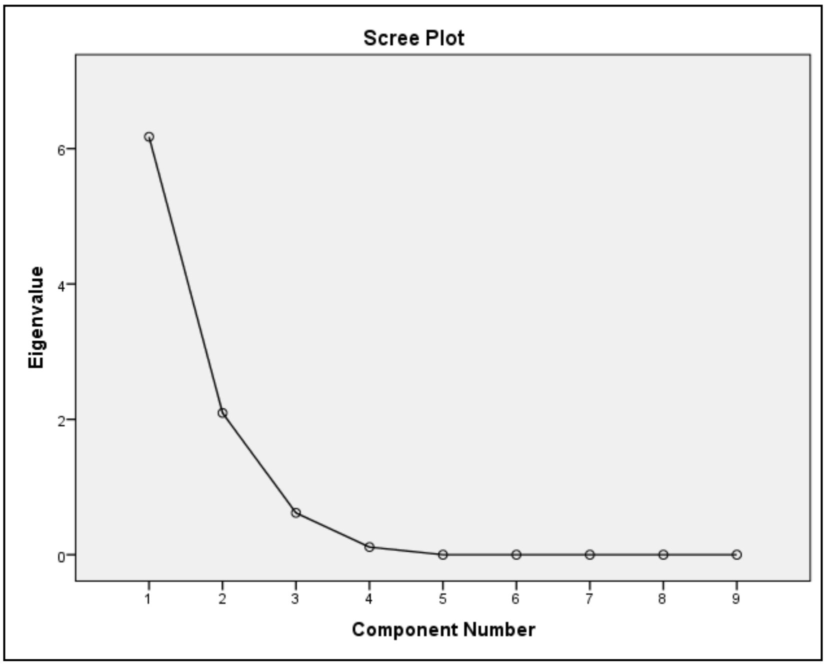

Figure F.1. Scree Plot for MMI=I

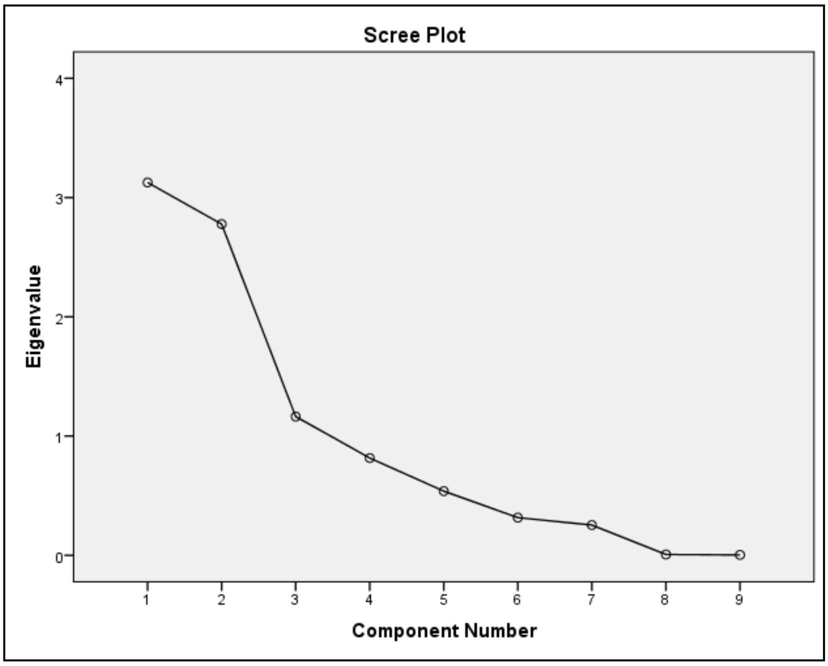

Figure F.2. Scree Plot for MMI=II

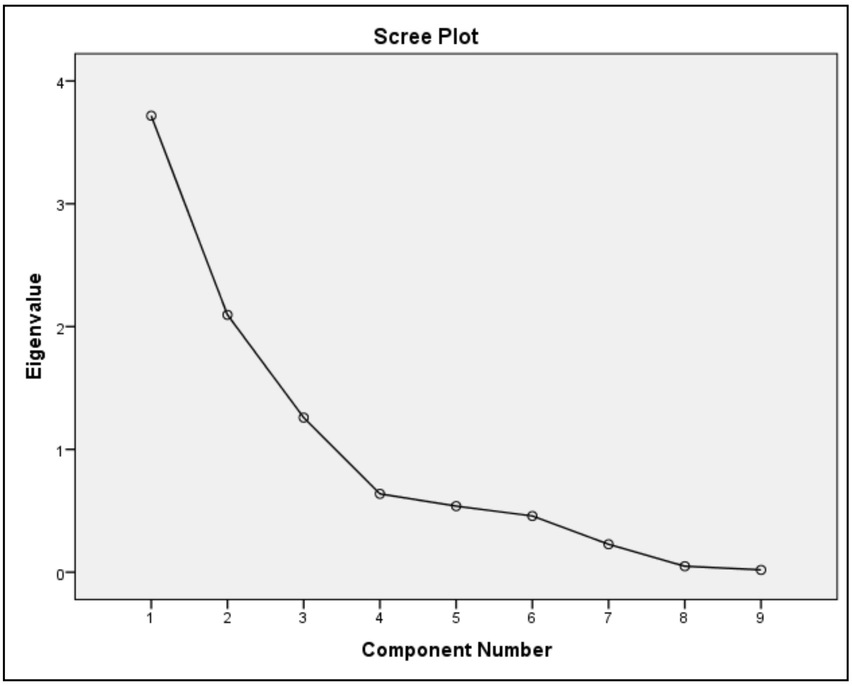

Figure F.3. Scree Plot for MMI=III

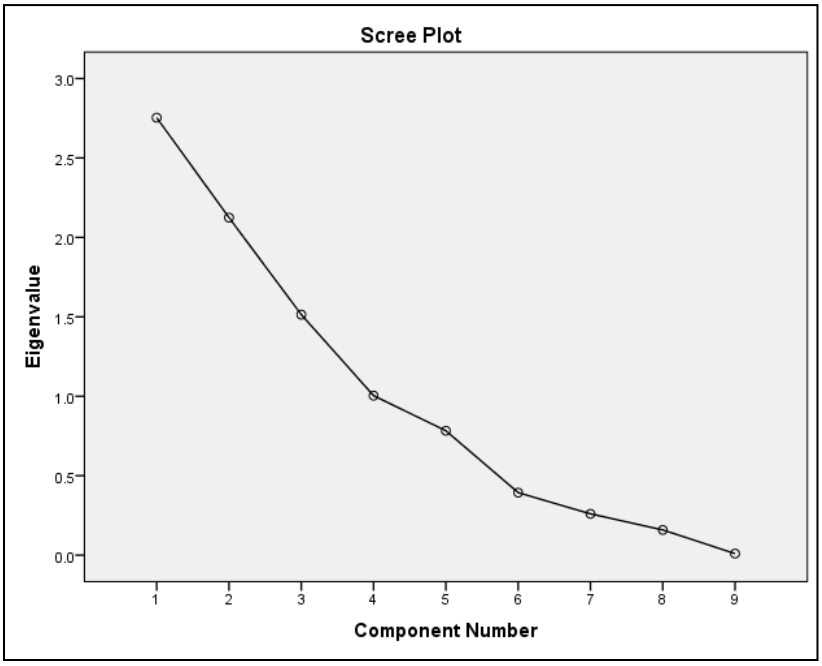

Figure F.4. Scree Plot for MMI=IV

Figure F.5. Scree Plot for MMI=V

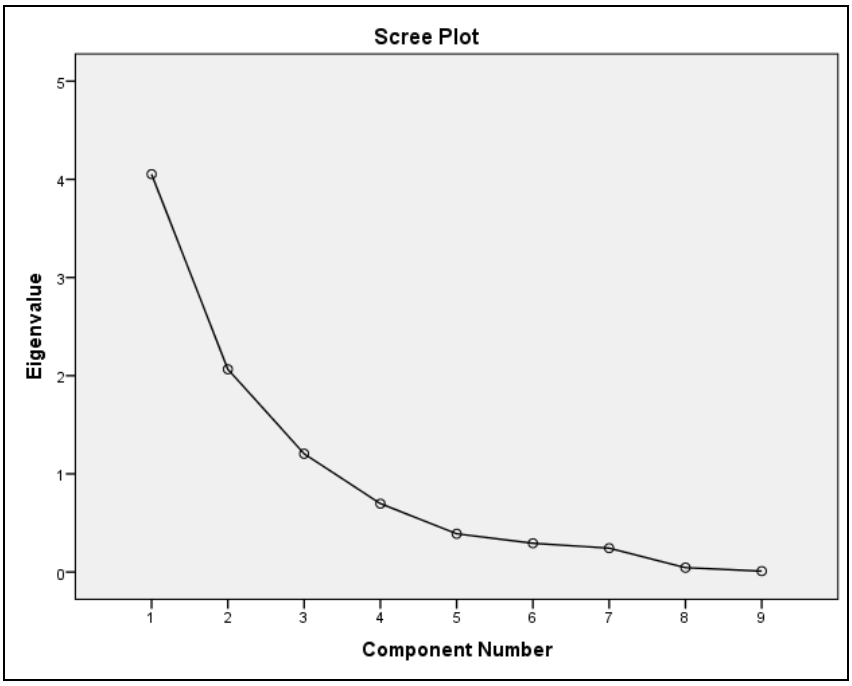

Figure F.6. Scree Plot for MMI=VI

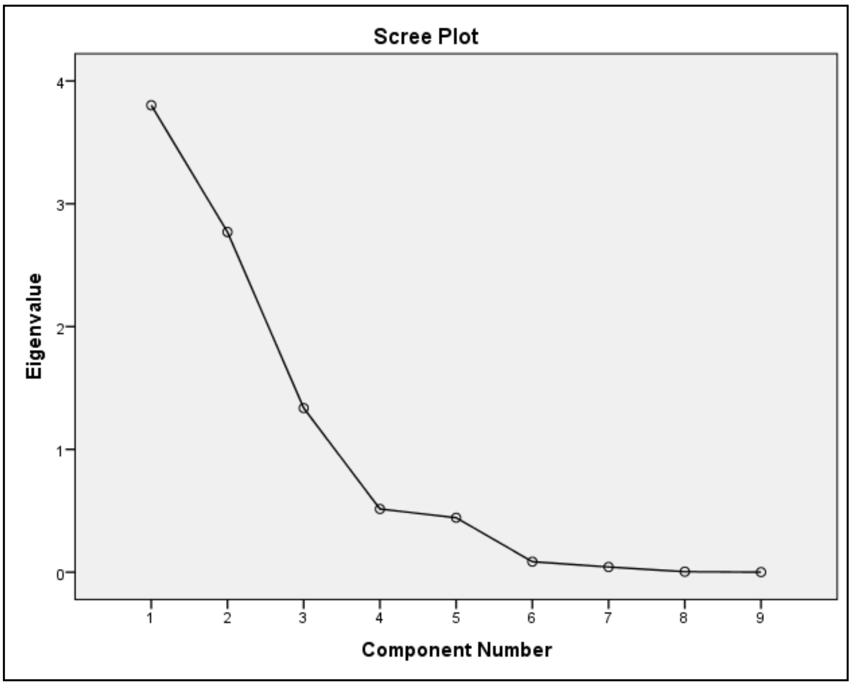

Figure F.7. Scree Plot for MMI=VII

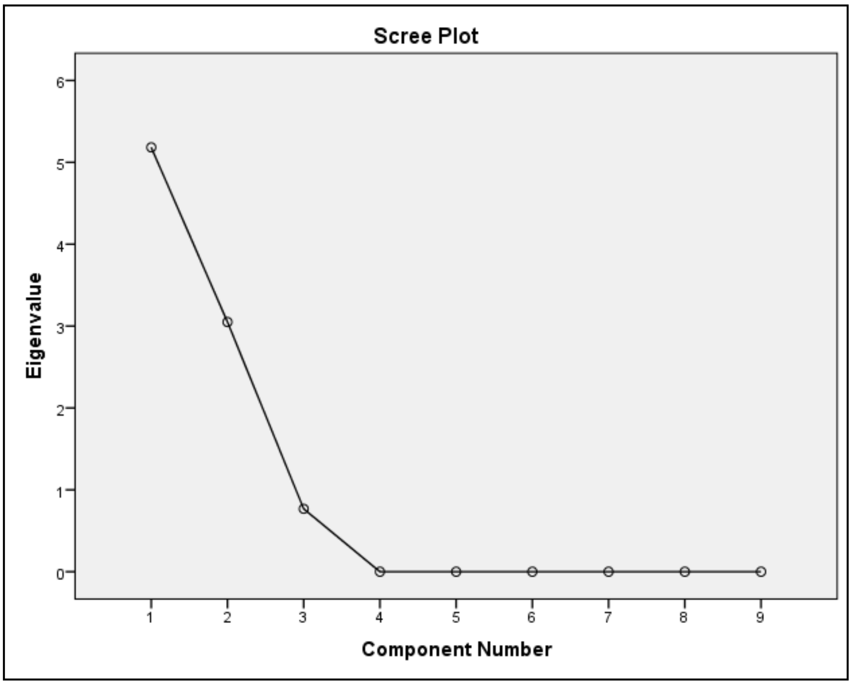

Figure F.8. Scree Plot for MMI=VIII

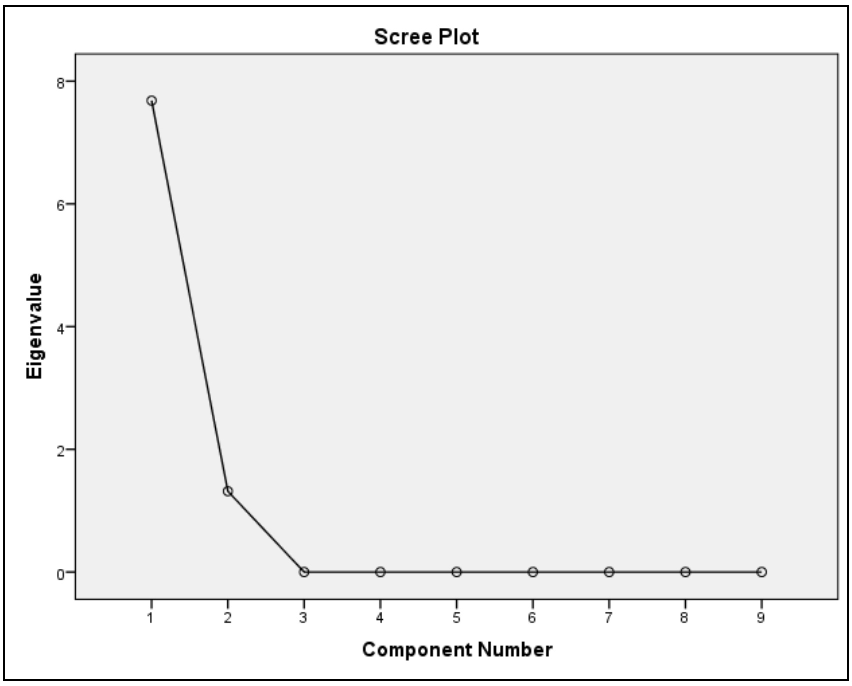

Figure F.9. Scree Plot for MMI=X

G. Principal Component Analysis-Component Matrix

Table G.1. *Component Matrix for MMI=I*

Component Matrix[a,b]		
	Component	
	1	2
PGV	0.975	0.204
FD	0.972	0.185
Mw	0.972	0.185
PGA	0.953	-0.271
SD	-0.893	0.299
AI	0.862	-0.497
PGD	0.805	0.582
ED	-0.234	-0.894
SC	-0.427	0.661
Extraction Method: Principal Component Analysis.		
a. 2 components extracted.		
b. Only cases for which MMI = 1 are used in the analysis phase.		

Table G.2. *Component Matrix for MMI=II*

Component Matrix[a,b]			
	Component		
	1	2	3
PGA	-0.868	0.170	0.451
ED	0.833	-0.150	0.261
AI	-0.773	0.264	0.549
SD	0.744	0.160	0.269
PGV		0.936	-0.127
PGD		0.922	-0.132
FD	0.286	0.737	
SC	-0.374	0.505	-0.265
Mw	0.540	0.330	0.638
Extraction Method: Principal Component Analysis.			
a. 3 components extracted.			
b. Only cases for which MMI = II are used in the analysis phase.			

Table *G.3. Component Matrix for MMI=III*

Component Matrix[a,b]			
	Component		
	1	2	3
PGV	0.959		
AI	0.958		0.135
PGA	0.948	-0.166	0.153
FD	0.695	0.424	0.115
Mw	0.250	0.852	
ED	-0.390	0.725	
SD	-0.237	0.694	0.340
SC		-0.113	0.903
PGD	0.473	0.363	-0.511
Extraction Method: Principal Component Analysis.			
a. 3 components extracted.			
b. Only cases for which MMI = III are used in the analysis phase.			

Table *G.4. Component Matrix for MMI=IV*

Component Matrix[a,b]				
	Component			
	1	2	3	4
Mw	0.776		0.427	
SD	0.739	-0.350	0.206	-0.217
PGV	0.703	0.386	-0.567	0.171
PGD	0.698	0.170	-0.660	0.174
ED	0.693	-0.509	0.302	
PGA		0.917	0.241	
AI		0.801	0.296	-0.114
FD	0.274	0.117	0.543	0.482
SC	-0.239	-0.248		0.805
Extraction Method: Principal Component Analysis.				
a. 4 components extracted.				
b. Only cases for which MMI = IV are used in the analysis phase.				

Table *G.5*. *Component Matrix for MMI=V*

Component Matrix[a,b]			
	Component		
	1	2	3
PGV	0.923	0.213	0.126
PGD	0.850	0.315	
AI	0.849	-0.138	
PGA	0.813	-0.397	
ED		0.930	
Mw	0.180	0.877	
SD		0.802	0.126
FD	0.361	-0.120	0.811
SC	-0.397		0.587
Extraction Method: Principal Component Analysis.			
a. 3 components extracted.			
b. Only cases for which MMI =V are used in the analysis phase.			

Table *G.6*. *Component Matrix for MMI=VI*

Component Matrix[a,b]			
	Component		
	1	2	3
PGA	0.960	0.180	
AI	0.915	0.252	-0.168
PGV	0.883	0.360	
ED	-0.712	0.503	-0.137
SD	-0.637	0.528	-0.254
PGD	0.558	0.432	0.422
FD		0.750	0.166
Mw	-0.499	0.708	0.237
SC	-0.199	-0.241	0.910
Extraction Method: Principal Component Analysis.			
a. 3 components extracted.			
b. Only cases for which MMI =VI are used in the analysis phase.			

Table *G.7*. *Component Matrix for MMI=VII*

Component Matrix[a,b]			
	Component		
	1	2	3
PGV	-0.912	0.217	
PGD	-0.818	0.199	
FD	0.785		0.557
SD	0.686	-0.118	-0.510
ED	0.666	-0.485	0.511
AI		0.897	0.166
PGA	-0.181	0.839	0.500
Mw	0.651	0.709	-0.172
SC	-0.558	-0.649	0.445
Extraction Method: Principal Component Analysis.			
a. 3 components extracted.			
b. Only cases for which MMI =VII are used in the analysis phase.			

Table *G.8*. *Component Matrix for MMI=VIII*

Component Matrix[a,b]		
	Component	
	1	2
SD	0.961	0.275
AI	-0.938	0.344
FD	-0.934	
SC	0.900	0.143
Mw	0.818	0.346
PGA	-0.760	0.649
PGV	0.205	0.957
PGD	0.405	0.886
ED	0.492	-0.770
Extraction Method: Principal Component Analysis.		
a. 2 components extracted.		
b. Only cases for which MMI =VIII are used in the analysis phase.		

Table *G.9. Component Matrix for MMI=X*

Component Matrix[a,b]		
	Component	
	1	2
FD	1.000	
SC	1.000	
Mw	1.000	
SD	0.999	
AI	-0.991	0.131
PGD	0.988	-0.156
PGV	-0.882	-0.470
PGA	-0.823	0.568
ED	0.521	0.854
Extraction Method: Principal Component Analysis.		
a. 2 components extracted.		
b. Only cases for which MMI =X are used in the analysis phase.		

H. Regression Plots for ANN Training Models

Table H.1. *Table showing the Regression Plots for ANN_Training Models*

Models	# of Hidden Neurons	Regression Plots
M1	3	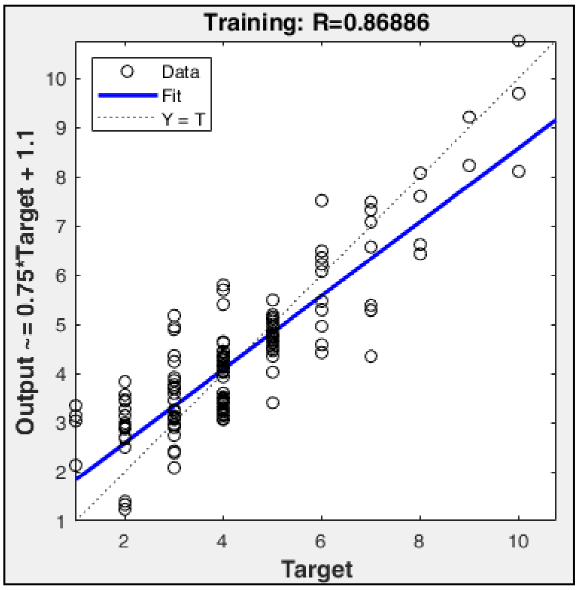
	4	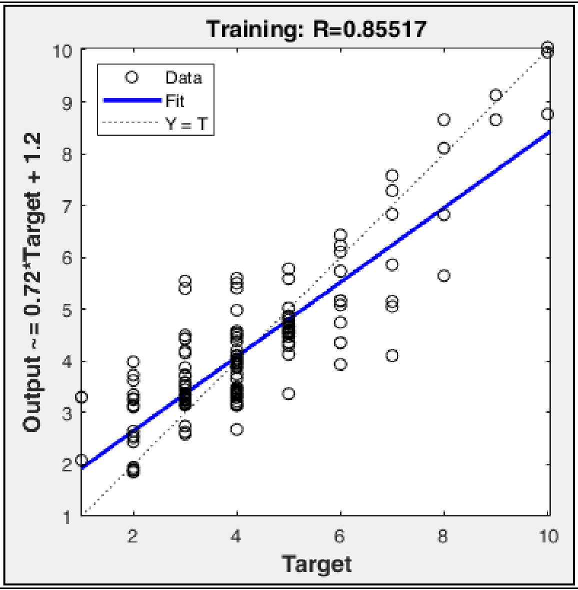

Table H.1. Table showing the Regression Plots for ANN_Training Models (continued)

Models	# of Hidden Neurons	Regression Plots
M2	4	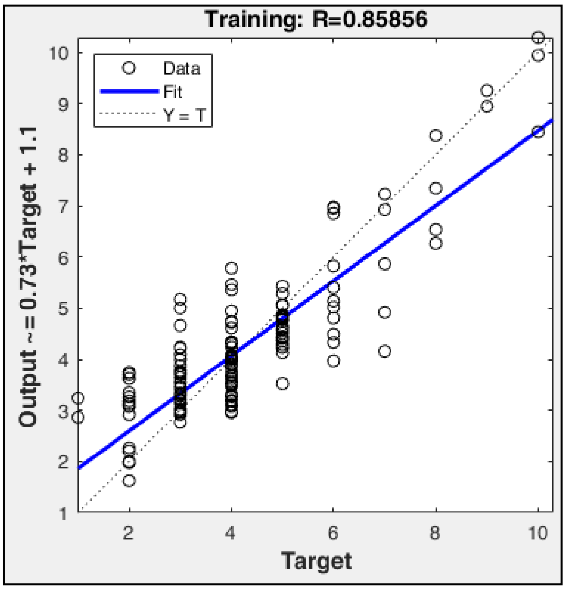
	5	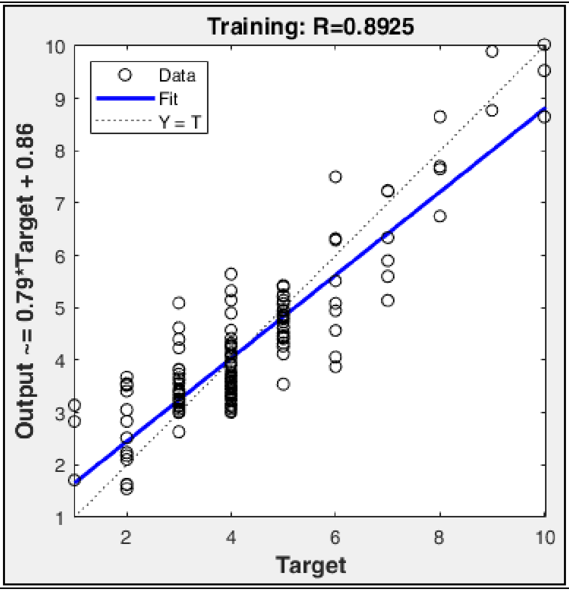

Table H.1. Table showing the Regression Plots for ANN_Training Models (continued)

Models	# of Hidden Neurons	Regression Plots
M3	5	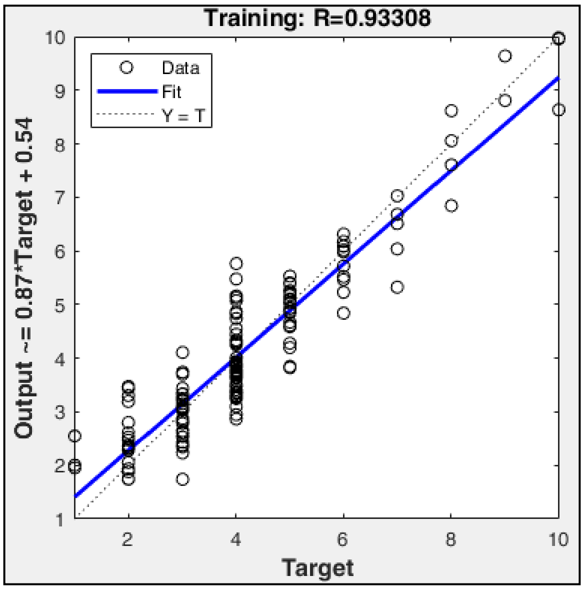
	6	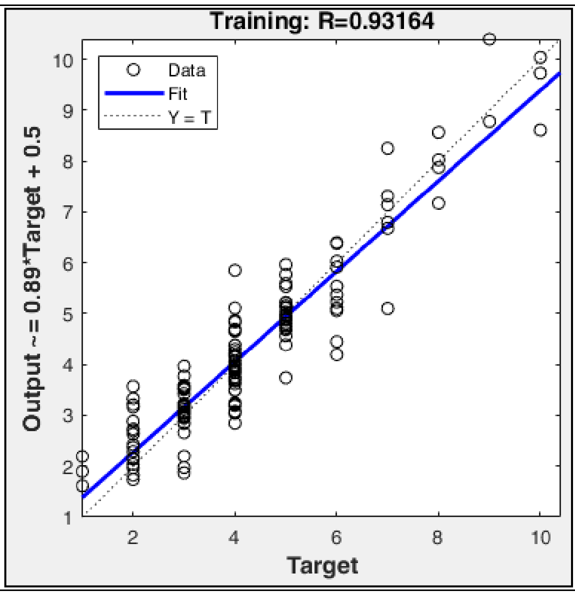

Table H.1. Table showing the Regression Plots for ANN_Training Models (continued)

<table>
<tr><th>Models</th><th># of Hidden Neurons</th><th>Regression Plots</th></tr>
<tr><td rowspan="2">M4</td><td>6</td><td>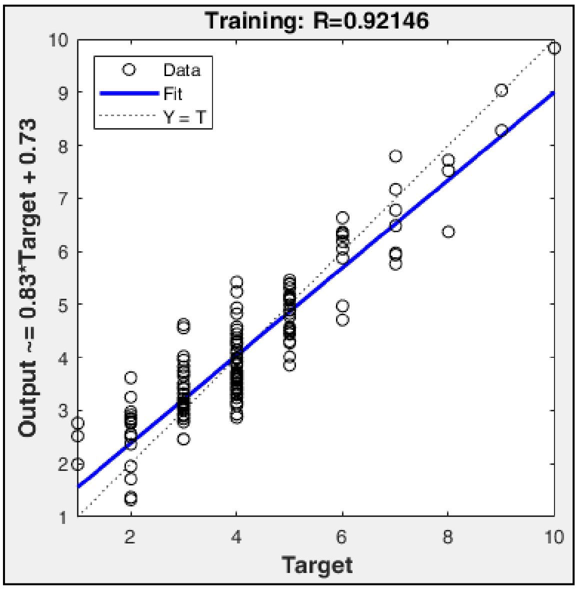
</td></tr>
<tr><td>7</td><td>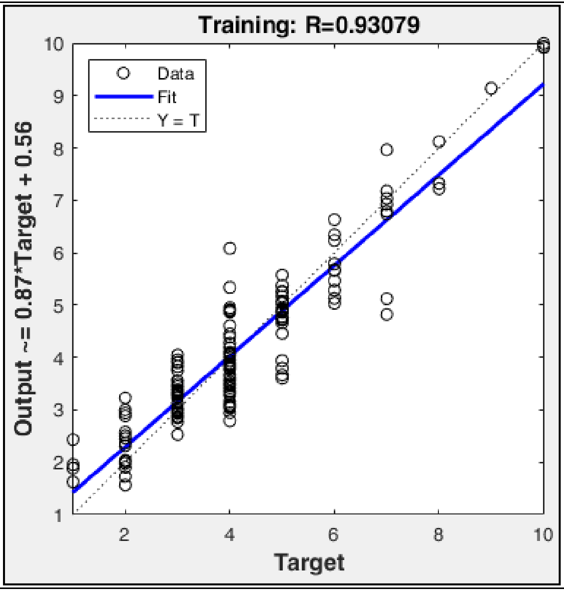
</td></tr>
</table>

Table H.1. Table showing the Regression Plots for ANN_Training Models (continued)

Models	# of Hidden Neurons	Regression Plots
M5	3	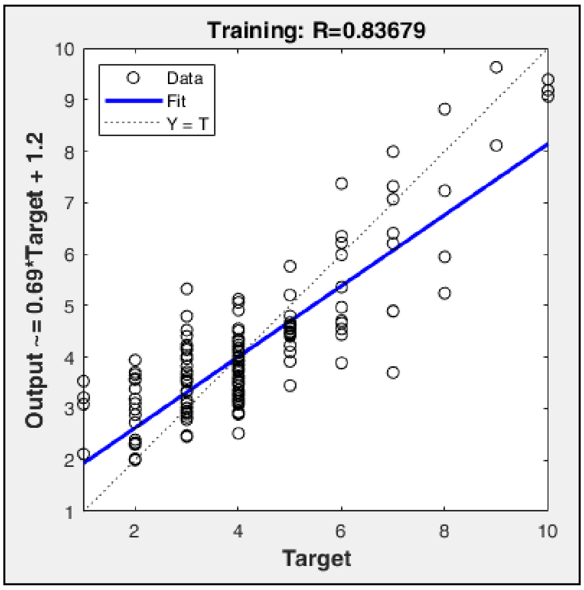
	4	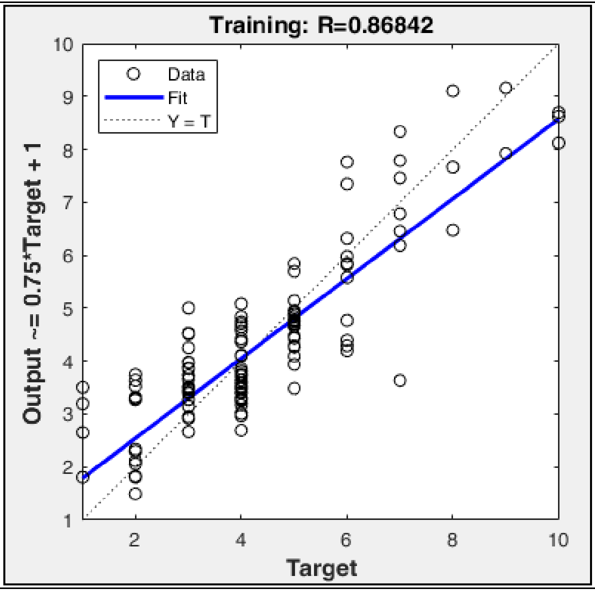

Table H.1. Table showing the Regression Plots for ANN_Training Models (continued)

<table>
<tr><th>Models</th><th># of Hidden Neurons</th><th>Regression Plots</th></tr>
<tr><td rowspan="2">M6</td><td>4</td><td>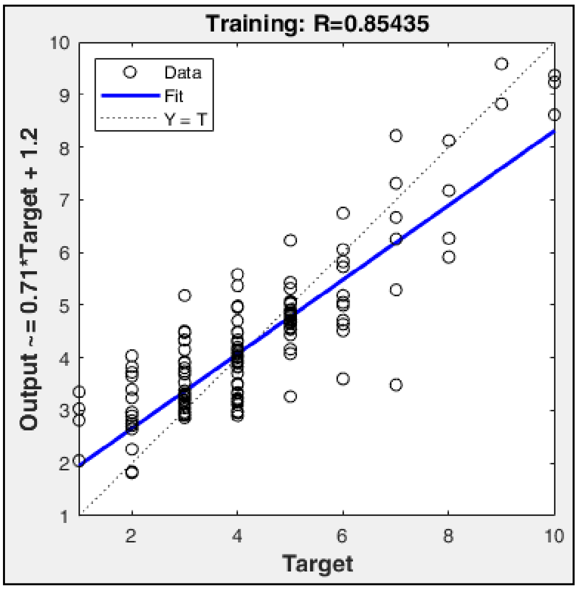
</td></tr>
<tr><td>5</td><td>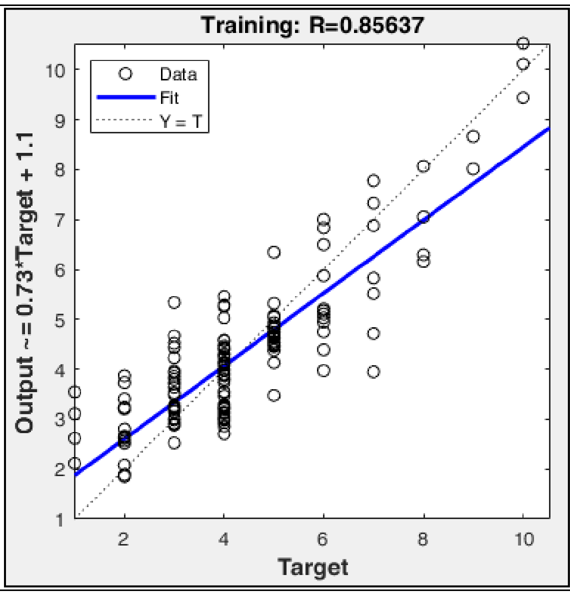
</td></tr>
</table>

Table H.1. Table showing the Regression Plots for ANN_Training Models (continued)

Models	# of Hidden Neurons	Regression Plots
M7	5	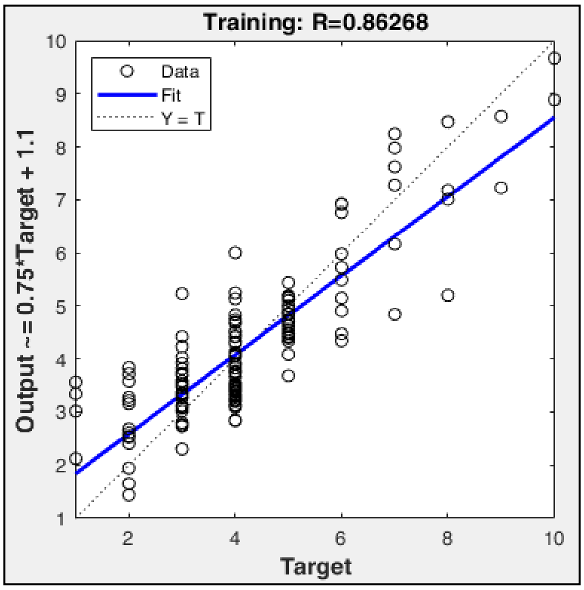
	6	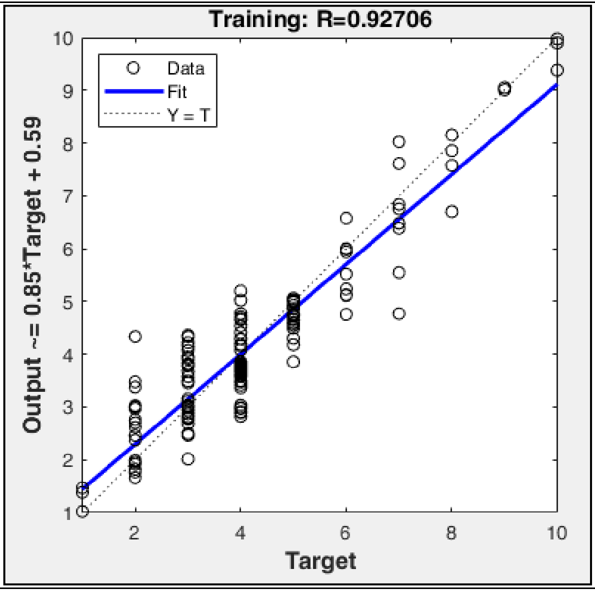

Table H.1. Table showing the Regression Plots for ANN_Training Models (continued)

Models	# of Hidden Neurons	Regression Plots
M8	6	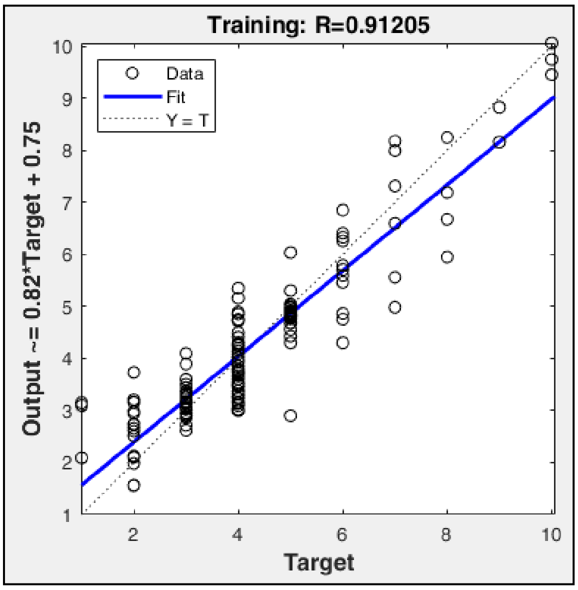
	7	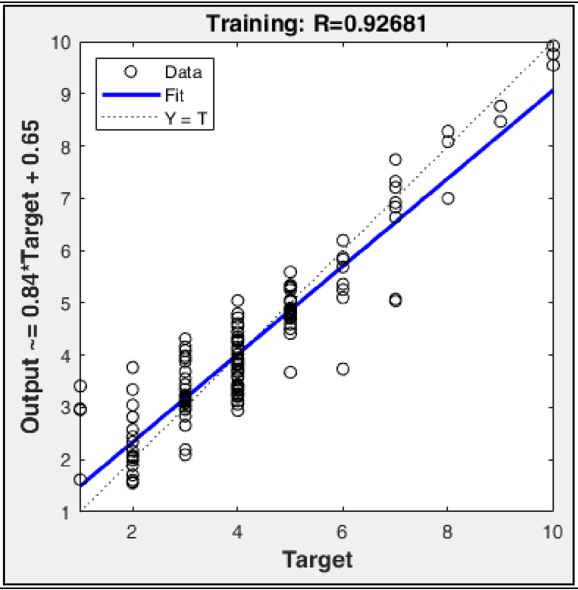

Table H.1. Table showing the Regression Plots for ANN_Training Models (continued)

Models	# of Hidden Neurons	Regression Plots
M9	3	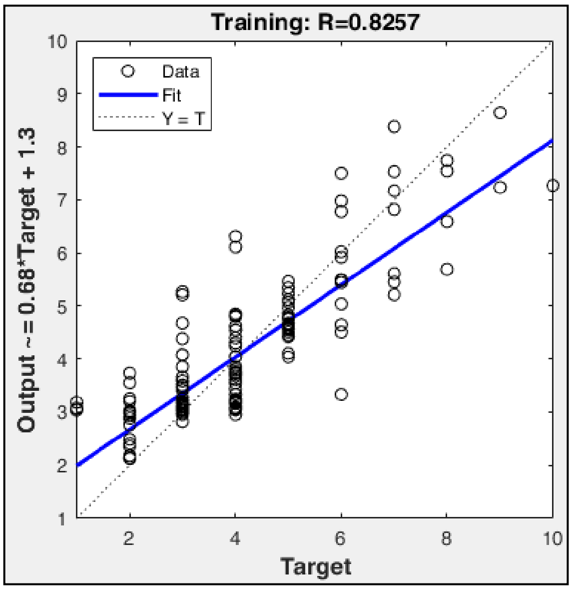
	4	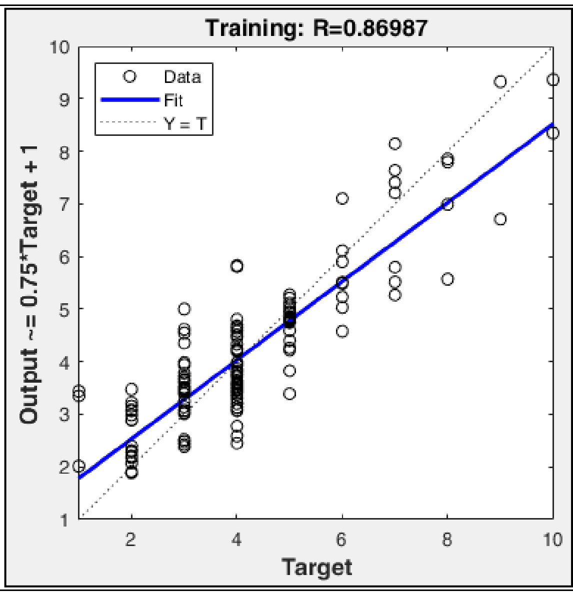

Table H.1. Table showing the Regression Plots for ANN_Training Models (continued)

Models	# of Hidden Neurons	Regression Plots
M10	4	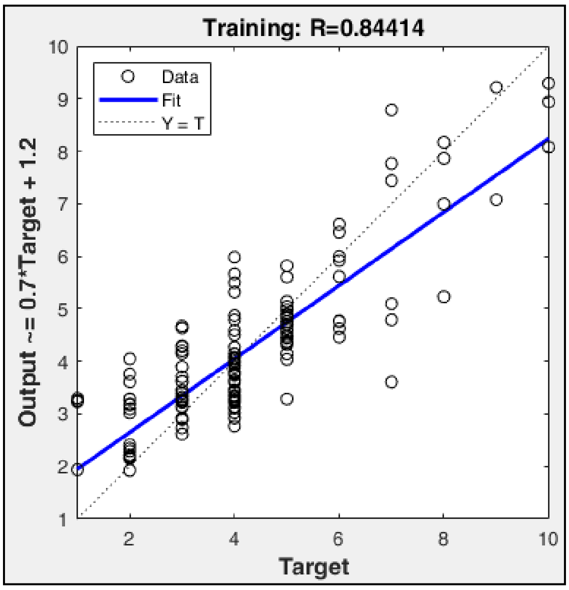
	5	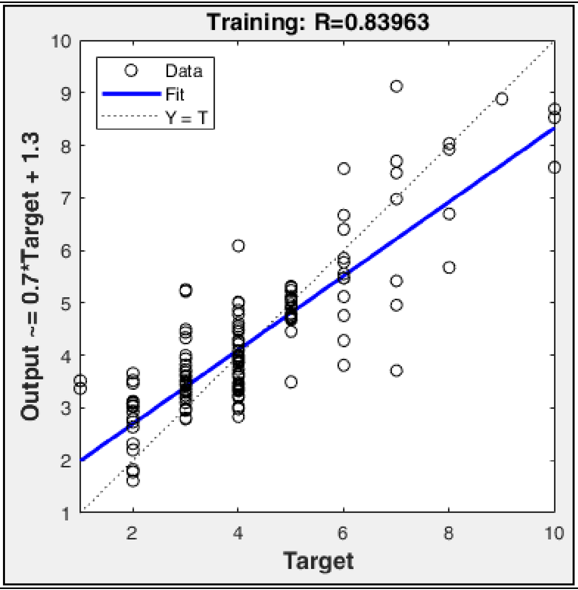

Table H.1. Table showing the Regression Plots for ANN_Training Models (continued)

<table>
<tr><th>Models</th><th># of Hidden Neurons</th><th>Regression Plots</th></tr>
<tr><td rowspan="2">M11</td><td>5</td><td>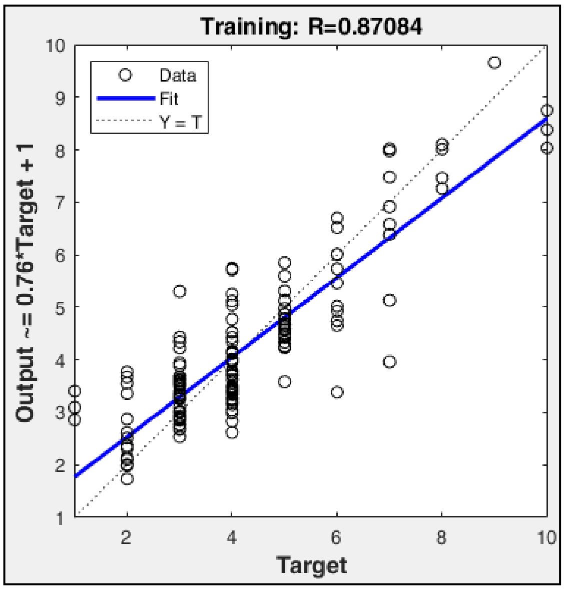
</td></tr>
<tr><td>6</td><td>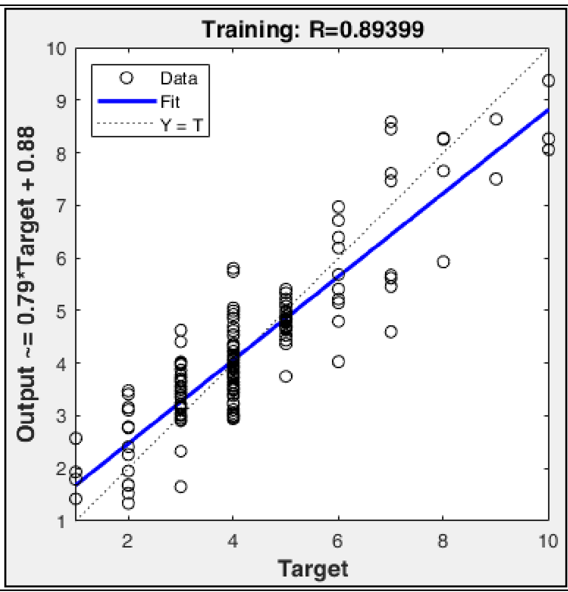
</td></tr>
</table>

Table H.1. Table showing the Regression Plots for ANN_Training Models (continued)

Models	**# of Hidden Neurons**	**Regression Plots**
M12	6	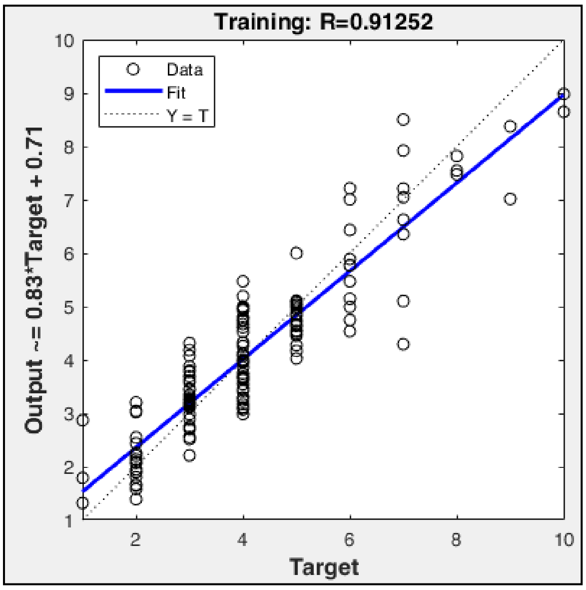
	7	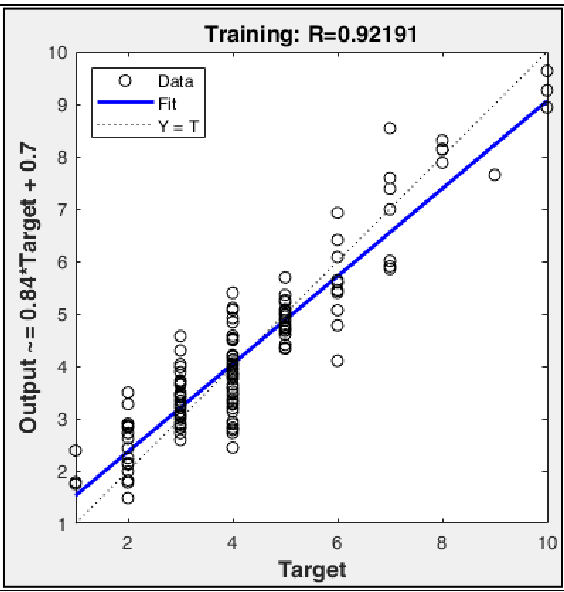

Table H.1. Table showing the Regression Plots for ANN_Training Models (continued)

Models	# of Hidden Neurons	Regression Plots
M13	3	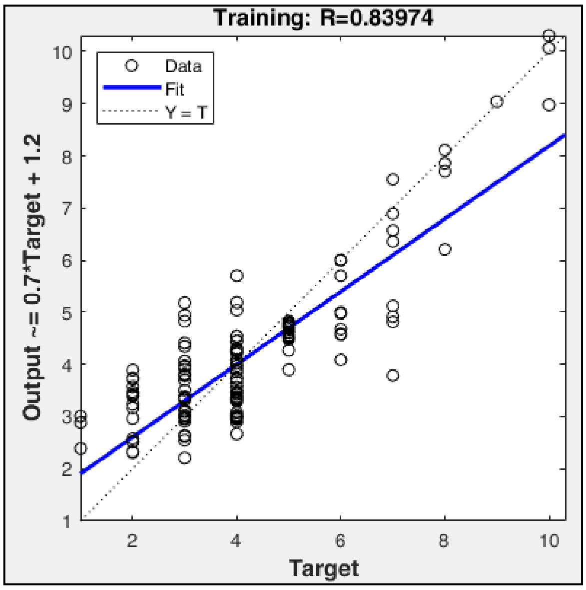
	4	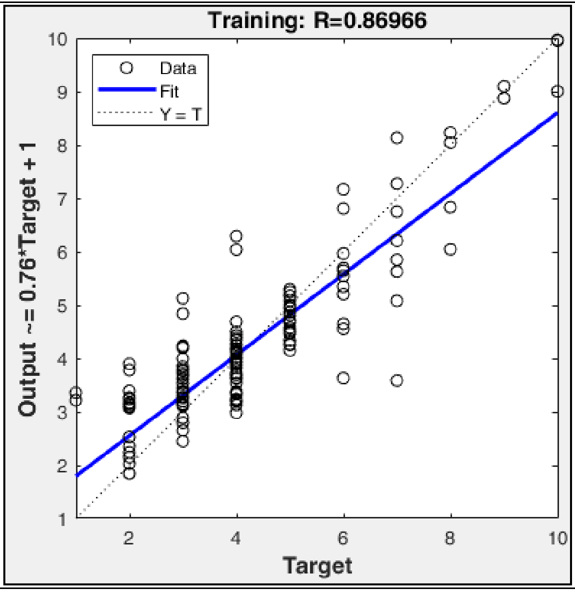

Table H.1. Table showing the Regression Plots for ANN_Training Models (continued)

Models	# of Hidden Neurons	Regression Plots
M14	4	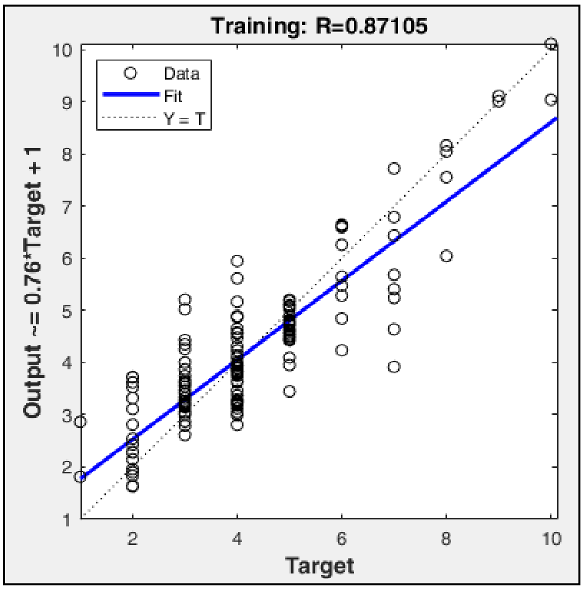
	5	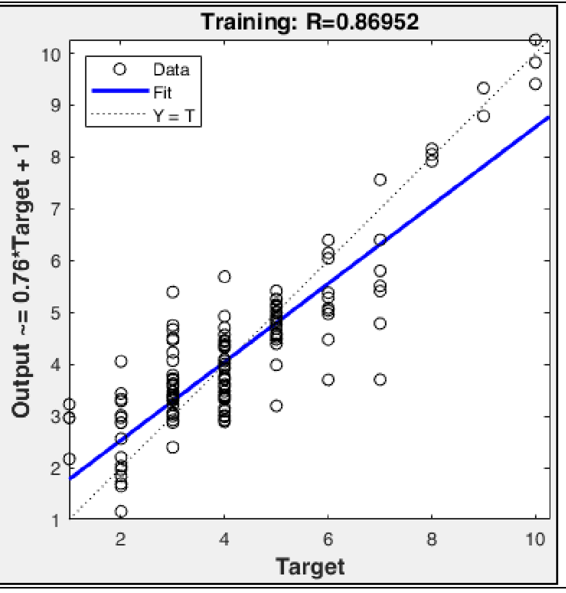

Table H.1. Table showing the Regression Plots for ANN_Training Models (continued)

Models	# of Hidden Neurons	Regression Plots
M15	5	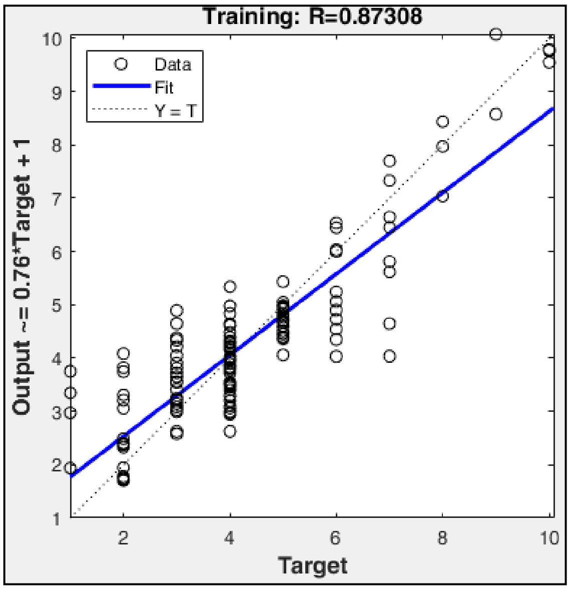
	6	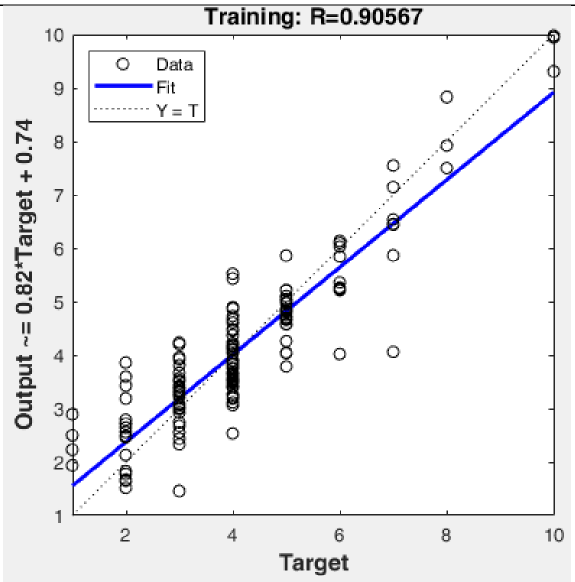

Table H.1. Table showing the Regression Plots for ANN_Training Models (continued)

Models	# of Hidden Neurons	Regression Plots
M16	6	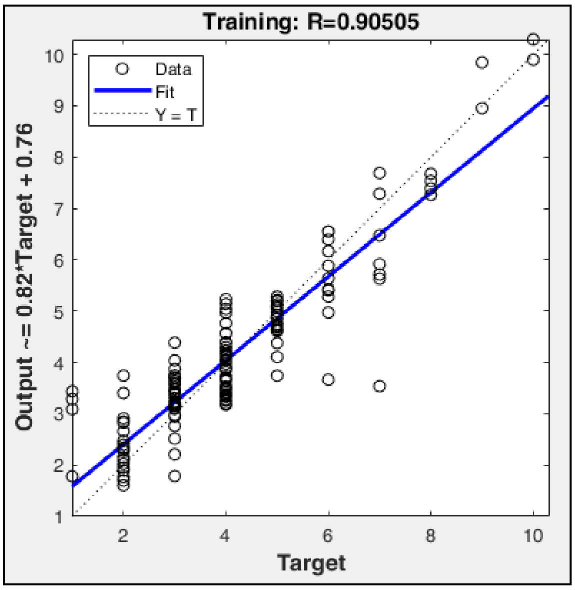
	7